

**JURASSIC-CRETACEOUS STRATIGRAPHIC AND STRUCTURAL EVOLUTION OF
THE NORTHERN YUCATAN MARGIN, GULF OF MEXICO BASIN**

A Thesis Presented to
the Faculty of the Department of Earth and Atmospheric Sciences
University of Houston

In Partial Fulfillment
of the Requirements for the Degree
Master of Science

By
Andrew Steier
May 2018

**JURASSIC-CRETACEOUS STRATIGRAPHIC AND STRUCTURAL EVOLUTION OF
THE NORTHERN YUCATAN MARGIN, GULF OF MEXICO BASIN**

Andrew Steier

APPROVED:

Dr. Paul Mann, Chairman

Dr. Jonny Wu

Ted Godo, Murphy Oil Corporation

**Dr. Dan Wells, Dean
College of Natural Sciences and Mathematics**

ACKNOWLEDGEMENTS

I would like to thank my research advisor, Dr. Paul Mann, for his guidance during my time at the University of Houston (UH), first as an undergraduate research assistant from 2015 to 2016 and then as a graduate student from 2016 to 2018. It was thanks to his academic guidance and his industry connections that I was able to gain valuable technical skills and access to a proprietary seismic dataset that set me apart from other students competing for jobs in the oil and gas industry. Truly, I would not be in the professional situation I am today without the support of Dr. Mann. Special thanks also go to Dr. Jonny Wu and Ted Godo, whose enthusiasm and thoughtful recommendations greatly improved this thesis. And I would like to thank Dr. Shuhab Khan, who in his role as the UH Undergraduate Advisor directed me to potential research advisors when I first arrived at UH as a lost post-baccalaureate student.

Thanks also go to those involved with the Conjugate Basins, Tectonics, and Hydrocarbons (CBTH) research consortium. This includes the corporate sponsors whose financial support funded my graduate studies and the company representatives who provided feedback on my project at various stages. I specifically would like to thank Mike Saunders and Laurie Geiger of Spectrum Geo for making the seismic data available to me for this study and the US and Mexican Gulf of Mexico teams at Total for helpful feedback that improved this thesis. Finally, I would like to thank the other CBTH students, both past and present, for their assistance, encouragement, and friendship during my time at UH.

And personally, I would like to thank Elda Smith and Heather Anderson for originally encouraging me to pursue a career in geology. I would like to thank my family for encouraging me along the way while keeping me grounded in my overall career goals. And most of all, I thank my wife, Jennifer, who has been there every step of the way, listening with a patient ear to every frustration and sharing in every celebration.

**JURASSIC-CRETACEOUS STRATIGRAPHIC AND STRUCTURAL EVOLUTION OF
THE NORTHERN YUCATAN MARGIN, GULF OF MEXICO BASIN**

An Abstract of a Thesis Presented to

the Faculty of the Department of Earth and Atmospheric Sciences

University of Houston

In Partial Fulfillment

of the Requirements for the Degree

Master of Science

By

Andrew Steier

May 2018

ABSTRACT

The Gulf of Mexico (GOM) basin formed during Triassic-late Jurassic rifting as the Yucatan continental block rifted to the southeast away from its northern GOM conjugate margin. During a second, late Jurassic-earliest Cretaceous drift phase, the Yucatan block rotated counterclockwise to its current location and produced an eastward-narrowing wedge of oceanic crust beneath the central GOM. The stratigraphy and structural evolution of the Florida margin is much better understood than its northern Yucatan conjugate because previous hydrocarbon exploration has been more extensive on the Florida margin.

In the northeastern GOM, the late Jurassic section near DeSoto Canyon records late Jurassic-Cretaceous gravity sliding of rafted blocks over distances of 25-40 km along a basinward-dipping layer of salt. This study uses a 117,000 km² grid of 2D seismic data tied to published regional seismic lines and wells to describe a previously unrecognized and coeval area of widespread, gravity sliding along the less-studied, northern Yucatan margin. I define three structural domains based on their distinctive salt structures and associated deformation: 1) the northeastern study area consists of relatively undeformed, late Jurassic-Cretaceous section underlain by 0-300 m-thick salt; 2) areas in the central and southwestern study area contain late Mesozoic gravity slides defined by normal faults rooted onto a 1-4° basinward-dipping salt detachment that controlled overlying, sedimentary growth wedges separated by intervening, 300-600 m-thick salt rollers; and 3) the distal margin of the western and central study area exhibits large salt diapirs up to 6 km tall that penetrate overlying units as young as the Pleistocene.

In the central study area containing late Mesozoic gravity slides, a sedimentary unit equivalent to the productive, Oxfordian Norphlet sandstone of the deep-water northeastern GOM is identified based on its similar seismic character. Reconstructing the Norphlet-equivalent unit

to its location during Oxfordian deposition places it adjacent to an extensive area of deep-water Norphlet sandstone mapped in a previous study. The reconstruction suggests an 84,000 km² fairway of potential aeolian, Jurassic reservoirs on the Yucatan and Campeche margins that includes areas of productive reservoirs in the southeastern Bay of Campeche which previous authors correlated with the Norphlet Formation.

TABLE OF CONTENTS

I. INTRODUCTION TO THIS THESIS.....	1
II. JURASSIC-CRETACEOUS STRATIGRAPHIC AND STRUCTURAL EVOLUTION OF THE NORTHERN YUCATAN MARGIN, GULF OF MEXICO BASIN	
1. Introduction.....	3
2. Regional geologic setting	
2.1 Tectonic evolution of the Gulf of Mexico.....	5
2.2 Structural settings of large gravity slides on the conjugate margins of the northeastern Gulf of Mexico and the Yucatan margin of Mexico.....	9
2.3 Geologic setting of the Yucatan margin and the southern Gulf of Mexico.....	11
3. Dataset.....	16
4. Structural and stratigraphic interpretation	
4.1 Late Jurassic-Cretaceous seismic interpretation.....	18
4.2 Distribution of salt structures.....	24
4.3 Basement structure and the continent-ocean boundary.....	25
5. Structural evolution of the Yucatan margin	
5.1 Cross-section restoration methodology.....	28
5.2 Structural evolution of the northeastern Yucatan area with minimal salt.....	31
5.3 Structural evolution of the central Yucatan area with prevalent salt rollers.....	31
5.4 Structural evolution of the southwestern Yucatan area with widespread diapirism...37	
6. Discussion	
6.1 Timing of salt-assisted gravity sliding on the Yucatan margin and implications for Gulf of Mexico basin evolution.....	49

6.2 Controls on post-salt sedimentation and structural evolution.....	59
6.3 Late Jurassic paleogeography and implications for hydrocarbon prospectivity.....	62
7. Conclusions.....	64
8. References.....	68

Figure Captions

Figure 1. The deep-water Gulf of Mexico (GOM) separates the passive margins of the Florida and Yucatan margins. The location of this study’s seismic dataset is shown in red with coverage extending from the Yucatan shelf into the deep-water GOM. Bathymetric contours are shown as blue lines at 500 m intervals.....4

Figure 2. A. The study area is shown on a basemap of the vertical gravity gradient from Sandwell et al.’s (2014) global gravity grid. Using this same grid, Nguyen and Mann (2016) mapped fracture zones and extinct spreading ridges (black) in the GOM and used their geometry to identify the Yucatan’s pole of rotation (blue) near northwest Cuba. Small circles (red) centered at the pole of rotation show the predicted opening directions for the GOM conjugate margins that include the study area of the Yucatan margin in Mexico. The mapped extent of Callovian salt on both conjugate margins is modified from Rowan et al. (2004) and is shown in pink. **B.** This tectonic reconstruction restores the Yucatan continental block to its paleo-position in late Jurassic time (Oxfordian; 161 Ma). During Oxfordian time, the Yucatan block transitioned from the northwest-southeast directed extension in the first phase of Triassic-middle Jurassic GOM opening to counter-clockwise rotation and seafloor spreading during the second, late Jurassic-earliest Cretaceous phase of GOM opening. During the Oxfordian, aeolian dunes of the Norphlet Formation were being deposited on both the Yucatan and northern GOM conjugate margins. The blue, dashed polygon represents the Balsas portal, which Mann et al. (2016) proposed was the entry point for Pacific seawater into the large sag basin that had formed by the end of the phase one rifting.....7

Figure 3. A. A seismic cross-section from Pilcher et al. (2014) trending northeast-southwest, southwest of the Florida Escarpment in deep-water shows the late Mesozoic section that has been deformed by gravity sliding along a salt detachment. This interval is underlain by Callovian salt

and capped by the Top Cretaceous unconformity. This section includes discontinuous, high-amplitude reflectors that overlie the Louann salt on the updip side of salt rollers. Pilcher et al. (2014) interpreted these high-amplitude reflectors as Norphlet sandstone. Similar packages of Norphlet sandstone have resulted in numerous hydrocarbon discoveries in the deep-water of the northeastern GOM (Godo, 2017). **B.** A southeast-northwest seismic cross-section from this study's seismic dataset on the northern Yucatan margin exhibits a gently-dipping detachment, salt rollers, high-amplitude reflectors overlying the salt, and limited deformation above the Top Cretaceous unconformity.10

Figure 4. Hudec et al. (2013) interpret steeply-rotated growth packages of late Jurassic strata above salt rollers that formed above a salt detachment along the northern Yucatan margin. These authors also note a sudden drop in the detachment level in the distal area from which large salt diapirs emerge. The approximate location of this seismic transect is shown in Figure 6.....12

Figure 5. A. Stratigraphic column correlating Mexican GOM and US GOM sedimentary units (modified from Angeles-Aquino and Cantu-Chapa, 2001; Goldhammer and Johnson, 2001; Mitra, 2007; and Gray, 2008). The aeolian sandstone member of the Ek-Balam Group is considered a lateral equivalent to the Norphlet Formation of the US GOM. **B.** Location map of the La Popa basin in eastern Mexico and Ek-Balam field in the Bay of Campeche.....14

Figure 6. Seismic dataset used in this study which covers the most distal areas of the Yucatan shelf and extends up to 150 km into the deep-water GOM. The seismic lines interpreted in this study are shown in green. The approximate location of Hudec et al.'s (2013) seismic line displaying salt rollers and overlying Jurassic growth wedges is shown in purple. To the southwest are fields in the Campeche area which have penetrated the Ek-Balam Group whose aeolian sandstones are suggested by Guzman et al. (2000) to be equivalent to the Norphlet Formation of the US GOM.17

Figure 7. A. Uninterpreted, dip seismic line located in the central region of the study area. **B.** Zoomed view of the uninterpreted, dip seismic line to highlight the late Mesozoic section. **C.** Interpreted, dip seismic line. The basal detachment (yellow) is a high-amplitude peak that is usually unfaulted, although numerous normal faults are rooted along this horizon. Bodies with internally chaotic reflections are interpreted as salt (pink). Discontinuous, high-amplitude troughs overlying the salt are interpreted as Norphlet-equivalent (blue). The Top Cretaceous unconformity (green) is recognized by its high amplitude peak-trough-peak configuration that frequently represents the upward termination of salt-related faulting.....20

Figure 8. A. Uninterpreted, strike seismic line. **B.** Zoomed view of the uninterpreted, strike seismic line to highlight the late Mesozoic section. **C.** Interpreted, strike seismic line. The basal detachment (yellow) is a high-amplitude peak that is rarely offset by faulting, although numerous normal faults are rooted in this horizon. Bodies with internally chaotic reflections are interpreted as salt bodies shown in pink. Discontinuous, high-amplitude troughs overlying the salt are interpreted as Norphlet-equivalent aeolian sandstone and are shown in blue. The Top Cretaceous unconformity (green) is a high amplitude peak-trough-peak configuration that frequently represents the upward termination of salt-related faulting.....22

Figure 9. A. Isochron of Louann-equivalent salt along the northern Yucatan margin with the limit of salt outlined in black. The continent-ocean boundary of Nguyen and Mann (2016) is shown in red. Outside of the study area, salt bodies mapped by Huffman et al. (2004) illustrate the overall GOM salt extent. **B.** Three different areas are defined based on the common salt structures present. Four fault families that affect the late Mesozoic stratigraphy are distinguished based on their age.....26

Figure 10. A. Interpreted depth to crystalline basement map for the Yucatan margin. Outlined is the outer marginal rift at the most distal extent of thinned continental crust. **B.** The outboard

boundary of the outer marginal rift is defined as the continent-ocean boundary (black, dashed). The fracture zones and extinct spreading ridges mapped by Nguyen and Mann (2016) are shown in yellow with projected fracture zones shown in green to illustrate the relationship between continent-ocean boundary geometry and fracture zone trajectory.....29

Figure 11. **A.** Location map of seismic cross-section. **B.** Dip-oriented seismic cross-section of the northeastern Yucatan area. **C-I.** Cenozoic strata are relatively undeformed and subhorizontal, except for small-offset, normal faults in the Miocene (F) and Oligocene (G) intervals. **J-K.** Small volumes of salt produce little deformation in the Mesozoic. **L.** The original salt volume overlies the pre-salt section on thinned continental crust prior to seafloor spreading.....32

Figure 12. **A.** Location map of seismic cross-section. **B.** Dip-oriented seismic cross-section of the central Yucatan area. **C-I.** Similar to the northeastern area, the Cenozoic strata are subhorizontal and show little deformation aside from small-offset, normal faults that are here more common in the Miocene (F) and Oligocene (G) sections. These units gradually onlap the Top Cretaceous surface. **J.** Normal faults rooted in the salt detachment are common and produce significant sedimentary wedges that thicken toward the fault. This indicates that much of the movement along these faults occurred during the Cretaceous. **K.** Less substantial sedimentary wedging is apparent in the Jurassic section indicating active normal faulting, salt migration, and the formation of salt rollers has begun. **L.** The original salt volume overlies the pre-salt section on thinned continental crust prior to seafloor spreading.38

Figure 13. **A.** Location map of seismic cross-section. **B.** Dip-oriented seismic cross-section of the southwestern Yucatan area. **C-E.** Recent and Plio-Pleistocene strata thin as they drape the growing diapirs outboard and show significant offset in the full graben inboard. **F-G.** Large thickness variation is evident on either side of the two diapirs where salt has been evacuated. Adjacent normal faults result from the downturning of strata toward the diapirs. **H-I.** Little

faulting is evident but thickening between and inboard from the diapirs suggests salt evacuation and diapiric growth is continuing. **J.** The two diapirs begin their vertical migration and few normal faults penetrate the Cretaceous as salt rollers are uncommon. **K.** Few normal faults deform the Jurassic as most of the updip salt migrates into the outer marginal rift. Salt extrudes onto the oceanic crust causing a thin Jurassic section which is subsequently onlapped by the Cretaceous section. **L.** The original salt volume overlies the pre-salt section on thinned continental crust prior to seafloor spreading.....44

Figure 14. Schematic restorations depicting the development of salt rollers, extensional faulting, and sedimentary growth wedges in the late Jurassic to Cretaceous section and the progressive onlapping of Cenozoic stratigraphy onto the Top Cretaceous surface. Modified from Pilcher et al. (2014) and Piedade and Alves (2017).....50

Figure 15. A. Location map of wells in subsidence analysis. Outline of Mississippi fan is shown in black, which heavily influences the total subsidence plots after the mid-Miocene. Location of the pseudo-well on the central Yucatan seismic cross-section is shown in blue in the inset. **B.** Plot of tectonic and total subsidence for the Cheyenne well in the US GOM after Ismael (2014). Mississippi fan sedimentation is not as clear as other wells as Ismael (2014) notes that total subsidence increases dramatically in the Paleocene, earlier than the other wells. Estimated paleobathymetry is shown in blue above the subsidence plot. **C.** Plot of tectonic and total subsidence for the Norton well in the US GOM. The effects of Mississippi fan sedimentation are not as evident as the other wells because of its western location away from the primary depocenter. The tectonic subsidence curve illustrates the slow, gradual subsidence of the basin beginning in the late Mesozoic. Estimated paleobathymetry is shown in blue above the subsidence plot. **D.** Plot of tectonic and total subsidence for the Titan well in the US GOM. Mississippi fan sedimentation affects the total subsidence curve greatly beginning in the Miocene.

The tectonic subsidence curve, however, removes the effects of sedimentation to reveal a slow, gradual history of basin subsidence. Estimated paleobathymetry is shown in blue above the subsidence plot. **E.** Plot of tectonic and total subsidence for the Vicksburg well in the US GOM. Similar to Titan, Mississippi fan sedimentation produces large effects on the total subsidence curve from the Miocene to present, but the tectonic subsidence curve again shows the slow, gradual history of basin subsidence. Estimated paleobathymetry is shown in blue above the subsidence plot. **F.** Tectonic and total subsidence curves for a pseudo-well along a Yucatan seismic cross-section. Despite fewer data points due to no biostratigraphic data, the same trend of slow, gradual subsidence is evident.....53

Figure 16. A. Mapped area of prevalent Norphlet-equivalent units on the northern Yucatan margin in relation to the mapping of Pilcher et al. (2014) on the Florida conjugate margin. Magnetic highs near these two areas suggest possible paleo-topographic highs that controlled sediment transport pathways and the direction of salt-assisted gravity sliding away from the area of high Mesozoic elevation. Notable oil (green) and gas (red) discoveries in the Norphlet Formation and Ek-Balam Group are overlaid. **B.** Zoomed view of the Florida margin with notable hydrocarbon discoveries in the Norphlet Formation labelled. **C.** Zoomed view of the Yucatan margin with notable hydrocarbon discoveries in the Ek-Balam Group’s aeolian member labelled.60

Figure 17. Oxfordian paleogeography showing proposed extent of aeolian sandstone deposition and salt bodies mapped in this study, by Lin (in prep.), and by Huffman et al. (2004). Magnetic data is used to identify paleo-topographic highs on the Yucatan margin where they are less studied than on the conjugate margin in the northeastern GOM. Reconstruction uses a fixed North American plate and restores the Yucatan block to its pre-drift position about a rotational pole from Nguyen and Mann (2016). The reconstructed magnetic grid illustrates the strong spatial

correlation between the Sarasota Arch and the Chiquila Magnetic Anomaly, and the DeSoto High and the Rio Lagartos Magnetic Anomaly on the conjugate margins.....63

Figure 18. Extent of proposed Oxfordian, sandstone reservoir fairway in the Mexican GOM based on this study’s mapping of Norphlet-equivalent and producing fields in the Bay of Campeche area. Lease blocks offered in the most recent bid rounds are outlined in pink (round 2.4) and blue (round 3.1)65

I. INTRODUCTION TO THIS THESIS

After completing my Bachelor of Arts degree in Classics and Honors Anthropology at the University of Notre Dame in 2012, I worked in the tourism and real estate industries in Steamboat Springs, Colorado and Houston. It was not until 2014 that I began undergraduate studies in geology at Houston Community College at night while continuing to work. In the fall of 2015, I began full-time coursework at the University of Houston and working for Dr. Paul Mann's Caribbean Basins, Tectonics, and Hydrocarbons (CBTH) consortium as an undergraduate research assistant. The next year I began the master's graduate program in geology with Dr. Mann as my thesis supervisor and was supported as a graduate research assistant by the CBTH project. For my master's research, I was granted access to a large grid of 2D seismic reflection data by Mike Saunders and Laurie Geiger of Spectrum Geo along the northern Yucatan margin in the Mexican Gulf of Mexico (GOM). The primary objective of the project was to explore the possibility of a Mexican equivalent to the productive Norphlet sandstone reservoirs of the US GOM.

An Oxfordian-age, aeolian sandstone reservoir producing in the Ek-Balam field of the Bay of Campeche was inferred by previous authors to represent a lateral-equivalent to the Norphlet Formation of the US GOM (e.g., Guzman-Vega and Mello, 1999; Guzman et al., 2000; Rosenfeld, 2003; Hunt et al., 2017). But no previous study has identified this Norphlet-equivalent in seismic data or suggested its areal distribution along the northern Yucatan margin of Mexico. Moreover, the distribution of various salt structures and the nature of deformation they cause to overlying strata like the Norphlet-equivalent unit had not been investigated by previous studies of the Yucatan margin. Hudec et al. (2013) and Pindell et al. (2014) are the only authors who have published seismic interpretations of salt rollers and diapirs on the northern Yucatan

margin. However, they did not map the areal distribution of these structures or provide a comprehensive explanation of their Mesozoic and Cenozoic evolution.

In this thesis, I map the salt structures and overlying strata including the Norphlet-equivalent unit in this under-studied region and propose an evolutionary history of these structures through a series of structural restorations. This study also places the salt and Norphlet-equivalent extents into the tectonic context of the late Jurassic GOM opening, using gravity (Sandwell et al., 2014) and magnetic (Maus et al., 2007) data to relate the distribution of salt rollers and potential hydrocarbon traps and reservoirs to the region's tectonic history.

In addition to Dr. Mann, my thesis committee includes Dr. Jonny Wu of the University of Houston and Ted Godo of Murphy Oil Corporation. Dr. Wu specializes in structural geology and tectonics and also has experience working in the oil and gas industry. Before joining Murphy, Ted Godo worked extensively on the development of deep-water Norphlet prospects in the US GOM that led to major oil discoveries at Appomattox, Rydberg, and many others (Godo, 2006; Godo et al., 2011; Godo, 2017).

Between the two years of my master's coursework and research, I was an exploration geology intern with Total E&P Americas in the summer of 2017, working with their Mexican GOM New Ventures team. This thesis greatly benefited from my experience with many different seismic datasets from the Mexican GOM at Total. In the fall of 2017, I was offered an extended, part-time internship with the same group at Total for the spring of 2018, and I will resume full-time work there following my May, 2018 graduation from the University of Houston.

II. JURASSIC-CRETACEOUS STRATIGRAPHIC AND STRUCTURAL EVOLUTION OF THE NORTHERN YUCATAN MARGIN, GULF OF MEXICO BASIN

1. INTRODUCTION

The Gulf of Mexico (GOM) basin was formed during a two-phase, Triassic-earliest Cretaceous rift history as the Yucatan continental block separated from the North America plate along its northern GOM conjugate margin (Pindell and Kennan, 2009; Eddy et al., 2014; Nguyen and Mann, 2016) (Fig. 1). In the second phase of GOM opening during the late Jurassic and earliest Cretaceous, 37° of counter-clockwise rotation of the Yucatan block (Nguyen and Mann, 2016) initiated seafloor spreading and passive margin formation that has allowed the GOM basin to become one of the most prolific hydrocarbon-producing basins in the world (Pindell and Kennan, 2009; Nguyen and Mann, 2016; Weimer et al., 2017; Godo, 2017) (Fig. 2).

Previous hydrocarbon exploration has been more extensive on the Florida conjugate margin in the US sector of the GOM than on the Yucatan margin in the Mexican sector, and therefore the stratigraphy and structural evolution of the Florida margin is much better-understood. In comparison, there are no deep-water wells penetrating the Mesozoic, no 3D seismic datasets, and only one, large 2D seismic dataset (Fig. 1) acquired in 2016 on the northern Yucatan margin where no acreage was offered in the 2017 deep-water bid rounds for the Mexican GOM (Fig. 18). As a result, the Yucatan margin remains relatively unexplored.

The most successful petroleum play of the deep-water, offshore northeastern US GOM since 2003 involves the productive aeolian sandstone reservoirs of the Oxfordian Norphlet Formation (Godo, 2006; Godo et al., 2011; Pilcher et al., 2014; Godo, 2017; Saunders et al., 2017; Weimer et al., 2017; Dunnahoe, 2018). Basinward of the Florida Escarpment in the deep-water GOM, numerous hydrocarbon discoveries have been made in the Norphlet sandstone incorporated and deformed in rafted fault blocks overlying salt detachments and completely

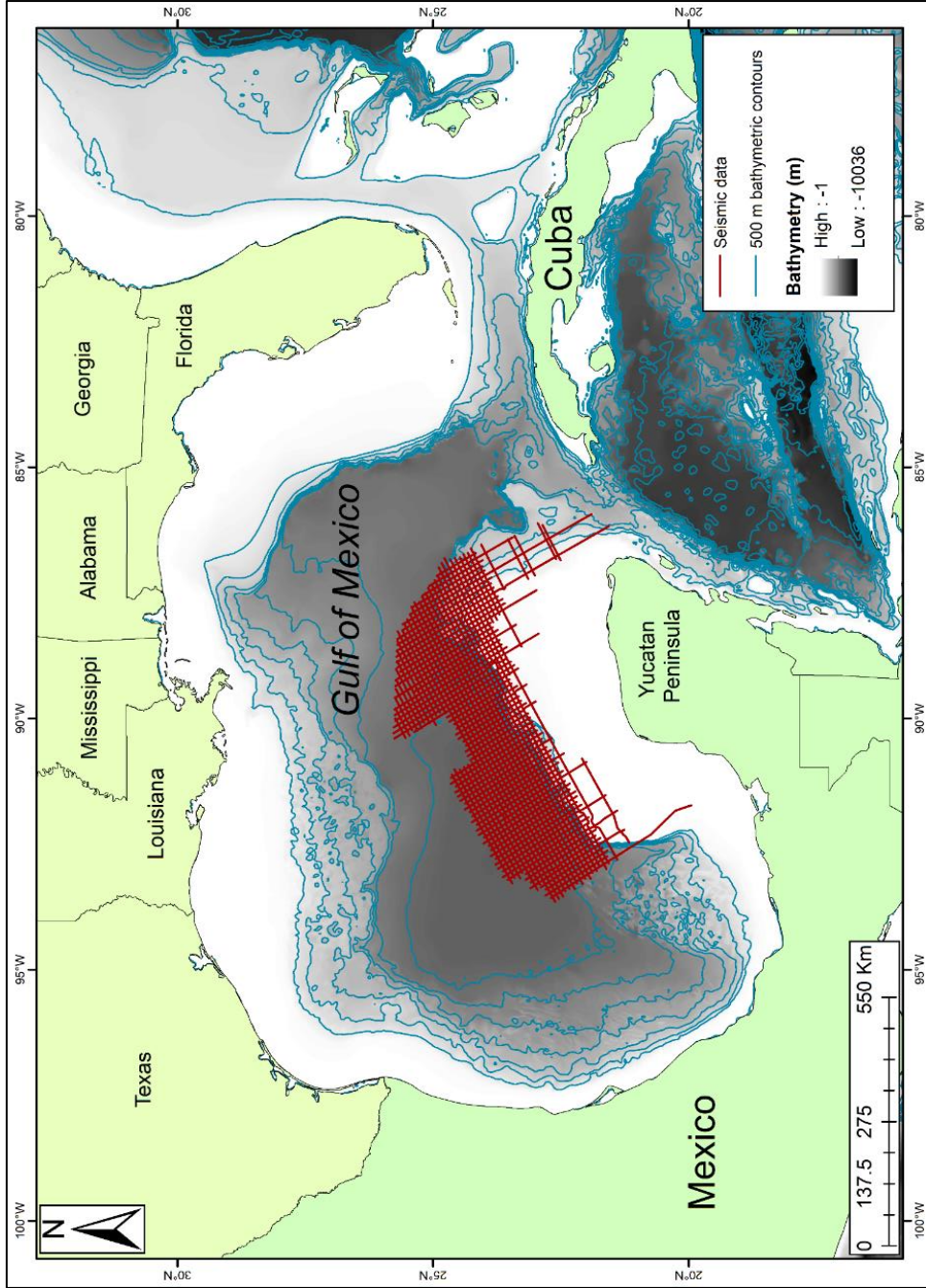


Figure 1. The deep-water Gulf of Mexico (GOM) separates the passive margins of the Florida and Yucatan margins. The location of this study's seismic dataset is shown in red with coverage extending from the Yucatan shelf into the deep-water GOM. Bathymetric contours are shown as blue lines at 500 m intervals.

separated by salt walls (Fig. 3). Similarly, hydrocarbon discoveries have been made in the Ek-Balam field in the Bay of Campeche in the southern GOM in fault-bounded, aeolian sandstone reservoirs also of Oxfordian age overlying the Callovian salt (Lopez, 1996; Guzman-Vega and Mello, 1999; Guzman et al., 2000; Mitra et al., 2007). These discoveries led Rosenfeld (2003) and Hunt et al. (2017) to suggest that this aeolian sandstone member of the Ek-Balam Group was equivalent to the Norphlet Formation of the northeastern GOM (Fig. 5).

This study focuses on the deep-water area northwest of the Yucatan platform (Fig. 1), which represents the conjugate, rifted margin to the Florida Escarpment. The Yucatan margin remains unexplored and largely unknown because there are no industry wells in this region and the few Deep Sea Drilling Project (DSDP) wells only penetrate the Paleogene section. Seismic interpretation of the 117,000 km² 2D seismic grid allows for identification and mapping of a potential Norphlet-equivalent sandstone along this margin and stratigraphic correlations to the northern GOM conjugate margin (Fig. 5). Improved mapping of the Callovian salt and interpretation of its evolution will illuminate areas of similar trapping styles as the northeastern GOM and could help predict the location of a large, Oxfordian, Norphlet sandstone reservoir fairway in this region.

2. REGIONAL GEOLOGIC SETTING

2.1 Tectonic evolution of the Gulf of Mexico

Most authors now agree that the GOM basin opened during two phases, although dating precision of the two-phase event is not sufficient to know if the two phases were pulsed or continuous (Marton and Buffler, 1994; Pindell and Kennan, 2009; Eddy et al., 2014; Nguyen and Mann, 2016). In the Triassic, northwest-southeast-directed rifting began between North America, the Yucatan continental block, and South America (Salvador, 1987; Galloway, 2008). During this time, the Yucatan block was translated southeastward and produced a series of southwest-

northeast lineaments in the basement fabric revealed by a regional pattern of southwest-northeast-trending magnetic highs and lows that can be reconstructed between the northeastern GOM and Yucatan by closing the area of oceanic crust created during the second phase of GOM opening (Hunter et al., 2014; Lin, in prep.) (Fig. 16).

A large, topographic sag basin formed in late Jurassic time above the phase-one rifts in an arcuate zone extending from eastern Mexico to south Florida. This sag basin subsequently filled with seawater as soon as the Balsas portal opened in central Mexico that allowed seawater from the Pacific Ocean to fill the large sag basin (Galloway, 2008; Mann et al., 2016; Padilla y Sanchez, 2017) (Fig. 2b). As rifting continued, salt deposition was favored in the restricted basin throughout the Callovian (Hudec et al., 2013). During the Oxfordian, salt deposition ceased as rifting was completed and seafloor spreading began (Nguyen and Mann, 2016).

The second phase of GOM opening began in the Oxfordian (Fig. 2b) as salt deposition and rifting ceased and oceanic spreading in the central GOM separated the single GOM salt basin into the distinct Louann and Campeche salt provinces of the northern and southern GOM, respectively (Hudec et al., 2013; Nguyen and Mann, 2016). At this transition between the first and second phases of GOM opening, the Yucatan block ceased its southeast translation and began to rotate counter-clockwise as late Jurassic oceanic crust was created. Nguyen and Mann (2016) used the tilt derivative of Sandwell et al.'s (2014) satellite-derived global gravity grid to map the fracture zones and extinct spreading ridges in the central GOM. These lineaments predict 37° of counter-clockwise rotation about a pole of rotation located in present-day northwestern Cuba (Nguyen and Mann, 2016), although multiple poles of rotation have been proposed by previous studies (Galloway, 2008; Pindell et al., 2016). By the Berriasian (Nguyen and Mann, 2016) or Valanginian (Pindell and Kennan, 2009; Snedden et al., 2014), the Yucatan block had reached its

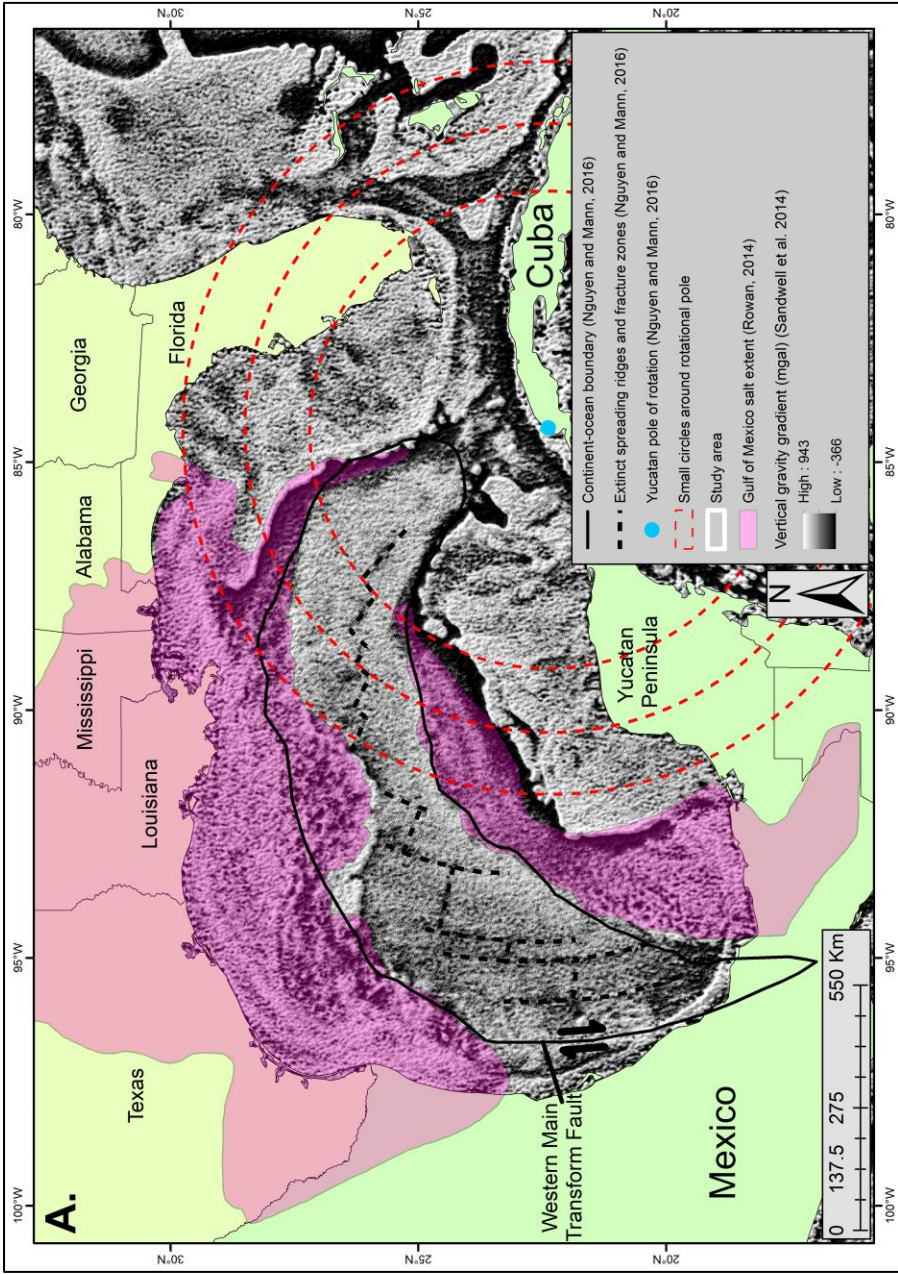


Figure 2. A. The study area is shown on a base map of the vertical gravity gradient from Sandwell et al.'s (2014) global gravity grid. Using this same grid, Nguyen and Mann (2016) mapped fracture zones and extinct spreading ridges (black) in the GOM and used their geometry to identify the Yucatan's pole of rotation (blue) near northwest Cuba. Small circles (red) centered at the pole of rotation show the predicted opening directions for the GOM conjugate margins that include the study area of the Yucatan margin in Mexico. The mapped extent of Cretaceous salt on both conjugate margins is modified from Rowan et al. (2004) and is shown in pink.

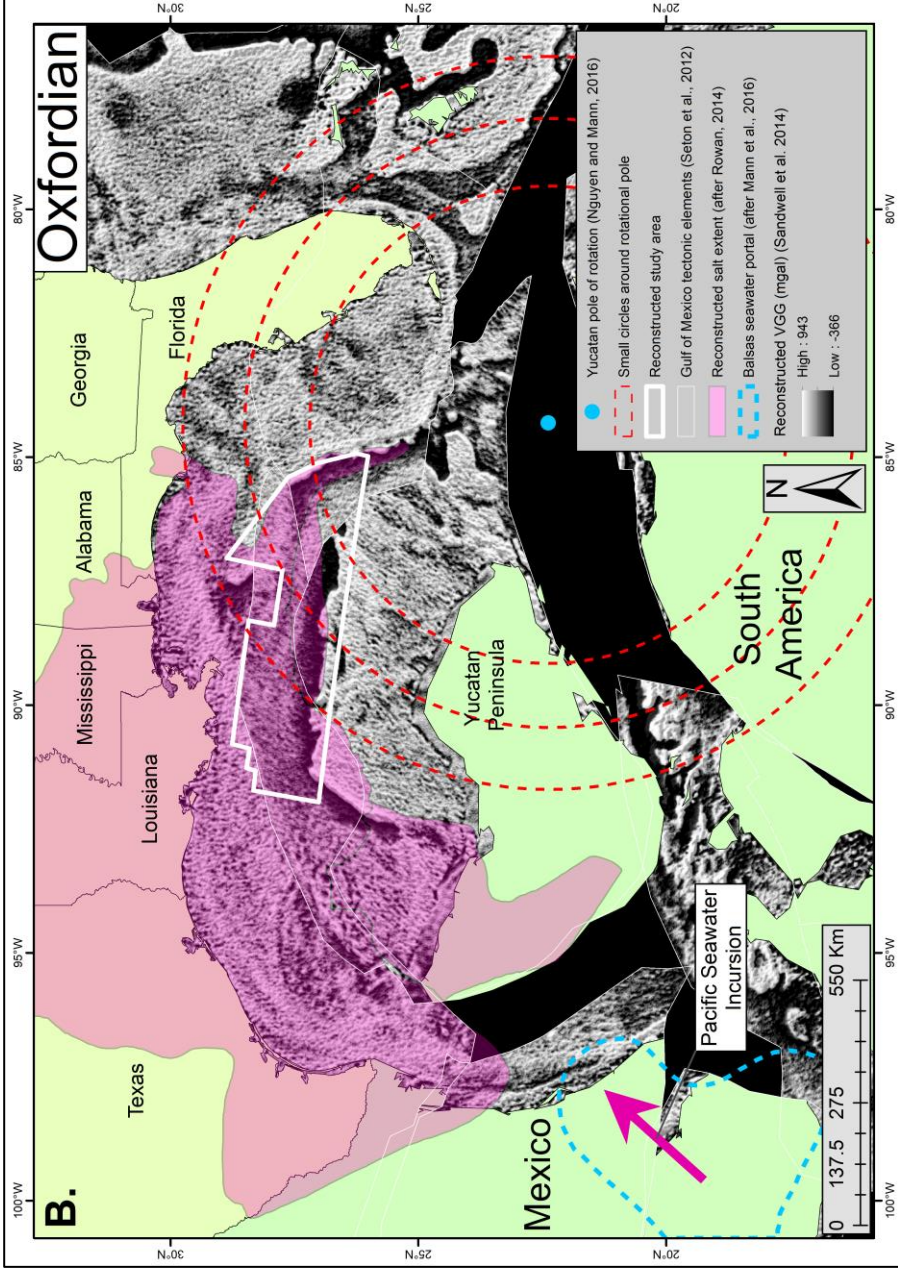


Figure 2 (cont.). B. This tectonic reconstruction restores the Yucatan continental block to its paleo-position in late Jurassic time (Oxfordian; 161 Ma). During Oxfordian time, the Yucatan block transitioned from the northwest-southeast directed extension in the first phase of Triassic-middle Jurassic GOM opening to counter-clockwise rotation and seafloor spreading during the second, late Jurassic-earliest Cretaceous phase of GOM opening. During the Oxfordian, aeolian dunes of the Norphlet Formation were being deposited on both the Yucatan and northern GOM conjugate margins. The blue, dashed polygon represents the Balsas portal, which Mann et al. (2016) proposed was the entry point for Pacific seawater into the large sag basin that had formed by the end of the phase one rifting.

present-day location and the passive margin phase of the Gulf of Mexico basin began (Galloway, 2008) (Fig. 2a).

2.2 Structural settings of large gravity slides on the conjugate margins of the northeastern Gulf of Mexico and the Yucatan margin of Mexico

In the northeastern GOM, Pilcher et al. (2014) mapped rafts of Norphlet sandstone in the deep-water southwest of the Florida Escarpment that were dispersed into a semi-circular distribution by gravity sliding away from a late Jurassic paleo-topographic high called the Middle Ground Arch (Hunt 2013; Hunt et al., 2017). The elevated area of the Middle Ground arch controlled the distribution of the radially-divergent rafts of Norphlet and overlying Smackover carbonate mudstone. The basinward movement of rafted blocks is confined to the late Jurassic and Cretaceous section (Fig. 3a). These strata slid as coherent blocks downdip and are separated by small (0-400 m thick) salt rollers overlying the salt detachment surface (Fig. 3a).

These salt rollers bound late Jurassic sedimentary units with slight wedge geometries that translated up to 5 km downdip along the salt detachment during the late Jurassic interval (Fig. 3a). The Cretaceous section, however, includes numerous growth packages as units expand on the downthrown side of listric, normal faults rooted in the salt detachment (Pilcher et al., 2014) (Fig. 3a). The late Mesozoic section is capped by the Cretaceous-Paleogene boundary deposit, a high-amplitude reflector that is generally not offset by deep faults rooted in the detachment (Sanford et al., 2016). Above this horizon, the strata are relatively undeformed, subhorizontal, and gradually onlap the Top Cretaceous surface (Fig. 3a).

The structural characteristics of the deep-water, salt-assisted gravity sliding on the northern Yucatan margin (Fig. 3b) are remarkably similar to those on the northern GOM conjugate margin (Fig. 3a). Above the deepest section of somewhat poor reflectivity, a high-amplitude peak representing the salt detachment gently dips basinward (Fig. 3b). This salt

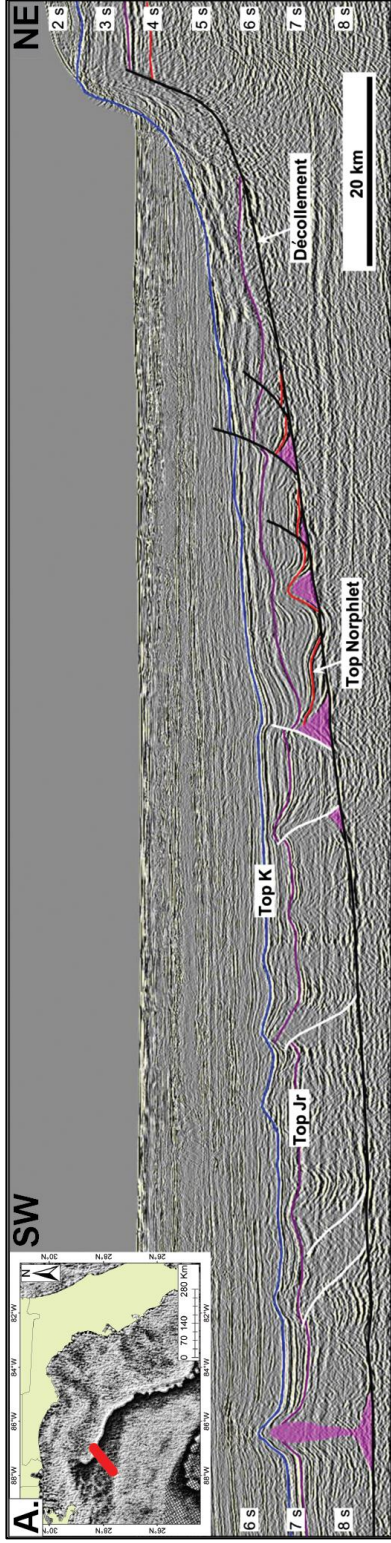


Figure 3. A. A seismic cross-section from Pilcher et al. (2014) trending northeast-southwest, southwest of the Florida Escarpment in deep-water shows the late Mesozoic section that has been deformed by gravity sliding along a salt detachment. This interval is underlain by Callovian salt and capped by the Top Cretaceous unconformity. This section includes discontinuous, high-amplitude reflectors that overlie the Louann salt on the updip side of salt rollers. Pilcher et al. (2014) interpreted these high-amplitude reflectors as Norphlet sandstone. Similar packages of Norphlet sandstone have resulted in numerous hydrocarbon discoveries in the deep-water of the northeastern GOM (Godo, 2017).

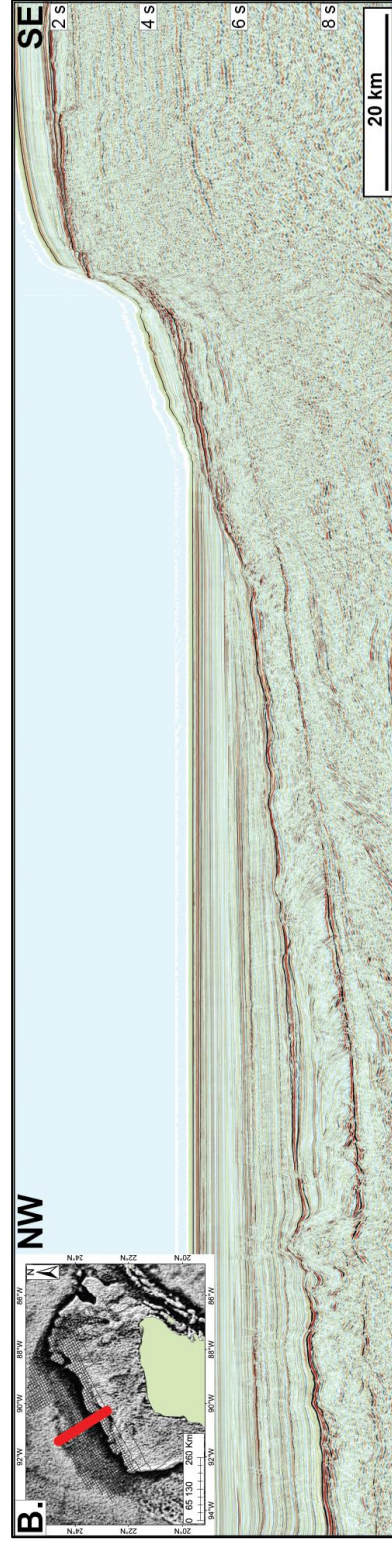


Figure 3 (cont.). B. A southeast-northwest seismic cross-section from this study's seismic dataset on the northern Yucatan margin exhibits a gently-dipping detachment, salt rollers, high-amplitude reflectors overlying the salt, and limited deformation above the Top Cretaceous unconformity.

detachment forms the base of the late Mesozoic section which has undergone salt-related deformation similar to the Florida margin. The high-amplitude Top Cretaceous surface is generally unaffected by the small salt rollers, although larger diapirs intermittently breach this surface in the more distal areas where the salt is thicker (Fig. 13).

Hudec et al. (2013) mapped 14 small salt rollers above the detachment updip and four large diapirs downdip along the Yucatan margin. They noted the detachment level drops dramatically near the continent-ocean boundary beneath the diapirs. In an elongate area that is roughly parallel to the margin, basement elevation decreases to define a 55-km-wide low that extends along the margin and comprises the distal extent of an area they termed the inner basin (Fig. 4). Goswami et al. (2017) used deep-penetration seismic imaging to interpret syn-rift sediments overlying thinned continental crust in the inner basin.

2.3 Geologic setting of the Yucatan margin and the southern Gulf of Mexico

The greater availability of seismic and well data in the US GOM (e.g. Pearson, 2011, Snedden et al., 2014; Weimer et al., 2007) combined with regional gravity datasets (Sandwell et al., 2014) has allowed for improved understanding of Mesozoic stratigraphy and its tectonic setting along the Florida margin. The Norphlet Formation exists on the entire northern GOM rim, although it is thickest in the northeastern GOM (Pearson, 2011). The Norphlet Formation is known from wells and seismic stratigraphy to overlie the Callovian Louann Salt in the offshore northeastern GOM (Tew et al., 1991; Obid, 2006; Pilcher et al., 2014; Snedden et al., 2014; Godo, 2017; Hunt et al., 2017; Payeur et al., 2017) (Fig. 3a).

Within the Norphlet Formation, four depositional facies have been described by previous authors: 1) basal black shales deposited in a lagoonal setting; 2) conglomerates deposited in alluvial fans near paleo-topographic highs; 3) arkosic sandstones and siltstones from distal

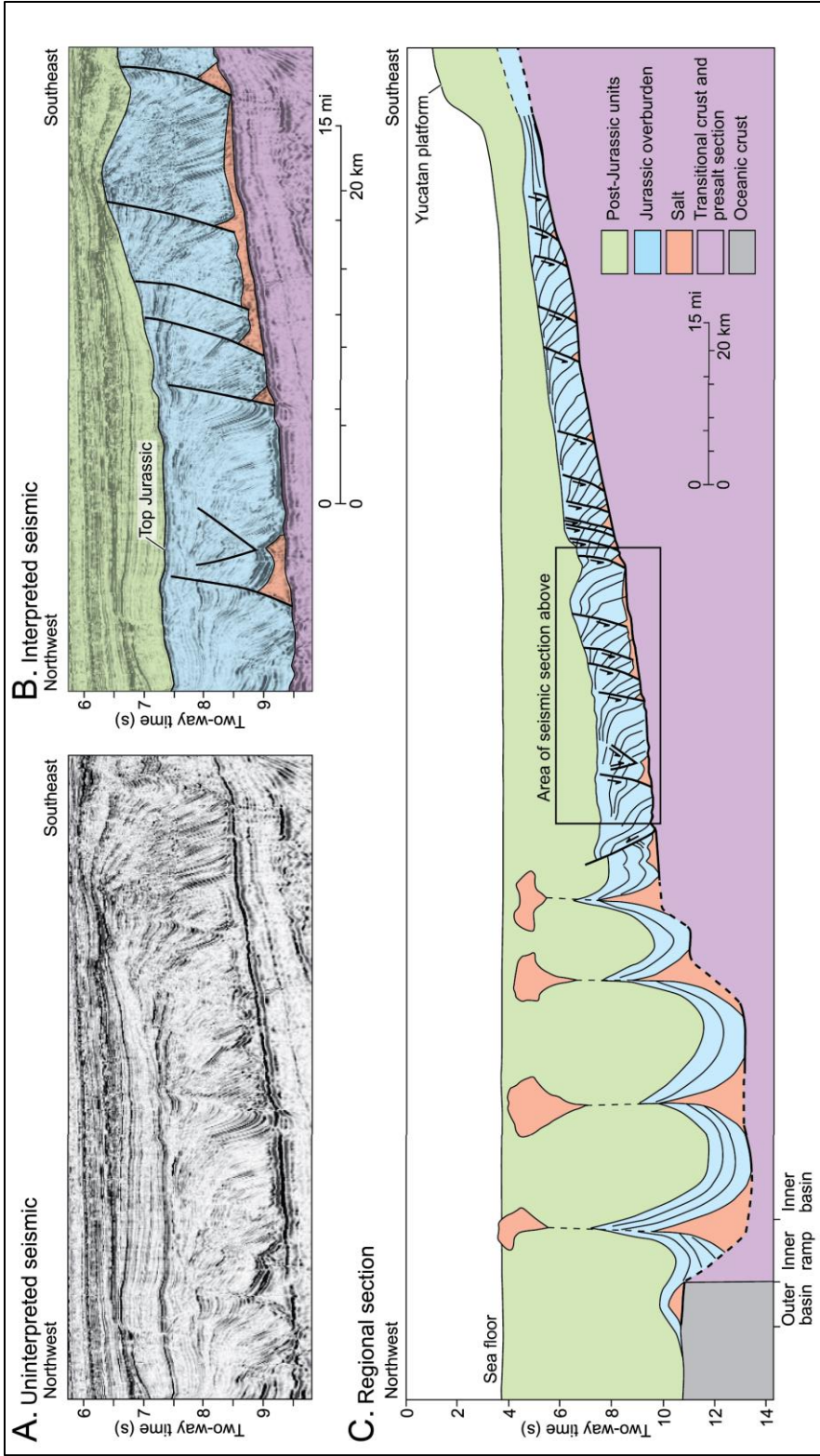


Figure 4. Hudec et al. (2013) interpret steeply-rotated growth packages of late Jurassic strata above salt rollers that formed above a salt detachment along the northern Yucatan margin. These authors also note a sudden drop in the detachment level in the distal area from which large salt diapirs emerge. The approximate location of this seismic transect is shown in Figure 6.

alluvial plain, fluvial, or wadi environments; and 4) the uppermost quartzose sandstones deposited in an aeolian environment and forming barchanoid and linear dune forms in the Destin Dome area (Pearson, 2011; Hunt et al., 2017).

The most productive hydrocarbon reservoir of these four units of the Norphlet Formation is the aeolian, quartzose sandstone facies consisting of well-rounded, well-sorted, quartz-rich, hematite-coated sands deposited with little to no clay matrix during a late Jurassic regression (Pearson, 2011). These aeolian, Norphlet reservoirs are producing in present-day Mississippi, Alabama, Florida, and the deep-water northeastern GOM (Godo, 2017). Marine flooding of this late Oxfordian desert resulted in a rapid transgression of the dunes, preserving their morphology and burying them with the anoxic, organic-rich, marine mudstones and carbonates of the Smackover Formation that acts as both the source and seal of the Norphlet reservoirs (Hunt et al., 2017).

The stratigraphic framework for the deep-water, northern Yucatan margin in my study area cannot be constrained by the few, available well penetrations (Fig. 6). The nearest Mesozoic well control and published stratigraphic column comes from the Bay of Campeche located 280 km south of the study area where Angeles-Aquino and Cantu-Chapa (2001) defined the Mesozoic stratigraphic units of the Mexican GOM including the Oxfordian Ek-Balam Group, which contains the aeolian sandstone reservoir producing in the Ek-Balam field. They equated this interval with the Oxfordian La Gloria sandstone of the La Popa basin. Later, Goldhammer and Johnson (2001) and then Gray (2008) related the La Gloria Formation to the Norphlet Formation of the US GOM (Fig. 5).

The results of Pilcher et al.'s (2014) stratigraphic study and the kinematic plate model for the opening of the GOM by Nguyen and Mann (2016) place the onset of Norphlet sandstone deposition approximately contemporaneous with the Yucatan block's rift-to-drift transition and

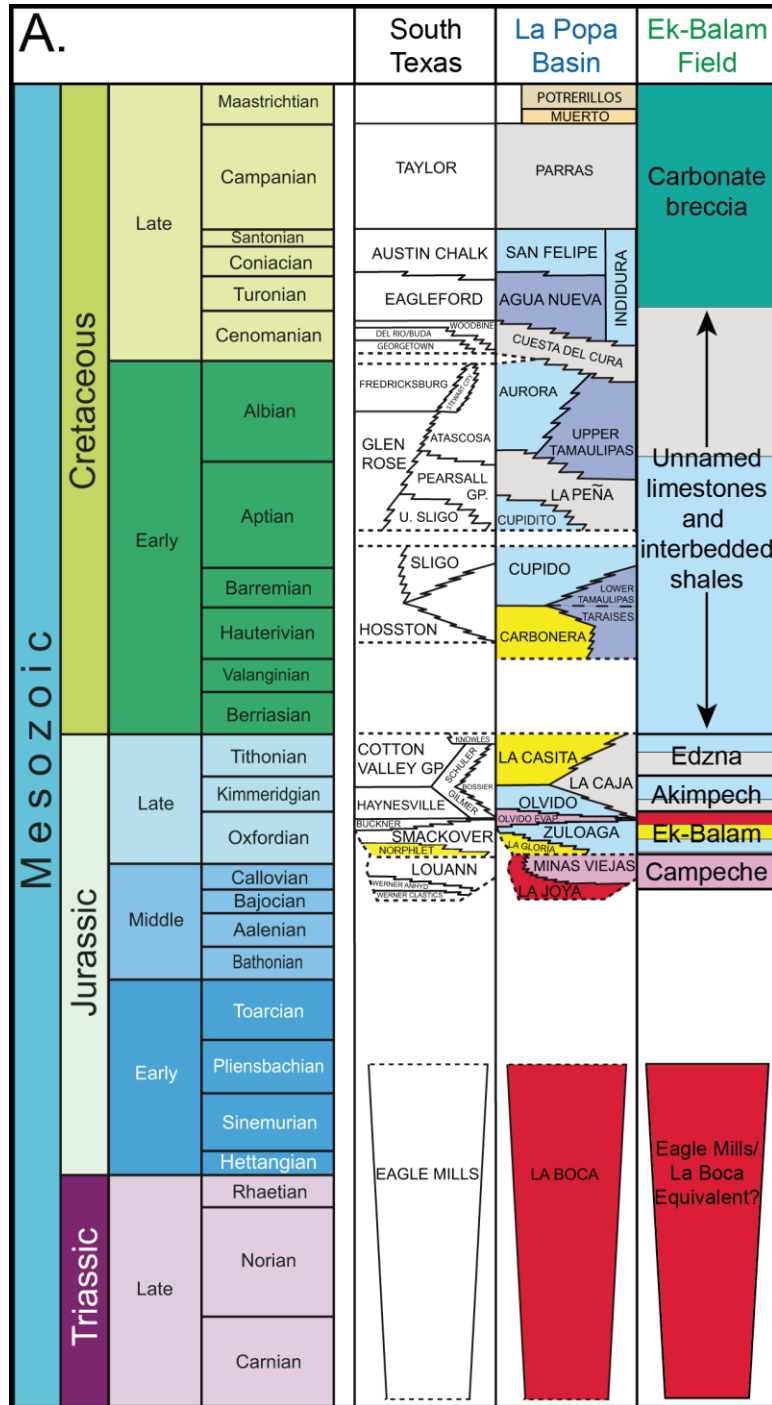


Figure 5. A. Stratigraphic column correlating Mexican GOM and US GOM sedimentary units (modified from Angeles-Aquino and Cantu-Chapa, 2001; Goldhammer and Johnson, 2001; Mitra, 2007; and Gray, 2008). The aeolian sandstone member of the Ek-Balam Group is considered a lateral equivalent to the Norphlet Formation of the US GOM.

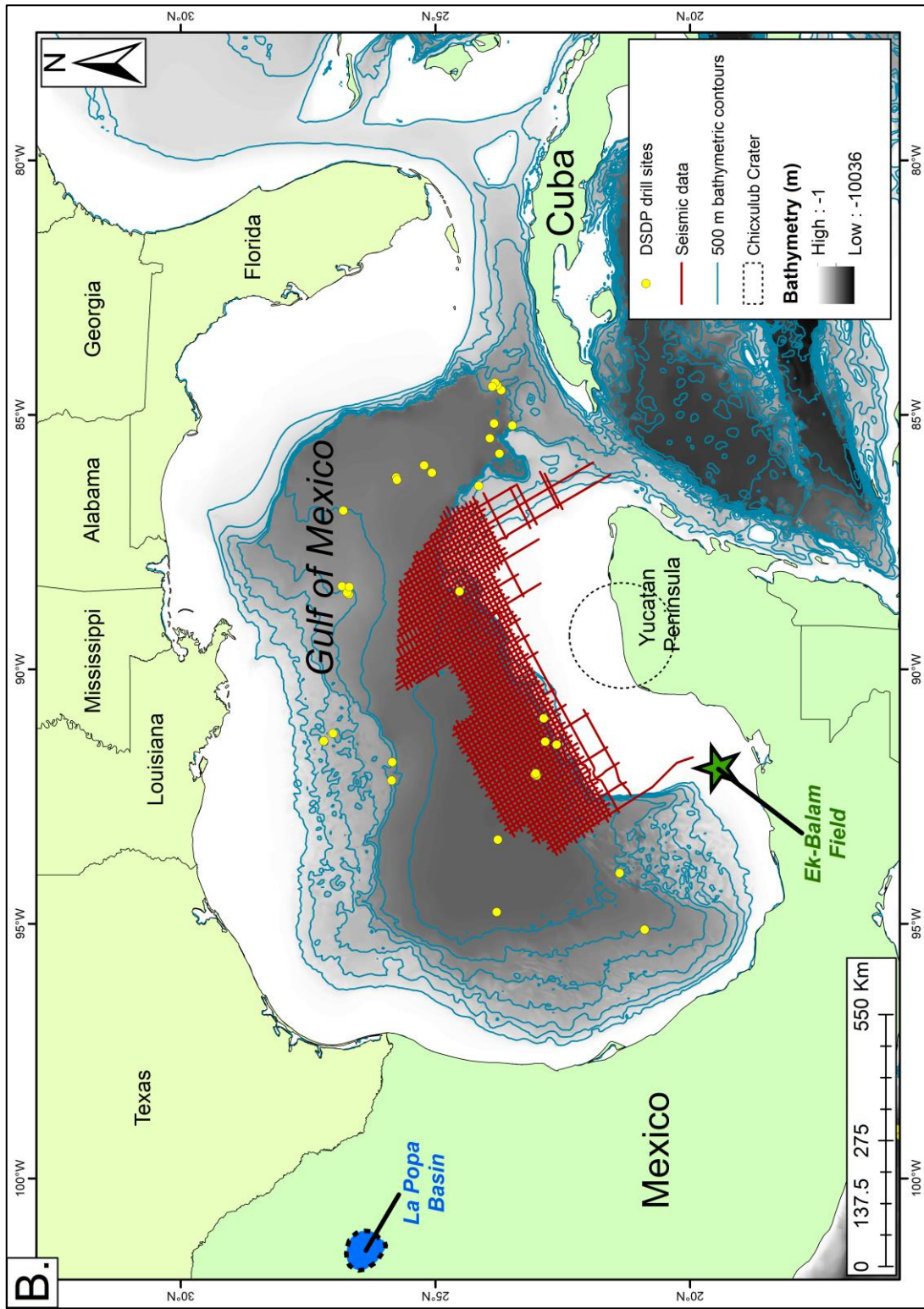


Figure 5 (cont.). B. Location map of the La Popa basin in eastern Mexico and Ek-Balam field in the Bay of Campeche.

initiation of seafloor spreading in the northeastern GOM (Fig. 2b). This suggests a potential post-rift and pre-drift continuous area of aeolian deposition in the Oxfordian GOM that would include both the Norphlet Formation of the US GOM and the Ek-Balam Group of the Mexican GOM (Fig. 5).

The possibility of the Ek-Balam Group representing a Norphlet-equivalent sandstone in the southern GOM and possibly extending along the northern Yucatan margin has been suggested by previous authors. After Guzman et al. (2000) and Guzman-Vega and Mello (1999) noted the aeolian hydrocarbon reservoirs of Oxfordian age in the Caan-1 and Caan-2 wells in the Bay of Campeche, Rosenfeld (2003) suggested the existence of both Norphlet- and Smackover-equivalents in the southern GOM. Hunt et al. (2017) reiterated that more extensive areas of reservoir-quality Norphlet-equivalent sandstones may exist in the Mexican GOM.

3. DATASET

My study uses approximately 24,500 line-km of 2D seismic reflection data in two-way travel time that was provided by Spectrum Geo for the purpose of this study. The seismic grid covers an area of approximately 117,000 km² along the northern Yucatan margin with 10 km line spacing (Fig. 6). The dataset spans the shelf, slope, and basinal areas that range in water depth from 50 m to 3800 m. Within this area, there are no published industry wells and seven publicly-available DSDP wells. Of these seven DSDP wells, four are in deep-water, none of which penetrate the Mesozoic section (Fig. 6). The difficulty in correlating seismic reflections from the shelf into the deep-water necessitated a different approach to assigning age constraints of seismic horizons beyond the shelf break.

This study has relied upon the published regional seismic lines of Rodriguez (2011) and Snedden et al. (2014) that intersect the deep-water area of this study's dataset and are tied to

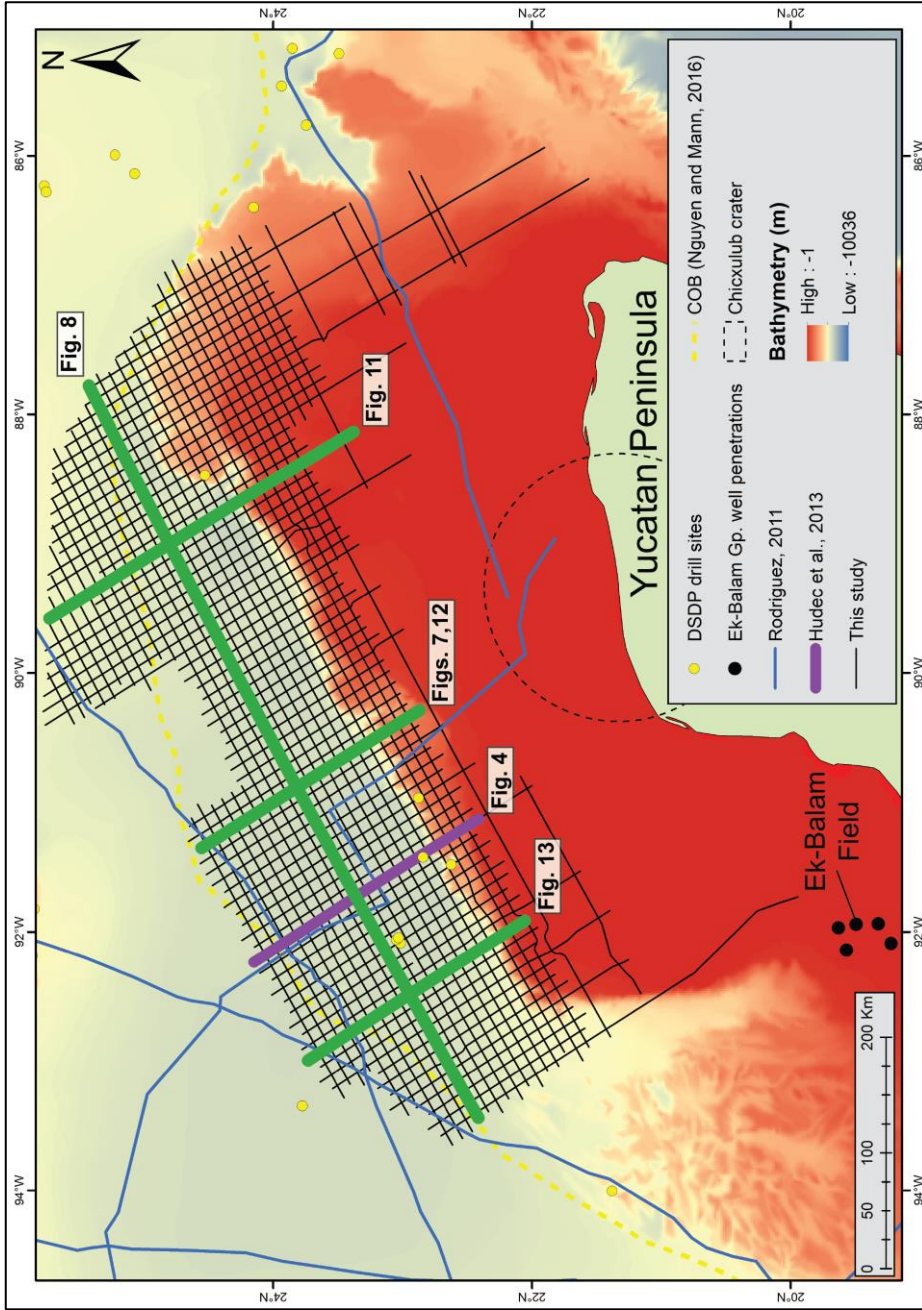


Figure 6. Seismic dataset used in this study which covers the most distal areas of the Yucatan shelf and extends up to 150 km into the deep-water GOM. The seismic lines interpreted in this study are shown in green. The approximate location of Hudec et al.'s (2013) seismic line displaying salt rollers and overlying Jurassic growth wedges is shown in purple. To the southwest are fields in the Campeche area which have penetrated the Ek-Balam Group whose aeolian sandstones are suggested by Guzman et al. (2000) to be equivalent to the Norphlet Formation of the US GOM.

industry and DSDP wells located outside of the study area penetrating the Mesozoic. Because of the cessation of seafloor spreading in the GOM in the earliest Cretaceous (Snedden et al., 2014; Nguyen and Mann, 2016), the Top Jurassic horizon cannot be correlated from the US GOM to the Mexican GOM across the extinct spreading center. This study's Top Jurassic pick (Figs. 11-14) is therefore speculative, but has been approximated from the thickness of post-salt Jurassic and Cretaceous sections observed in the deep-water US GOM where this interval is constrained by well data (Snedden et al., 2014; Pilcher et al., 2014).

The identification of stratigraphic units in the GOM with well-established seismic facies from previous studies was also used to constrain the age of seismic horizons. Chaotic reflections based by a high-amplitude peak dipping gently basinward are interpreted as salt bodies overlying a detachment surface and have been interpreted as Callovian in age by previous authors (Hudec et al., 2013). A package of very high-amplitude reflectors in a peak-trough-peak configuration above the salt onto which younger strata onlap is interpreted as the Top Cretaceous horizon related to the Chicxulub impact (Sanford et al., 2016).

4. STRUCTURAL AND STRATIGRAPHIC INTERPRETATION

4.1 Late Jurassic-Cretaceous seismic interpretation

The late Jurassic to Cretaceous section on the northern Yucatan margin is the most deformed by salt diapirism and salt-assisted gravity sliding along a basal salt detachment and holds the most commercial interest for hydrocarbon exploration. It is in this interval that salt-detached gravity sliding and vertical salt migration has resulted in various salt structures and deformation of the overlying strata that have created many potential hydrocarbon trap and seal configurations. For these reasons, this study focuses on the paleogeography and structural evolution of the late Mesozoic section.

In the deep-water northeastern GOM, the Louann salt, Norphlet Formation, and Smackover Formation can be identified in the subsurface based on their characteristic seismic responses. In Mobile Bay and south of the Middle Ground Arch, the high-velocity basal Smackover Formation produces a strong seismic peak, below which the Norphlet Formation is identified as a strong trough. The next peak below this is the top of the Louann Salt (Obid, 2006; Hunt, 2013; Hunt et al., 2017). Outboard of the Florida Escarpment, Pilcher et al. (2014) interpreted fault-bounded, high-amplitude seismic troughs that overlie the Louann salt on the updip side as the Norphlet Formation. This characteristic seismic expression forms this study's basis for identifying late Jurassic stratigraphic units in the Yucatan seismic data. Pilcher et al. (2014) also provided the most comprehensive mapping of deep-water Norphlet deposits to date, which are used in this study to examine spatial relationships between the distribution of deep-water Norphlet in the northeastern GOM and its potential equivalent on the Yucatan margin.

On the northern Yucatan margin, above the deepest section of relatively low-amplitude, often-chaotic seismic reflectors lies a high-amplitude, gently basinward-dipping peak that can be easily followed from near the shelf break basinward until it abruptly becomes unrecognizable at the distal inner basin (Hudec et al., 2013), or outer marginal trough (Pindell et al., 2014) (Figs. 4c, 7a). This surface is rarely offset by faulting, but forms the base of frequent listric, normal faults in the overlying horizons. Above this surface, irregularly-shaped bodies with internally chaotic seismic reflections arise. These often appear triangular in dip cross-sections (Fig. 7b) and more irregular in strike cross-sections (Fig. 8b) in the updip areas and taller and mushroom-shaped in the downdip areas, particularly in the southwest where salt accumulations are thicker. These bodies are interpreted as Callovian salt rollers and diapirs with the underlying high-amplitude surface interpreted as the detachment surface down which overlying strata have slid (Fig. 7c).

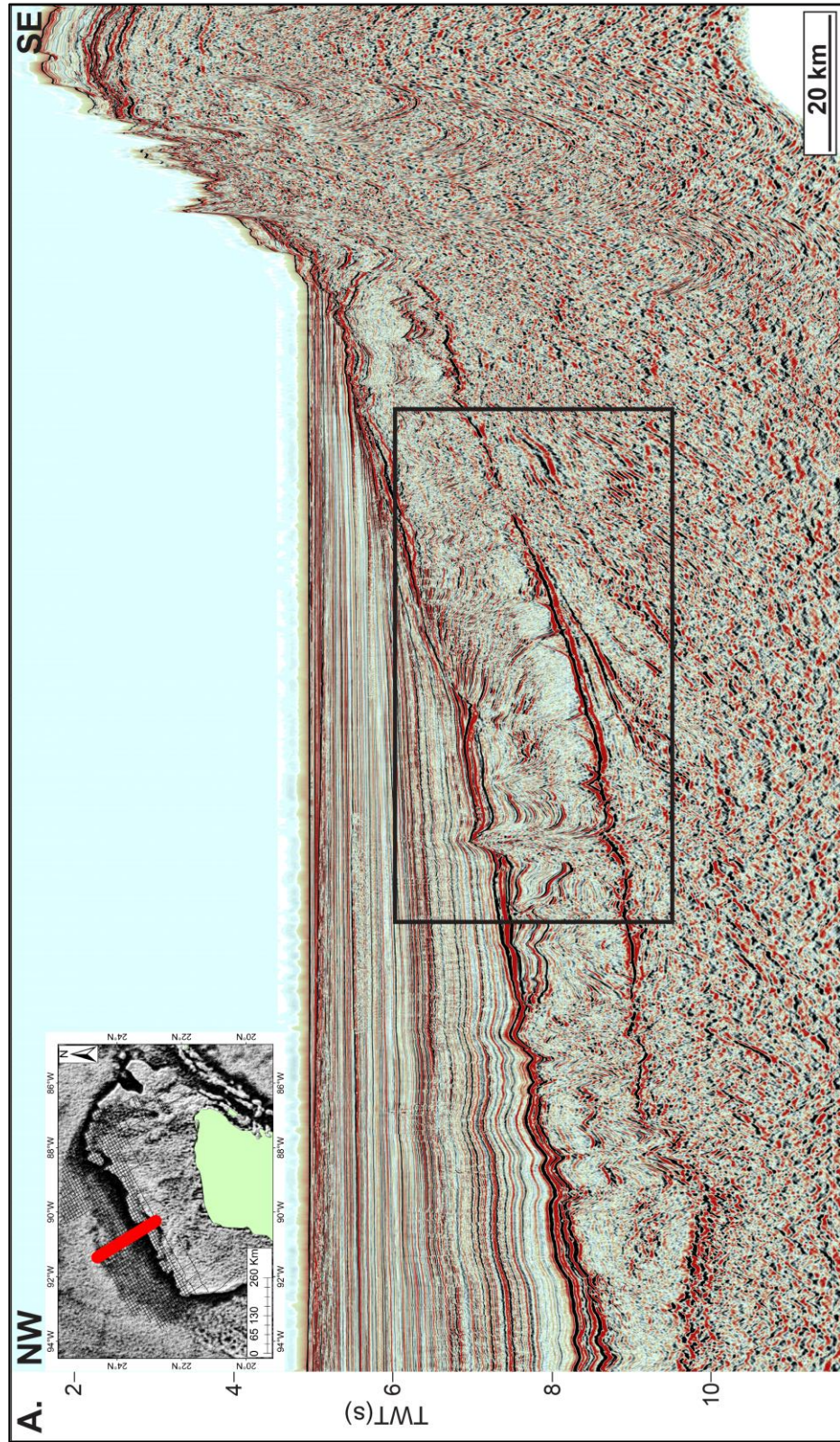


Figure 7. A. Uninterpreted, dip seismic line located in the central region of the study area.

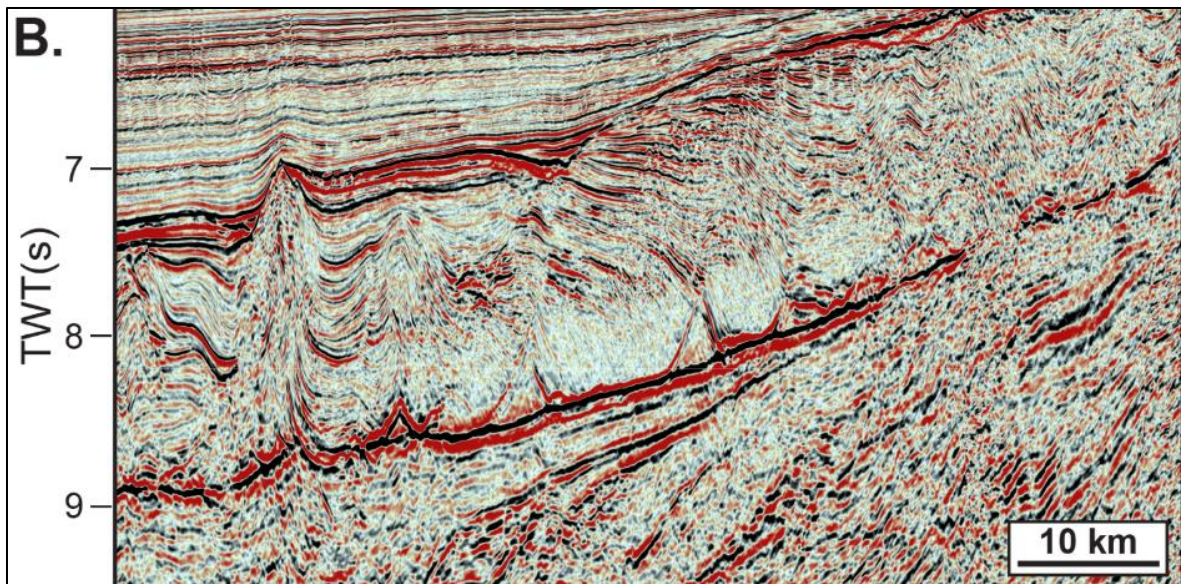


Figure 7 (cont.). B. Zoomed view of the uninterpreted, dip seismic line to highlight the late Mesozoic section.

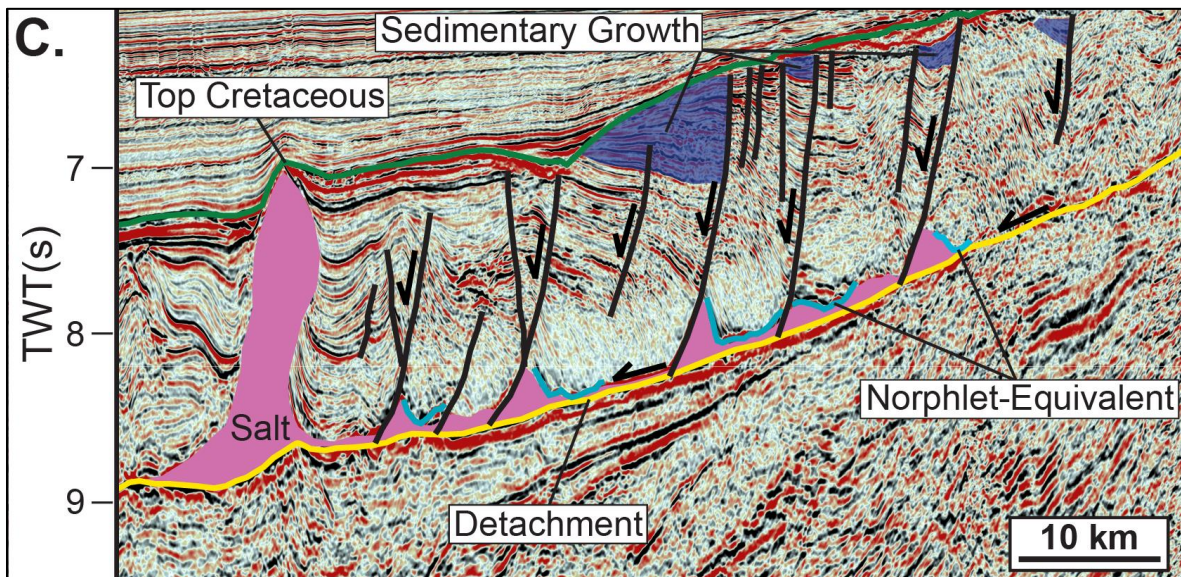


Figure 7 (cont.). C. Interpreted, dip seismic line. The basal detachment (yellow) is a high-amplitude peak that is usually unfaulted, although numerous normal faults are rooted along this horizon. Bodies with internally chaotic reflections are interpreted as salt (pink). Discontinuous, high-amplitude troughs overlying the salt are interpreted as Norphlet-equivalent (blue). The Top Cretaceous unconformity (green) is recognized by its high amplitude peak-trough-peak configuration that frequently represents the upward termination of salt-related faulting.

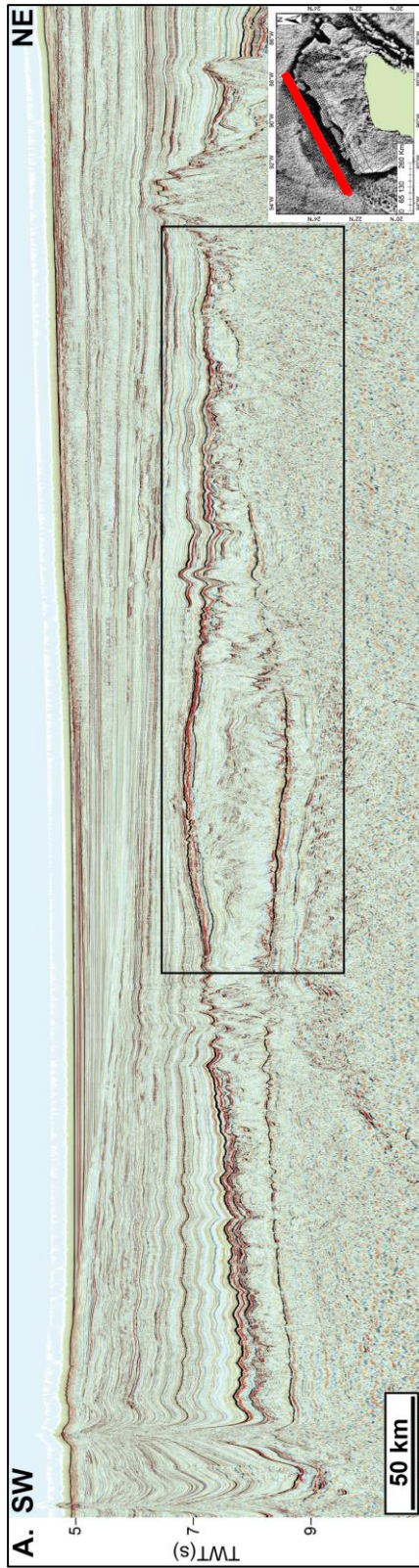


Figure 8. A. Uninterpreted, strike seismic line.

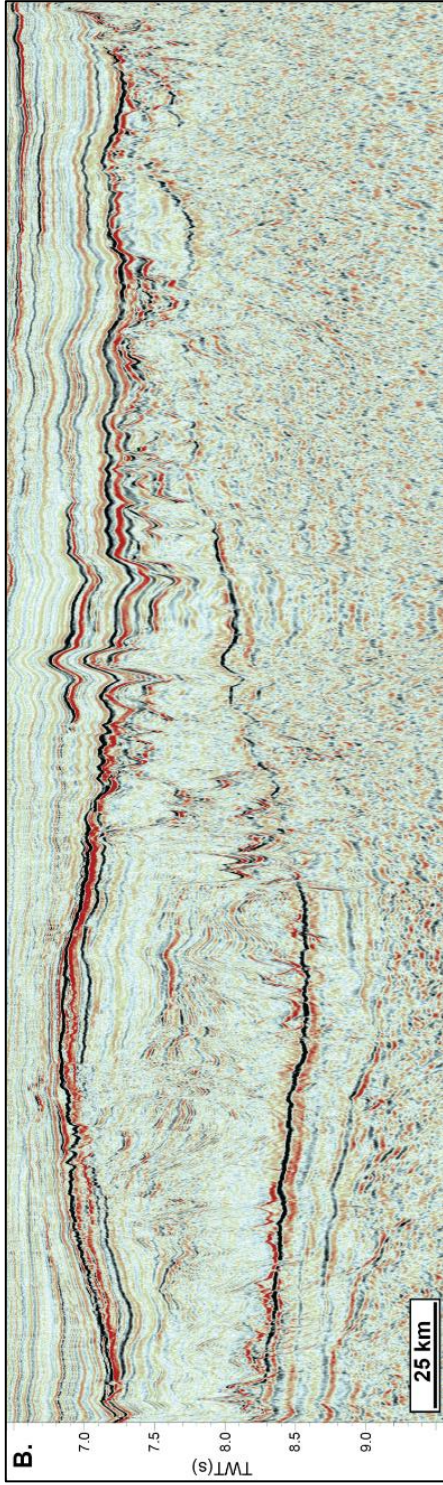


Figure 8 (cont.). B. Zoomed view of the uninterpreted, strike seismic line to highlight the late Mesozoic section.

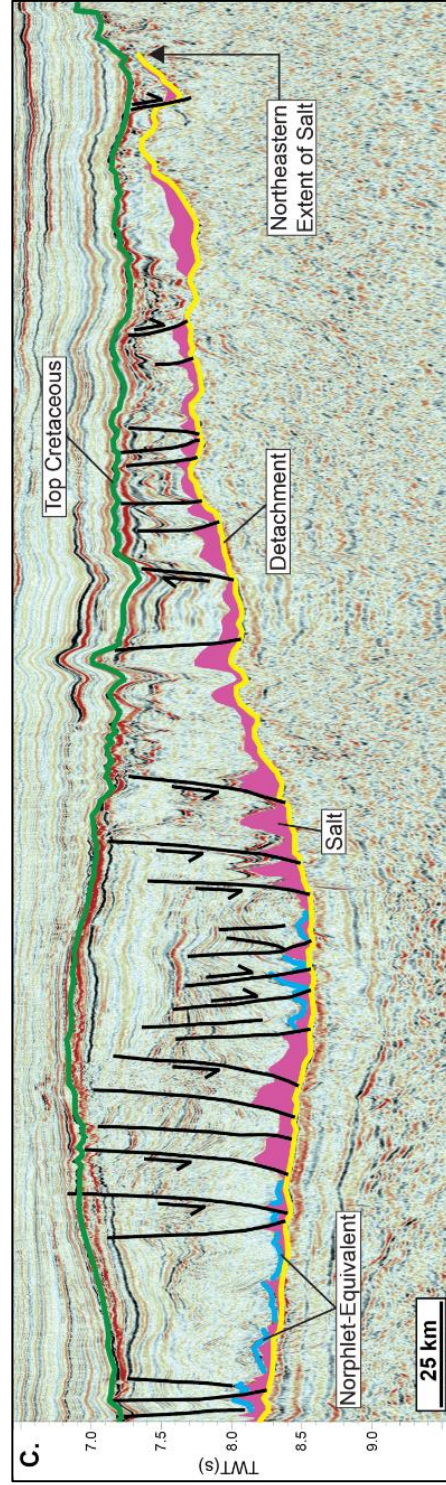


Figure 8 (cont.). C. Interpreted, strike seismic line. The basal detachment (yellow) is a high-amplitude peak that is rarely offset by faulting, although numerous normal faults are rooted in this horizon. Bodies with internally chaotic reflections are interpreted as salt bodies shown in pink. Discontinuous, high-amplitude troughs overlying the salt are interpreted as Norphlet-equivalent aeolian sandstone and are shown in blue. The Top Cretaceous unconformity (green) is a high amplitude peak-trough-peak configuration that frequently represents the upward termination of salt-related faulting.

High-amplitude troughs in the Yucatan seismic data that overlie salt on the updip side, terminate updip, and are bounded downdip by salt rollers are very similar in appearance to those interpreted by Pilcher et al. (2014) as the Norphlet Formation (Figs. 7b-7c). After previous studies (Obid, 2006; Hunt, 2013; Pilcher et al., 2014; Hunt et al., 2017), these troughs are interpreted as the top of a Norphlet-equivalent sedimentary unit. On strike lines, a similar geometry and seismic character for the interpreted Norphlet-equivalent unit was observed with: 1) fault-bounded, high-amplitude troughs directly overlying the top evaporite surface; and 2) rapid changes in the time elevation of the interpreted Norphlet-equivalent unit due to salt deformation (Figs. 8b-8c).

4.2 Distribution of salt structures

By subtracting the detachment horizon from the top salt horizon, a salt isochron is calculated for the Yucatan margin (Fig. 9a). Salt is notably absent in the northeastern portion of the study area (Fig. 8c) but progressively thickness westward. In the center of the study area, salt rollers up to 400 ms in time thickness are most prevalent with few salt diapirs in the most distal areas (Fig. 9a). The salt reaches its greatest thickness in the southwestern region of the study area where large diapirs up to 4.5 s in time thickness frequently deform Cenozoic strata and affect local bathymetry (Figs. 9a, 13). Large diapirs are most common in distal areas where salt has filled the outer marginal rift (Fig. 10) near the basinward extent of thinned continental crust and migrated vertically after sediment loading.

From the salt isochron, two different styles of salt deformation can be identified. A large region of the central study area and a smaller region of the southwestern study area (Fig. 9b) commonly contain salt rollers whose evolution created sedimentary growth wedges in the late Jurassic and Cretaceous sections, but rarely cause deformation above the Top Cretaceous

unconformity (Fig. 7c). Further basinward, an extensive region of salt diapirs (Fig. 9b) can be defined. The diapirs are generally rooted in the outer marginal rift (Fig. 10b) in the most distal area of extended continental crust where salt filled in a paleobathymetric low during late Jurassic rifting and seafloor spreading (Fig. 13). These diapirs become more common in the southwest (Fig. 9b) where salt thicknesses are generally greater, perhaps supporting the Pacific origin of GOM seawater (Mann et al., 2016).

Faults large enough to be correlated between the 2D seismic lines are categorized into four different fault families based on their timing (Fig. 9b): 1) Listric, normal faults rooted in the salt detachment that do not cause any offset of the Top Cretaceous horizon are common in the salt roller province in the central study area; 2) In deeper water, greater salt thicknesses and mobility cause larger salt-related faulting that offsets the Top Cretaceous; 3) Southeast of the salt rollers are more recent normal faults that produce offsets of late Mesozoic strata and are active into the Paleogene; 4) The largest and youngest faults occur in the southwest and produce extensional half and full graben structures that can affect pre-Callovian strata and are active into the Neogene, sometimes even creating fault scarps on the seafloor (Fig. 13).

4.3 Basement structure and the continent-ocean boundary

Mapping the top of the crystalline basement along the northern Yucatan margin reveals basement features with significant implications for GOM opening and salt migration history. Most prominent is the outer marginal rift (Fig. 10a). Similar to the interpretations of previous authors (Hudec et al., 2013; Ismael, 2014; Pindell et al., 2014; Goswami et al., 2017), the top of the basement on the distal, northern Yucatan margin decreases in elevation as it moves distally until it reaches its maximum depth before a sharp rise as the thinned continental crust transitions to oceanic crust (Figs. 11-13). The point at which the top of the basement first begins its descent

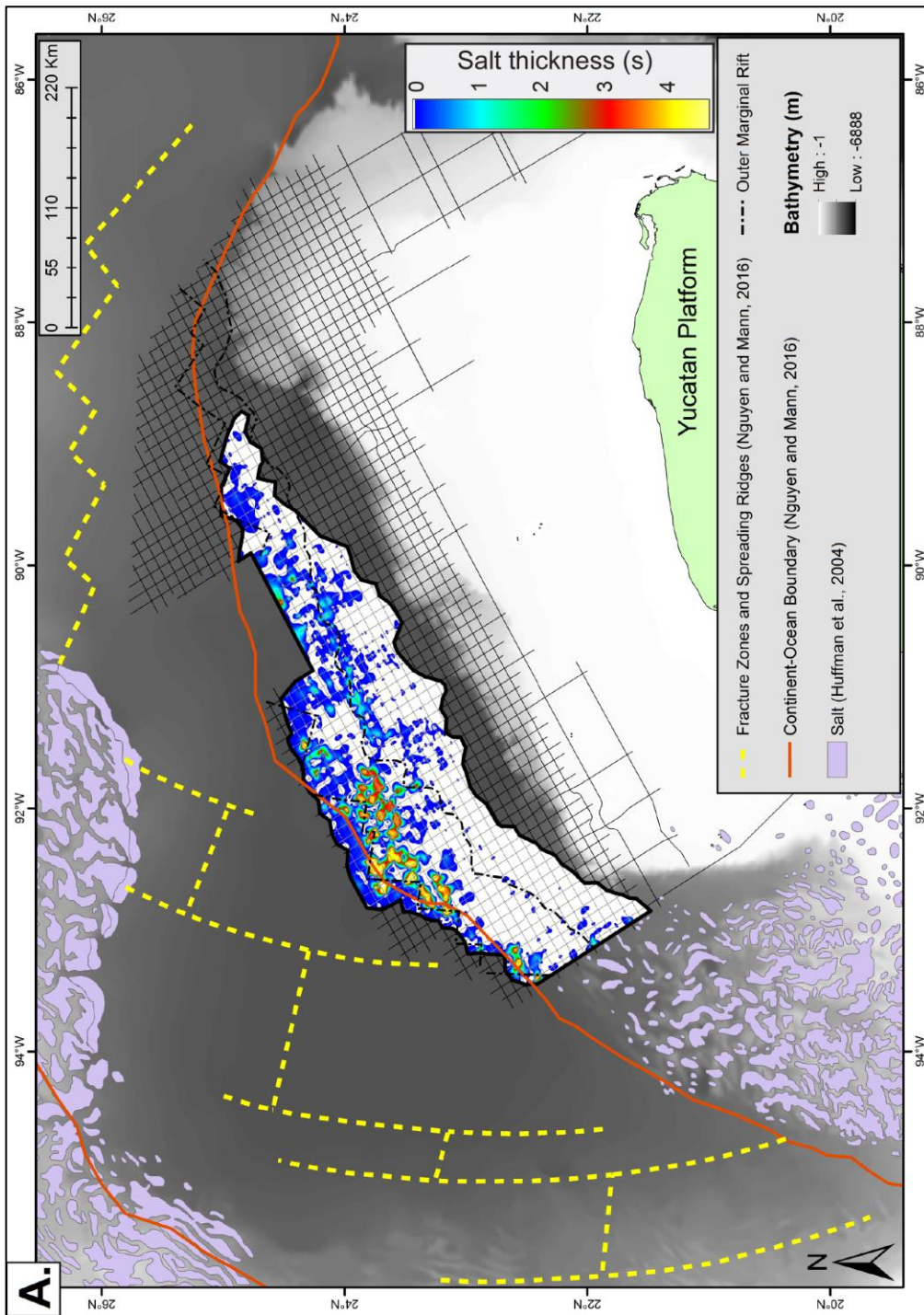


Figure 9. A. Isochron of Louann-equivalent salt along the northern Yucatan margin with the limit of salt outlined in black. The continent-ocean boundary of Nguyen and Mann (2016) is shown in red. Outside of the study area, salt bodies mapped by Huffman et al. (2004) illustrate the overall GOM salt extent.

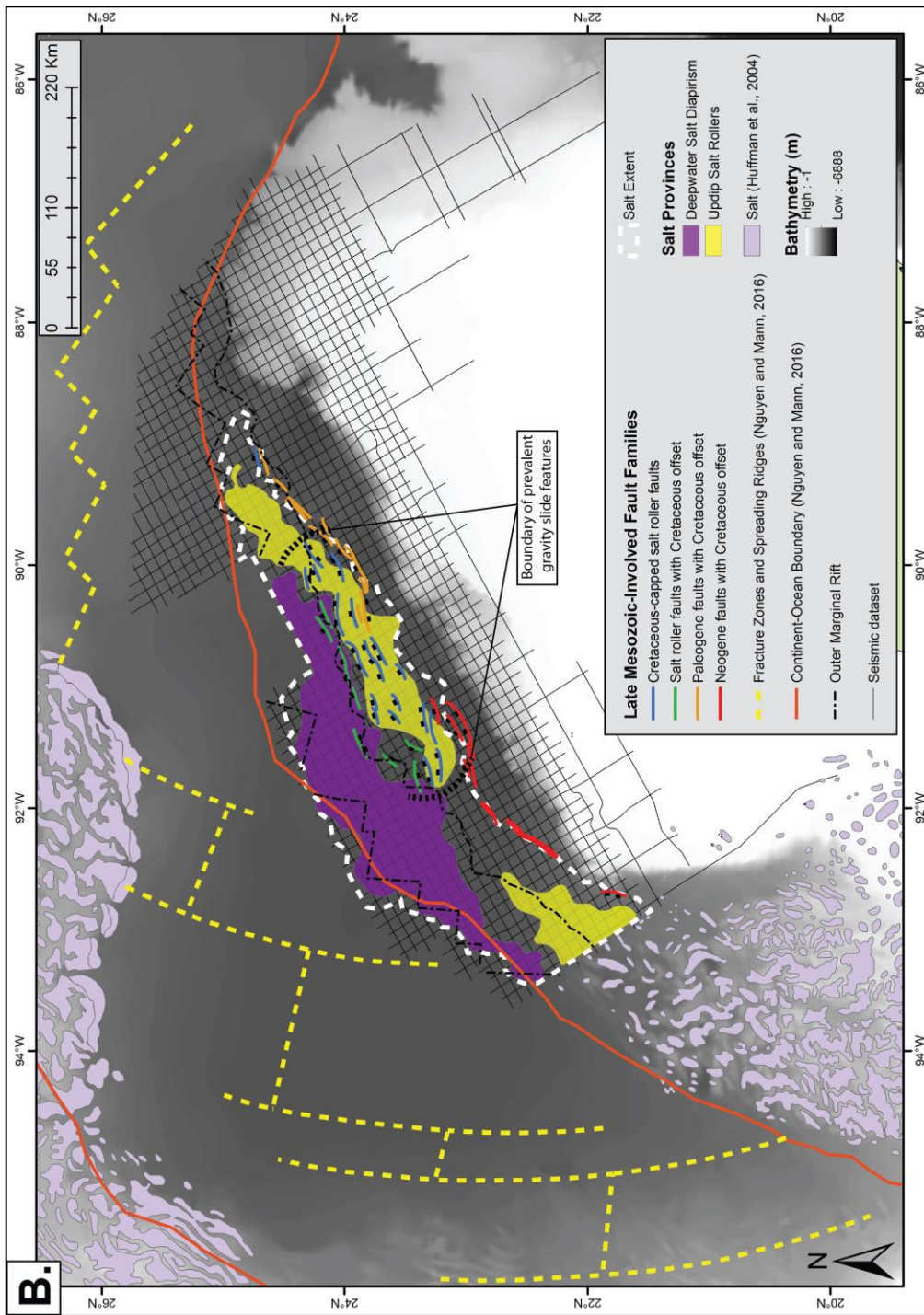


Figure 9 (cont.). B. Three different areas are defined based on the common salt structures present. Four fault families that affect the late Mesozoic stratigraphy are distinguished based on their age.

from typical oceanic crust depths to the outer marginal rift is defined as the continent-ocean boundary (Fig. 10b).

Notably, the boundary between oceanic crust and thinned continental crust is not parallel to the shelf's trajectory. Rather, there are significant landward and basinward jumps in this point between adjacent seismic lines. Mapping these points on dip-oriented seismic lines produces a stair-step pattern in the continent-ocean boundary. This may relate to the geometry of fracture zones and extinct spreading ridges mapped by Nguyen and Mann (2016) (Fig. 10b), similar to the stair-step continent-ocean boundary suggested by Pindell et al. (2016).

This definition of the continent-ocean boundary also illustrates the areas in the southwest where salt has mobilized onto oceanic crust as it translated downdip (Fig. 10b), causing the increased elevation of late Jurassic and Cretaceous strata in the oceanic crustal domain and subsequent onlapping of those units (Fig. 13b). Where the interpreted continent-ocean boundary exits the seismic data coverage in the study area, the vertical gravity gradient of Sandwell et al. (2014) was used to interpolate the continent-ocean boundary between control points (Fig. 10b).

5. STRUCTURAL EVOLUTION OF THE YUCATAN MARGIN

5.1 Cross-section restoration methodology

To better illustrate the large variation in salt deformation history and structural evolution of different regions of the study area, three seismic time sections are restored using Midland Valley Move software at various time intervals since Callovian salt deposition (Figs. 11-13). For each interval, the top horizon is backstripped, the underlying sedimentary layers are decompacted, movement along major faults are restored, and the remaining section is flattened to a generalized paleobathymetry after restorations by previous authors (Hudec and Jackson, 2004; Pilcher et al., 2014). As there are no Mesozoic well penetrations in the study area, the porosities and depth coefficients used in the decompaction for each sedimentary unit were estimated to an

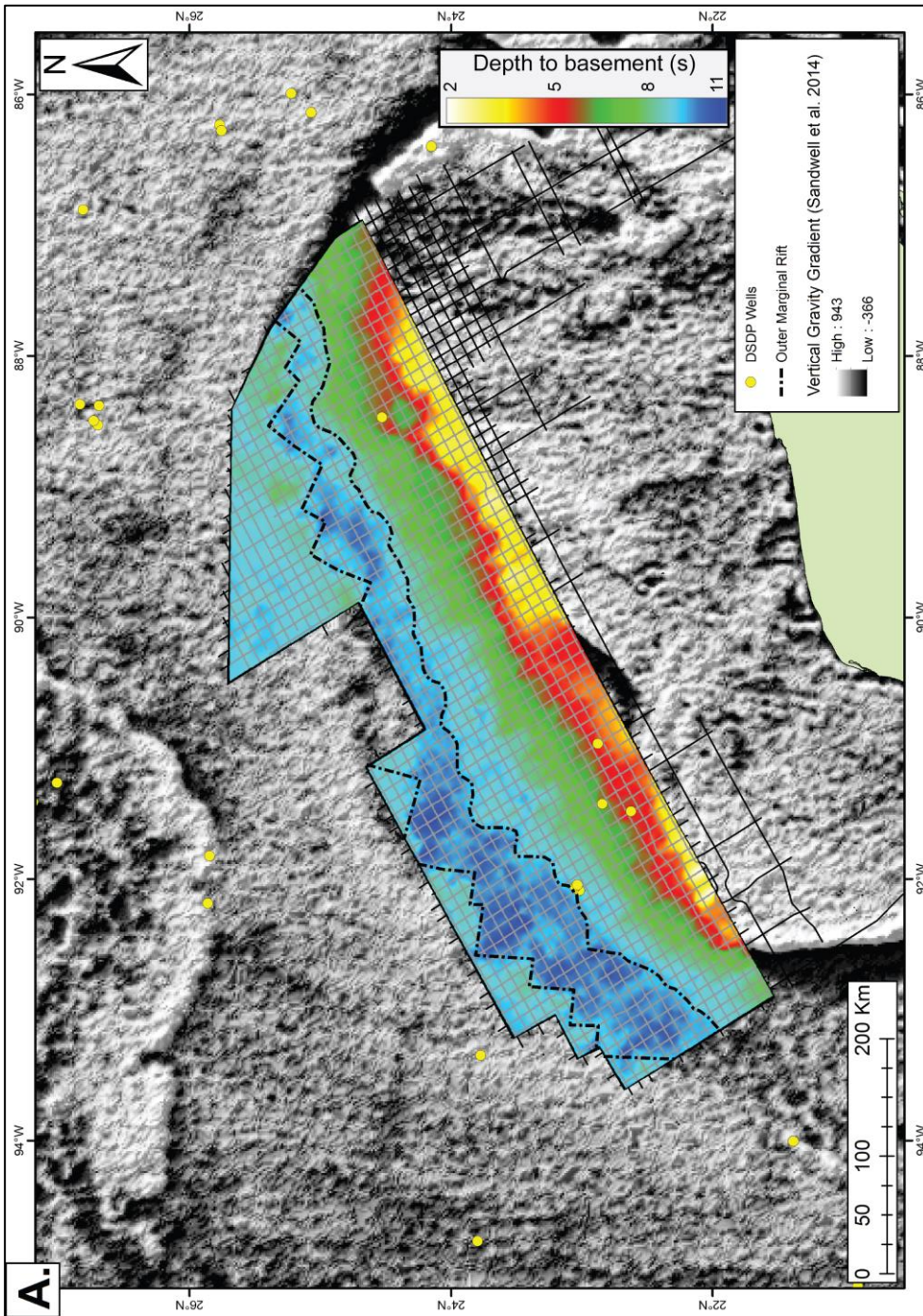


Figure 10. A. Interpreted depth to crystalline basement map for the Yucatan margin. Outlined is the outer marginal rift at the most distal extent of thinned continental crust.

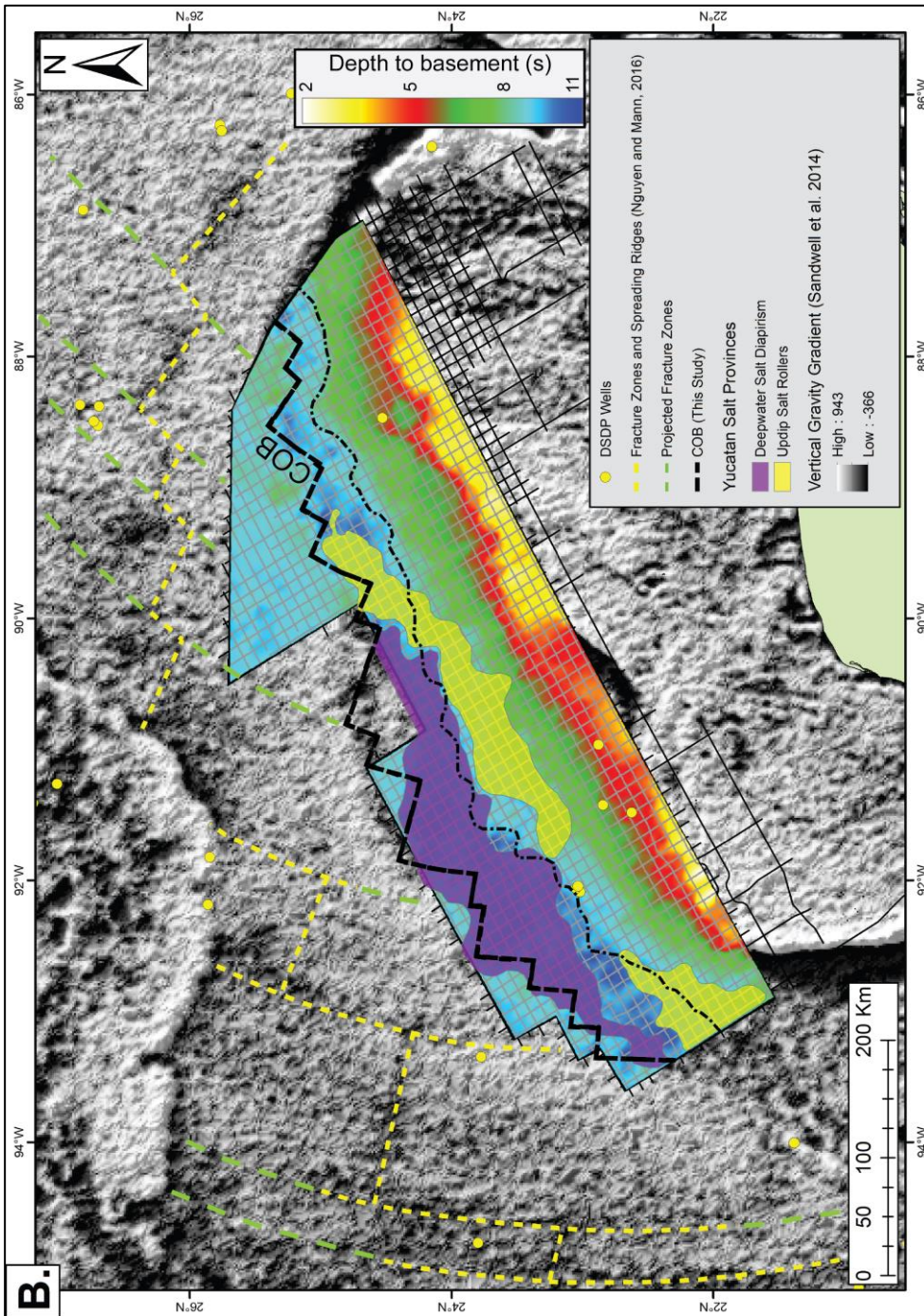


Figure 10 (cont.). B. The outboard boundary of the outer marginal rift is defined as the continent-ocean boundary (black, dashed). The fracture zones and extinct spreading ridges mapped by Nguyen and Mann (2016) are shown in yellow with projected fracture zones shown in green to illustrate the relationship between continent-ocean boundary geometry and fracture zone trajectory.

intermediate value between those expected for carbonate and clastic rocks. Decompactions were performed using the Sclater-Christie compaction curve (Sclater and Christie, 1980) and unfolding utilized a simple shear restoration algorithm after Rowan and Ratliff (2012). Manual restorations were performed to better model mobilized salt, particularly in the southwest where salt deformation is most complex. In these instances, the cross-sectional areas of sedimentary layers were maintained within 1% of the calculated decompacted areas.

5.2 Structural evolution of the northeastern Yucatan area with minimal salt

The northeastern Yucatan margin exhibits minimal salt (Figs. 11b, 11c) and therefore the late Mesozoic section remains relatively undeformed with no gravity slide structures (Figs. 11j, 11k). Cenozoic strata are subhorizontal and progressively onlap the Top Cretaceous surface. Normal faults are common distally in the Oligocene (Fig. 11g) and Miocene (Fig. 11f) intervals but do not deform the Mesozoic section and appear to be thin-skinned normal faults confined to the Cenozoic section. Systematic restorations illustrate the structurally quiescent history of this portion of the study area during the passive margin phase (Figs. 11c-11j) that followed Triassic-Jurassic rifting. This is indicative of the small salt volumes that did not promote gravity sliding as seen to the southwest in the central area.

5.3 Structural evolution of the central Yucatan area with prevalent salt rollers

The central region of the northern Yucatan margin features frequent salt rollers with few diapirs (Figs. 12b, 12c). Similar to the northeastern margin, the Cenozoic strata are subhorizontal and relatively undeformed with the exception being the distal Oligocene (Fig. 12g) and Miocene (Fig. 12f) sections. In this interval, frequent, small-offset normal faults are present, dipping both landward and basinward. These thin-skinned faults often terminate in the Oligocene, rarely reach

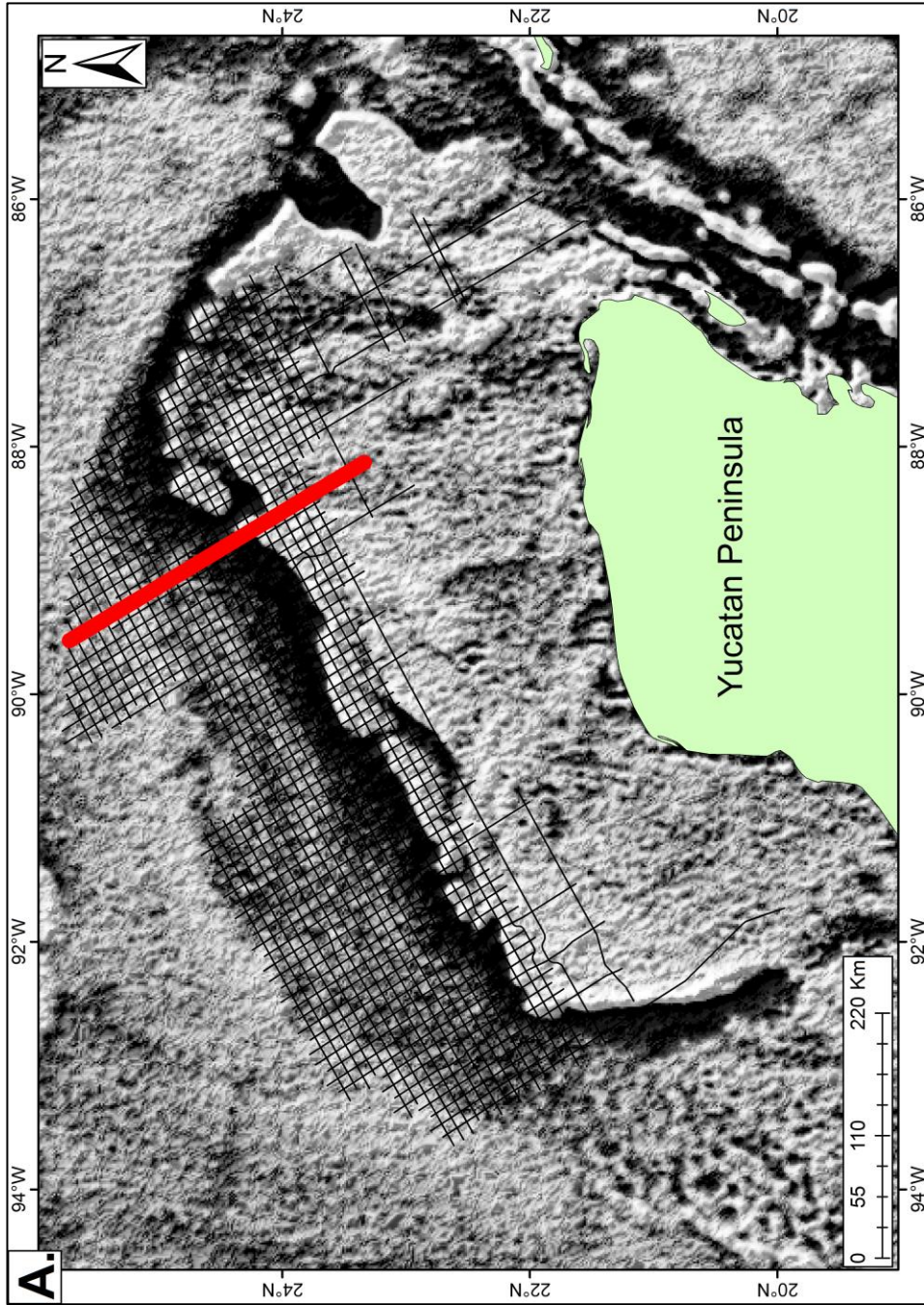


Figure 11. A. Location map of seismic cross-section of the northeastern Yucatan area. C-I. Cenozoic strata are relatively undeformed and subhorizontal, except for small-offset, normal faults in the Miocene (F) and Oligocene (G) intervals. J-K. Small volumes of salt produce little deformation in the Mesozoic. L. The original salt volume overlies the pre-salt section on thinned continental crust prior to seafloor spreading.

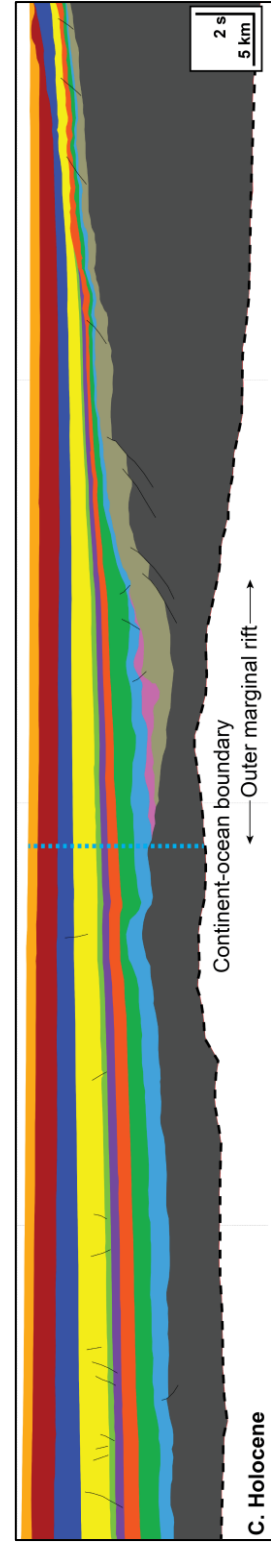
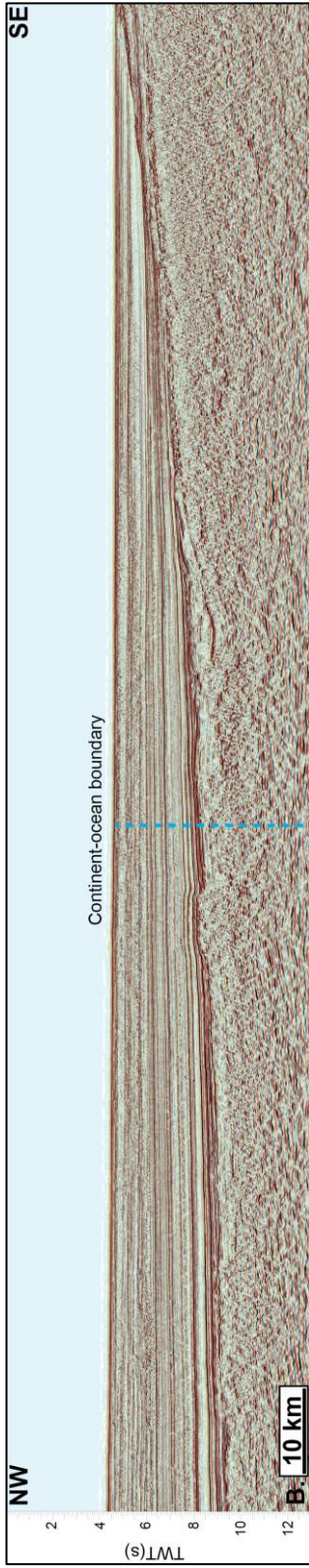
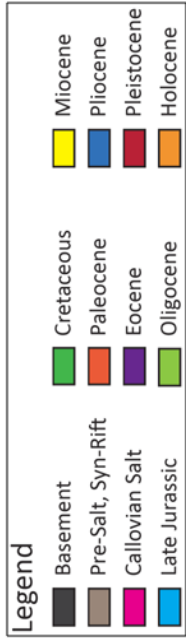


Fig. 11, cont.

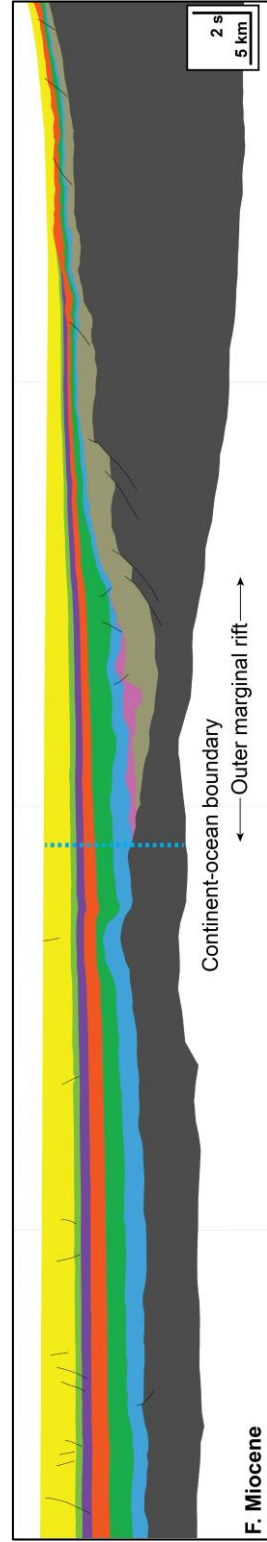
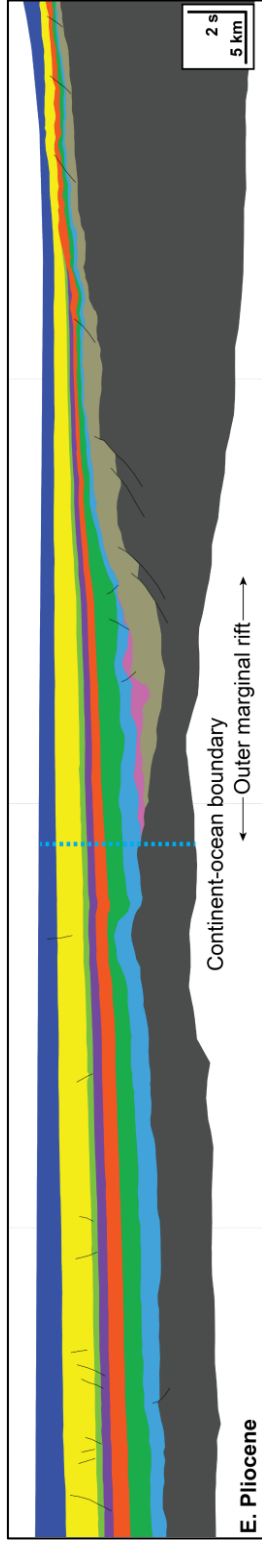
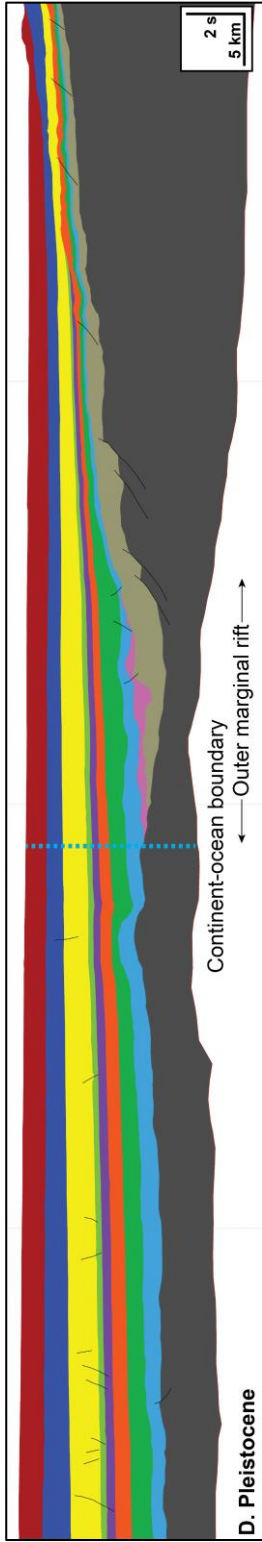


Fig. 11, cont.

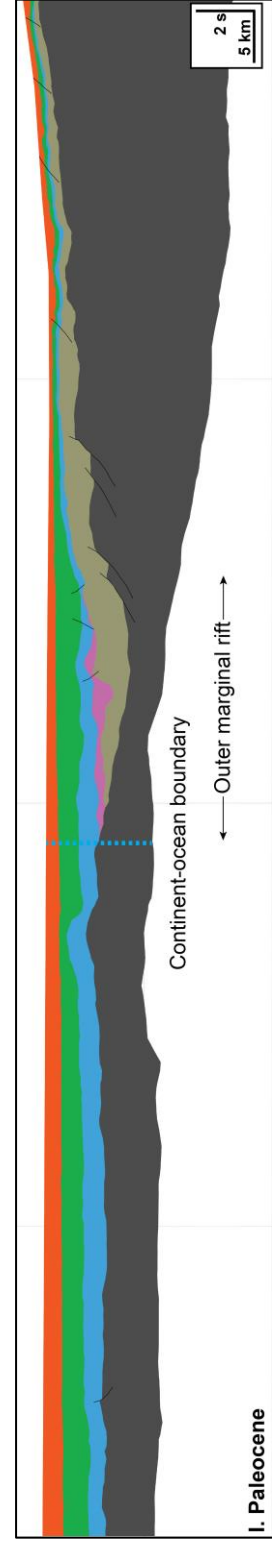
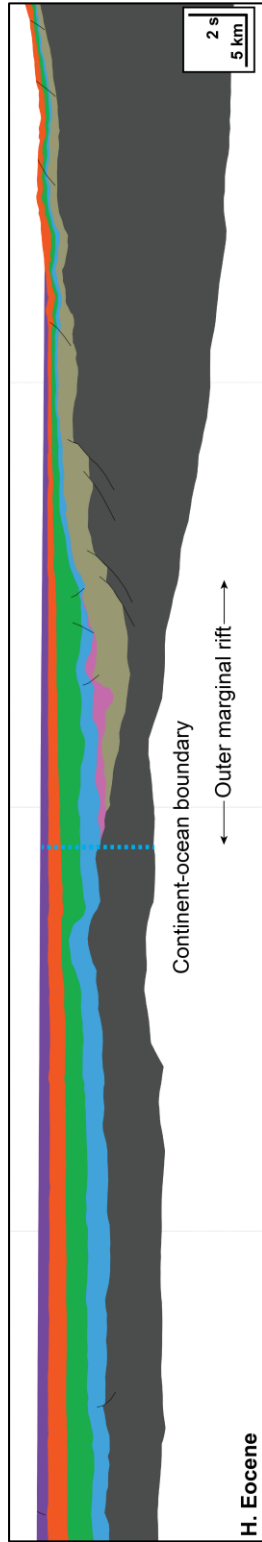
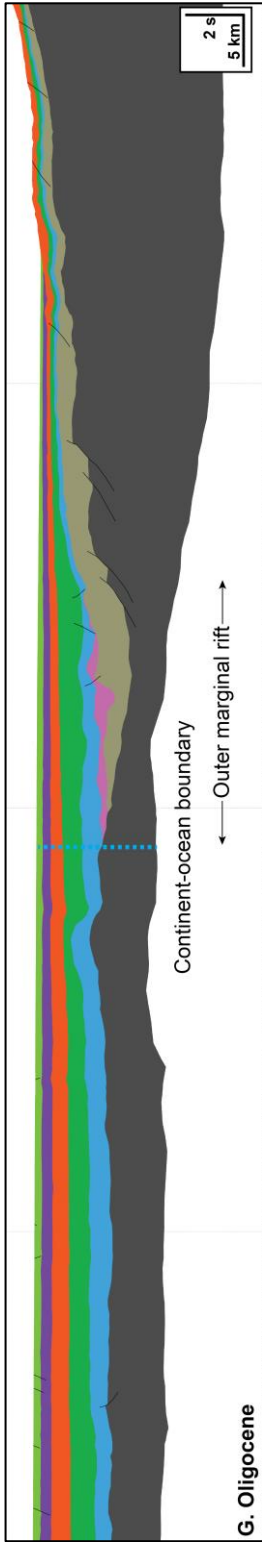


Fig. 11, cont.

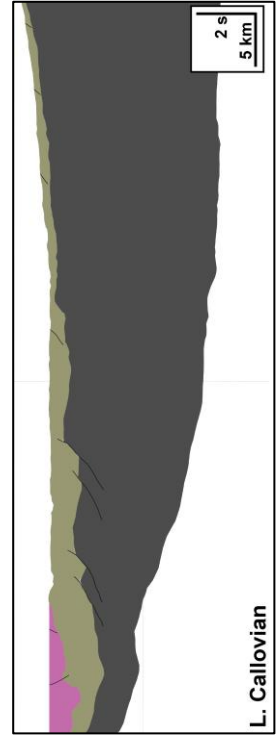
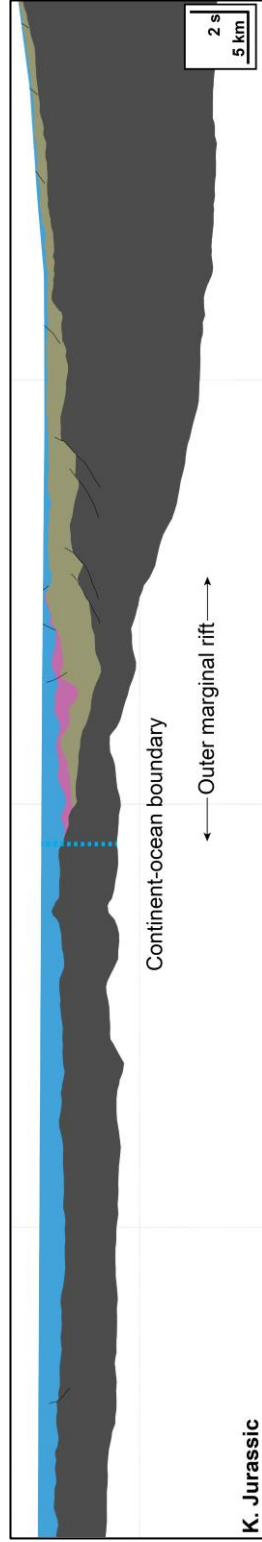
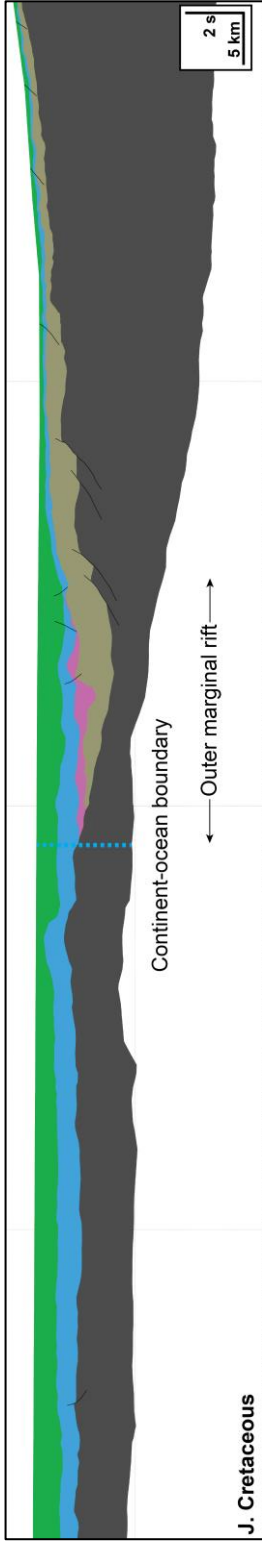


Fig. 11, cont.

the Eocene (Fig. 12h), and do not deform the Mesozoic section. The Cenozoic strata again show progressive onlapping of the Top Cretaceous horizon (Figs. 12c-12i).

Most notable in this central area is the development of salt rollers and associated sedimentary growth wedges (Figs. 12j, 12k). The lack of Cenozoic deformation (Fig. 12c) indicates that gravity sliding and salt migration ceased by the end of the Cretaceous. The substantial wedge geometry in the post-salt Jurassic section (Fig. 12k) and the Cretaceous section (Fig. 12j) suggest that downdip translation and extensional faulting began in the late Jurassic and continued into the Cretaceous, similar in timing to the rafts of the northeastern GOM (Pilcher et al., 2014). During the late Jurassic and early Cretaceous, salt migrated into the outer marginal rift, then extruded onto oceanic crust, and began to form the large diapirs that penetrate the whole section (Figs. 12j, 12k). This resulted in the elevation of the Jurassic and early Cretaceous strata and subsequent onlapping by the late Cretaceous to Paleocene interval which thins as it drapes the structure (Fig. 12i).

The small diapir distal from the salt rollers (Fig. 12c) shows that this transect is nearing the southwestern area of thicker salt accumulations that promote salt diapirism (Fig. 9b). The elevation change of the Top Cretaceous horizon suggests that the diapir was still growing during the Cenozoic (Fig. 12c). The Paleocene (Fig. 12i) and Eocene (Fig. 12h) sections thin as they drape the structure and show little elevation change over the diapir. This, along with the lack of thickness or elevation change in the Oligocene section (Fig. 12g), indicate that this small amount of diapiric growth ended in the Eocene, unlike the larger diapirs to the southwest (Fig. 13).

5.4 Structural evolution of the southwestern Yucatan area with widespread diapirism

The southwestern area of the northern Yucatan margin features few salt rollers but numerous large diapirs along the distal margin in the outer marginal rift (Figs. 10b, 13b, 13c).

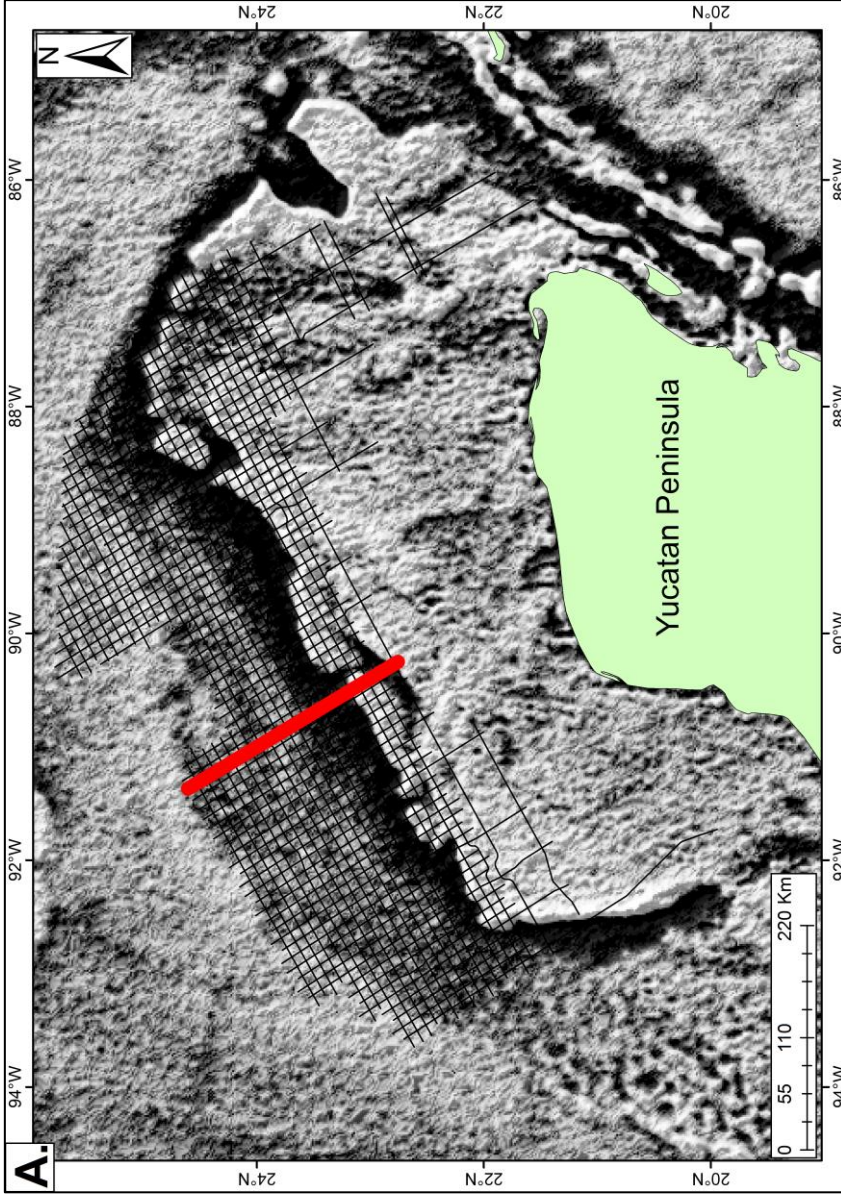


Figure 12. A. Location map of seismic cross-section of the central Yucatan area. **C-I.** Similar to the northeastern area, the Cenozoic strata are subhorizontal and show little deformation aside from small-offset, normal faults that are here more common in the Miocene (F) and Oligocene (G) sections. These units gradually onlap the Top Cretaceous surface. **J.** Normal faults rooted in the salt detachment are common and produce significant sedimentary wedges that thicken toward the fault. This indicates that much of the movement along these faults occurred during the Cretaceous. **K.** Less substantial sedimentary wedging is apparent in the Jurassic section indicating active normal faulting, salt migration, and the formation of salt rollers has begun. **L.** The original salt volume overlies the pre-salt section on thinned continental crust prior to seafloor spreading.

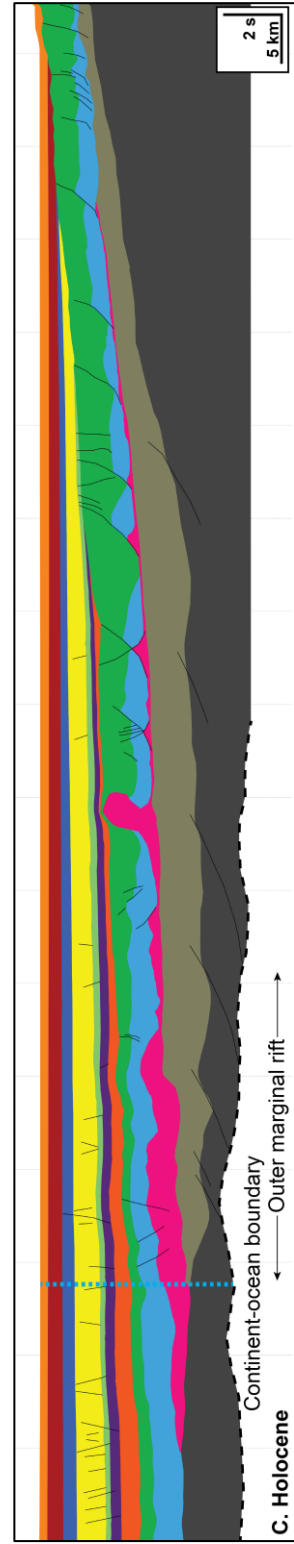
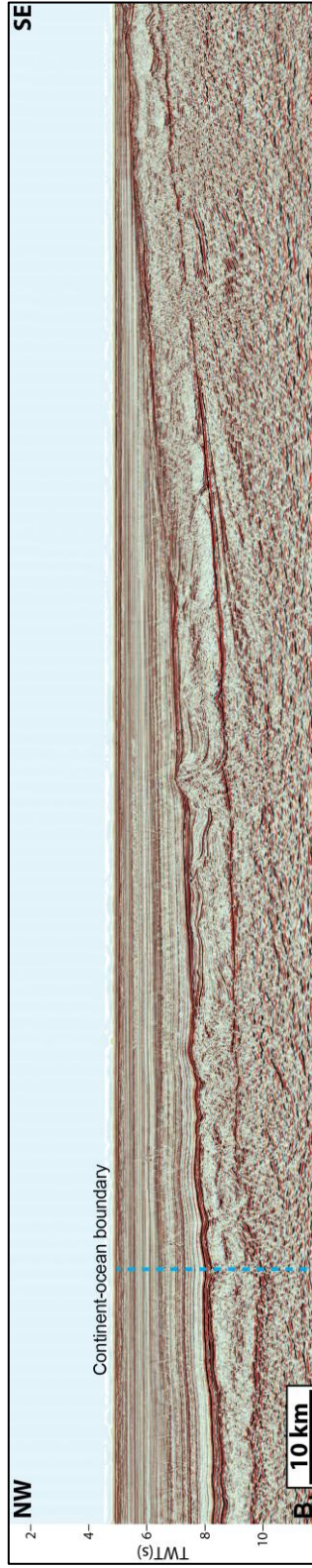
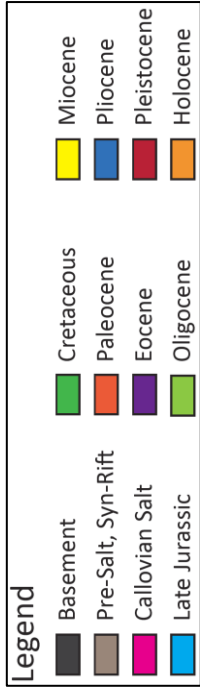


Fig. 12, cont.

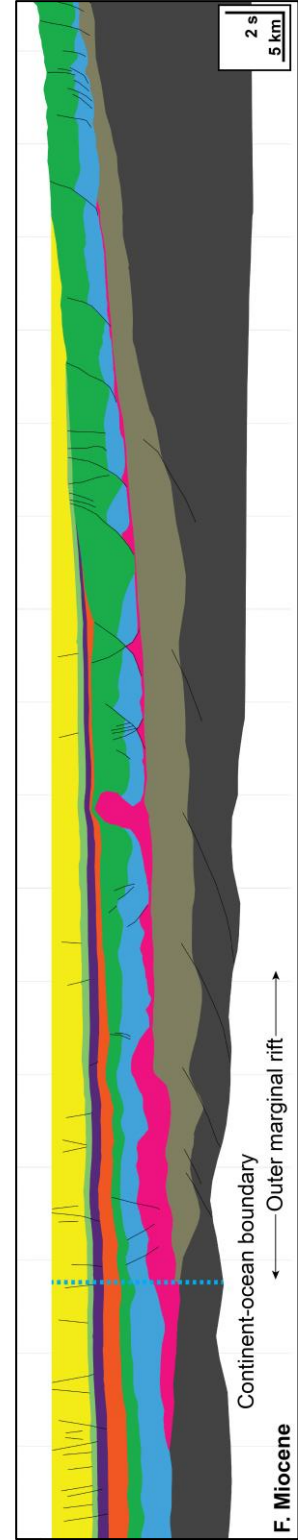
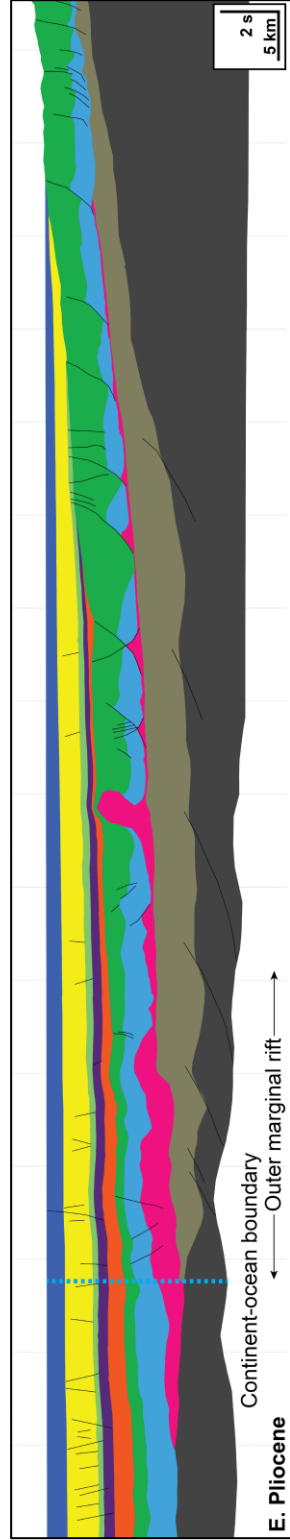
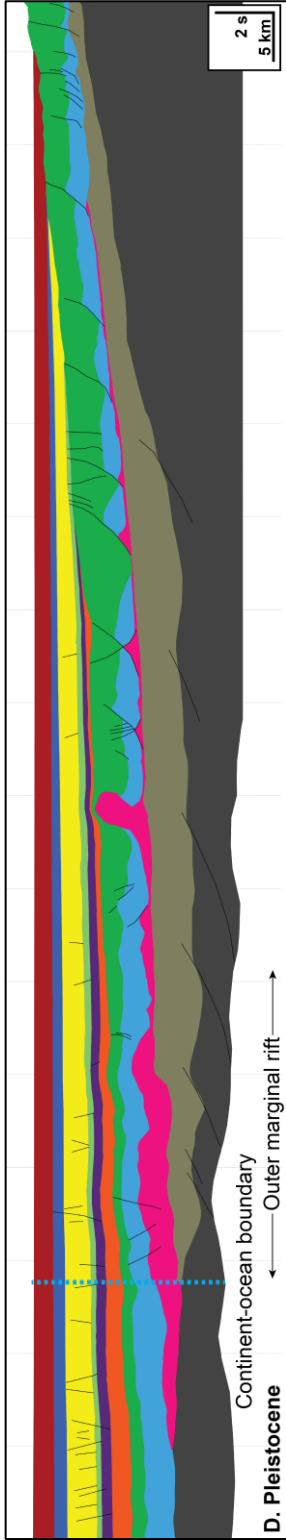


Fig. 12, cont.

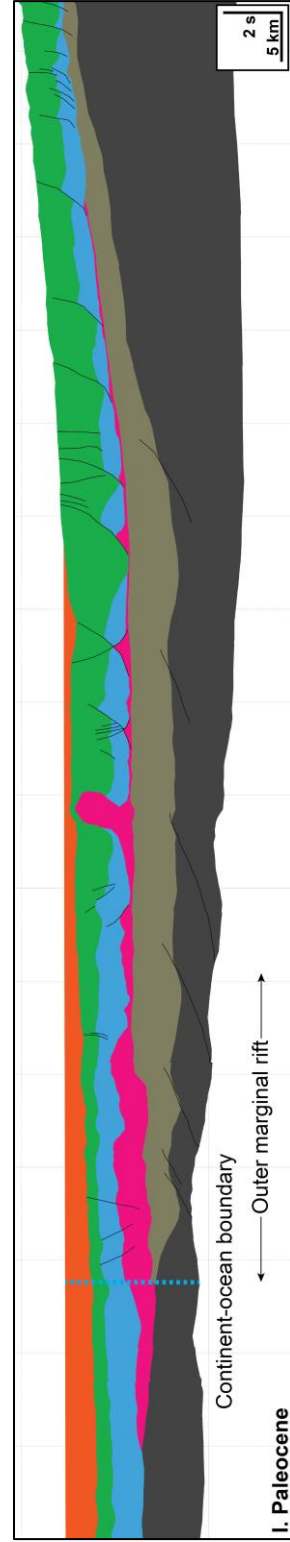
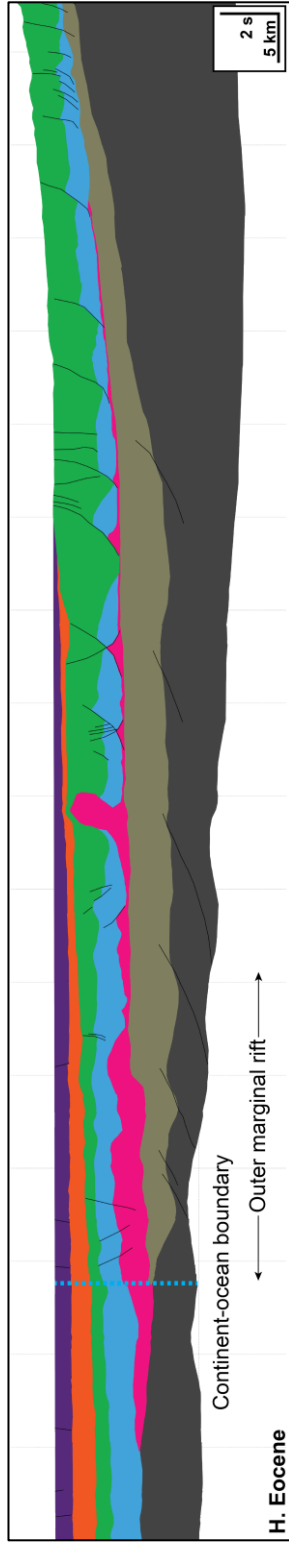
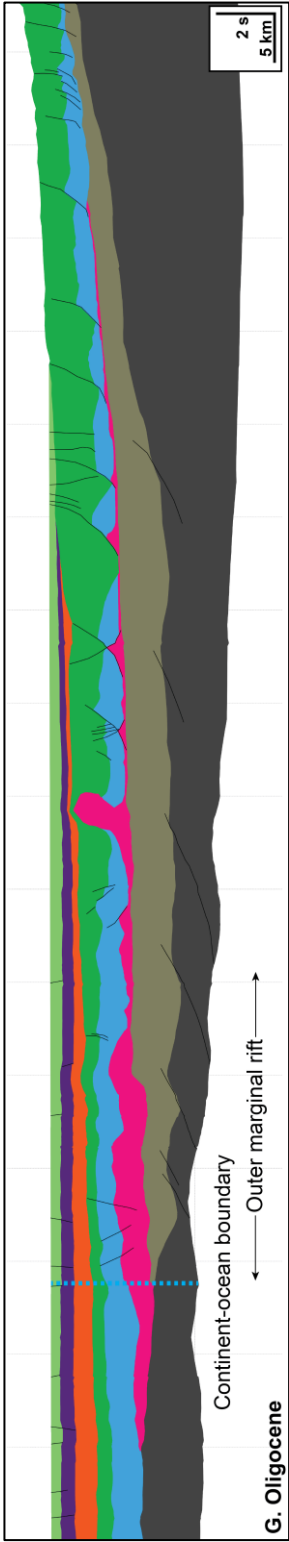


Fig. 12, cont.

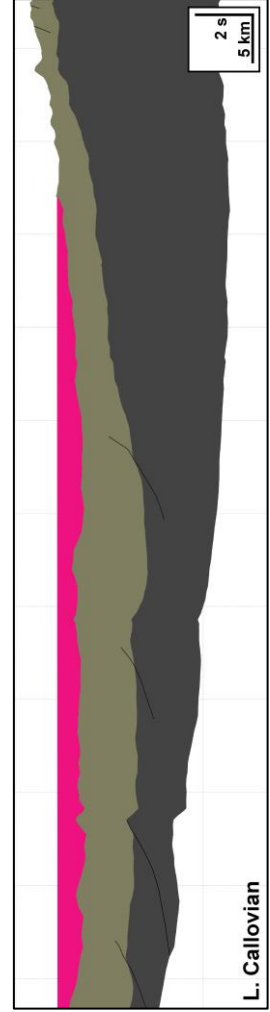
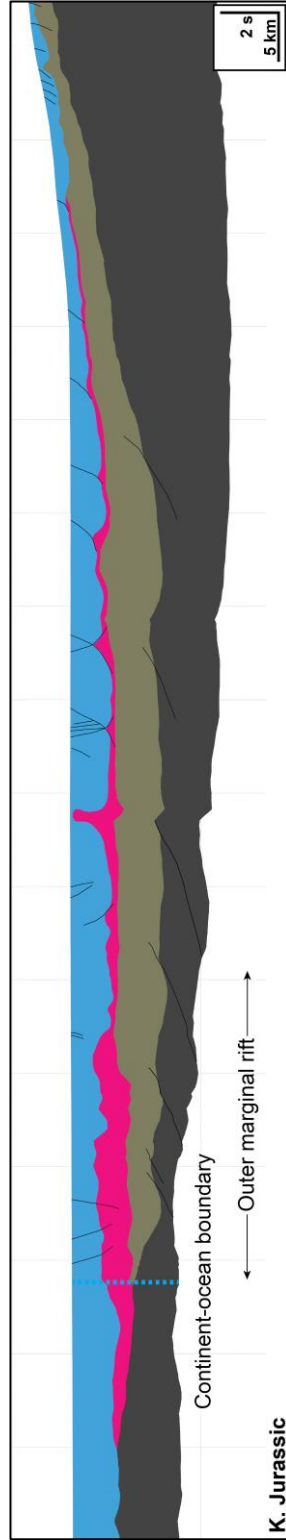
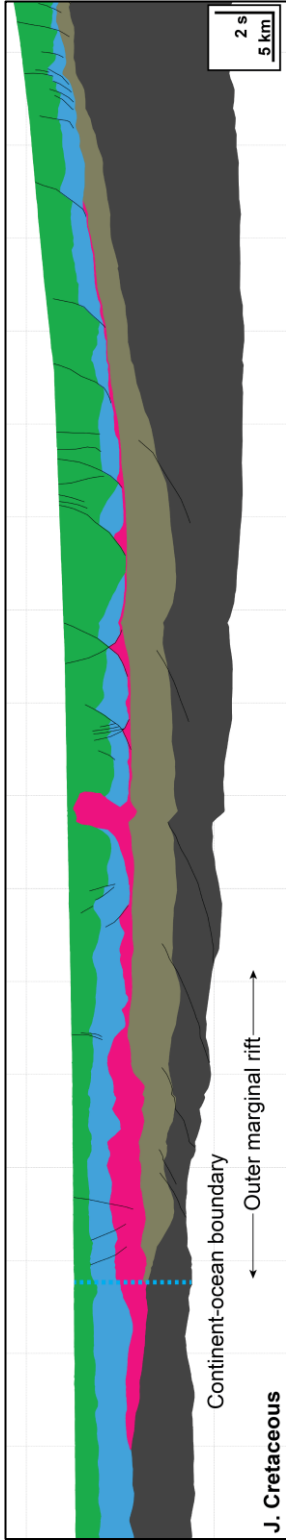


Fig. 12, cont.

In contrast to the two prior sections (Figs. 11, 12), the diapirs here are large enough to deform strata as young as the Holocene (Fig. 13c) as the vertically mobilized salt affects local bathymetry. More proximally, the most recent sedimentary units are also affected by the large full graben that causes offset down to the Mesozoic section and is still active, evidenced by fault scarps present on the seafloor (Fig. 13b).

Minimal diapiric motion is evident in the Pliocene (Fig. 13e) and Pleistocene sections (Fig. 13d). The Miocene section (Fig. 13f), however, exhibits large thickness variations that allow an inferred Miocene age for significant salt withdrawal northwest of the two large diapirs, within the mini-basin between the diapirs, and southeast of the diapirs where the elevation of the salt detachment decreases into the outer marginal rift.

Systematic backstripping reveals a notable difference in the history of salt withdrawal beside these diapirs. While the changes in thickness across every Cenozoic and Mesozoic interval document progressive salt evacuation southeast of the diapirs (Figs. 13c-13k), this is not the case northwest of the diapirs. The thickness of the Miocene section (Fig. 13f) is far greater just outboard of the diapirs than it is distally in the oceanic crustal domain.

Below this interval, however, the older units do not thicken near the diapirs and instead only thin as they onlap the growing structure (Figs. 13g-13j). This indicates that significant salt withdrawal only occurred during the Miocene northwest of the diapirs, despite the continuous salt withdrawal in more proximal locations. Salt evacuation during diapiric growth is also recorded by the Eocene to Miocene (Figs. 13f-13h) normal faulting, both inboard and outboard of the diapirs. Although these faults are also present lower in the section, the majority occur during the Miocene (Fig. 13f) when thickness changes suggest that salt withdrawal was most active, creating hinge zones where Miocene and younger strata rotated downward.

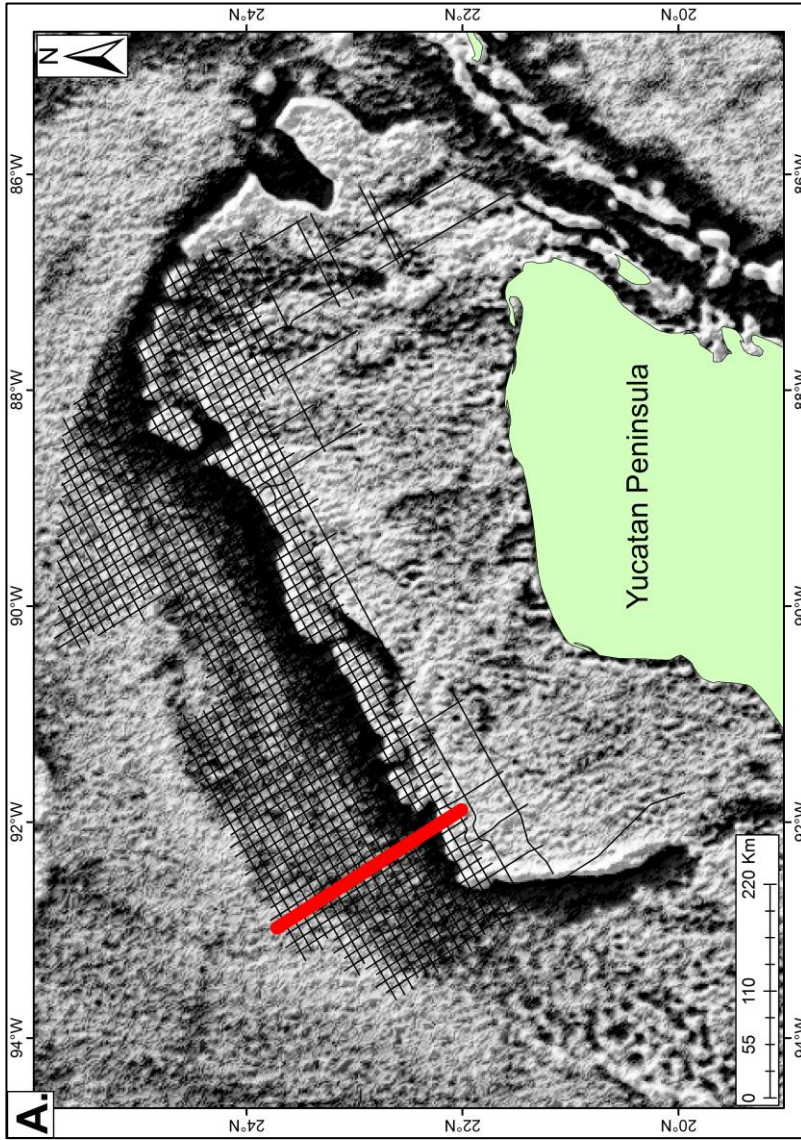


Figure 13. **A.** Location map of seismic cross-section. **B.** Dip-oriented seismic cross-section of the southwestern Yucatan area. **C-E.** Recent and Plio-Pleistocene strata thin as they drape the growing diapirs outboard and show significant offset in the full graben inboard. **F-G.** Large thickness variation is evident on either side of the two diapirs where salt has been evacuated. Adjacent normal faults result from the downturning of strata toward the diapirs. **H-I.** Little faulting is evident but thickening between and inboard from the diapirs suggests salt evacuation and diapiric growth is continuing. **J.** The two diapirs begin their vertical migration and few normal faults penetrate the Cretaceous as salt rollers are uncommon. **K.** Few normal faults deform the Jurassic as most of the updip salt migrates into the outer marginal rift. Salt extrudes onto the oceanic crust causing a thin Jurassic section which is subsequently overlapped by the Cretaceous section. **L.** The original salt volume overlies the pre-salt section on thinned continental crust prior to seafloor spreading.

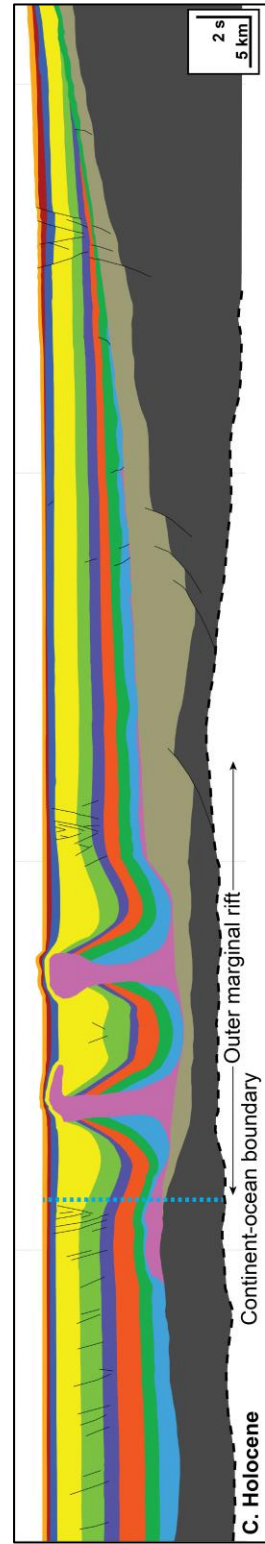
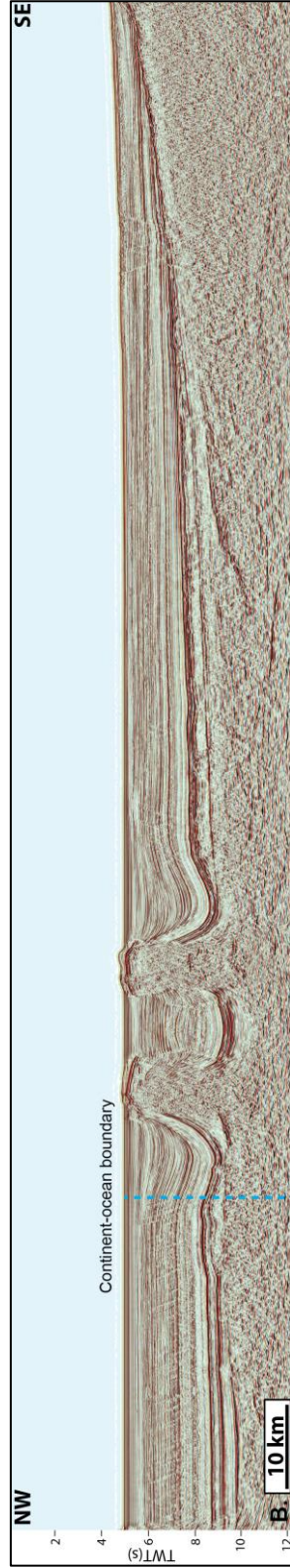
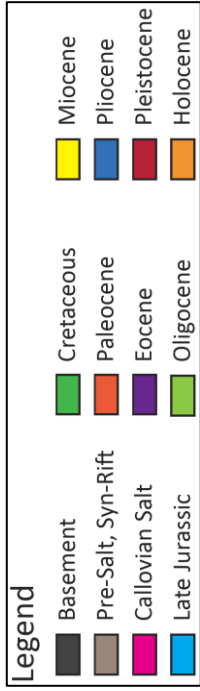


Fig. 13, cont.

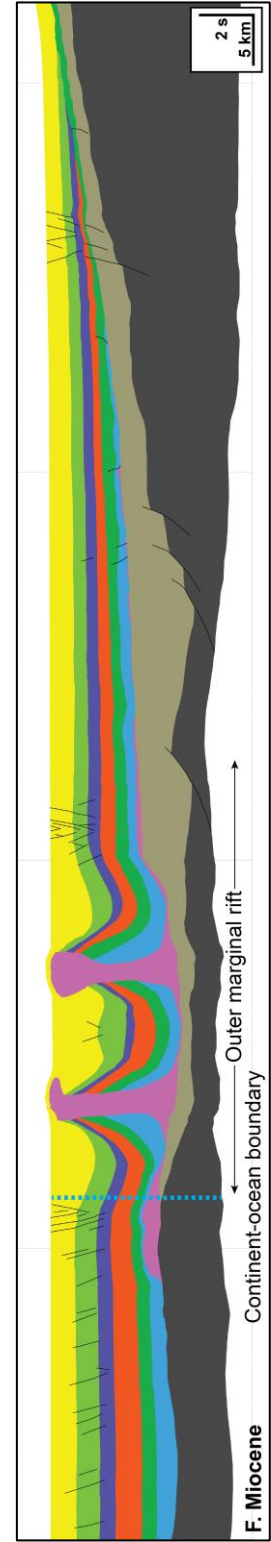
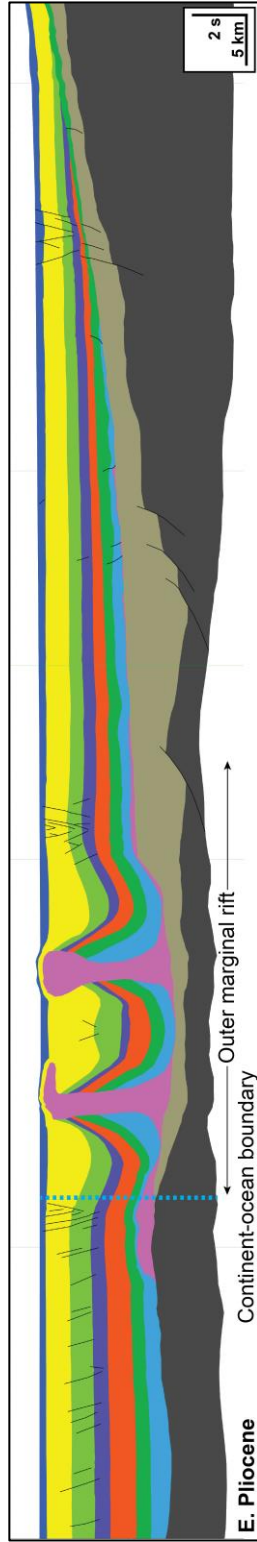
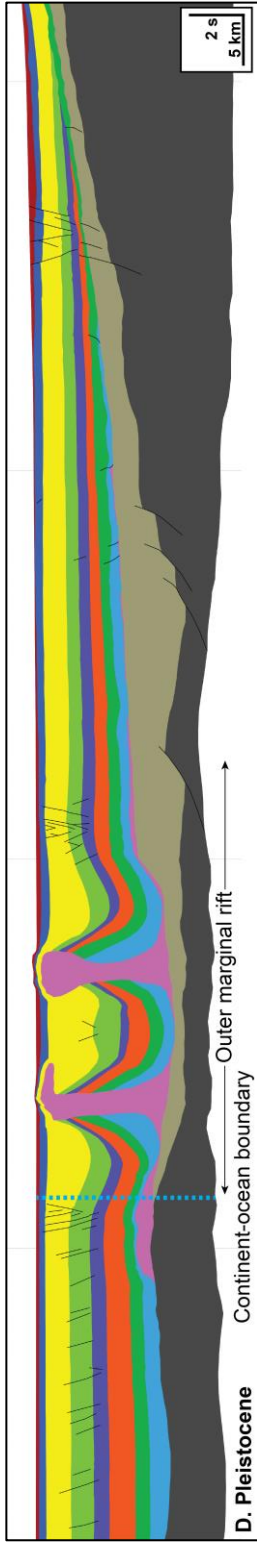


Fig. 13, cont.

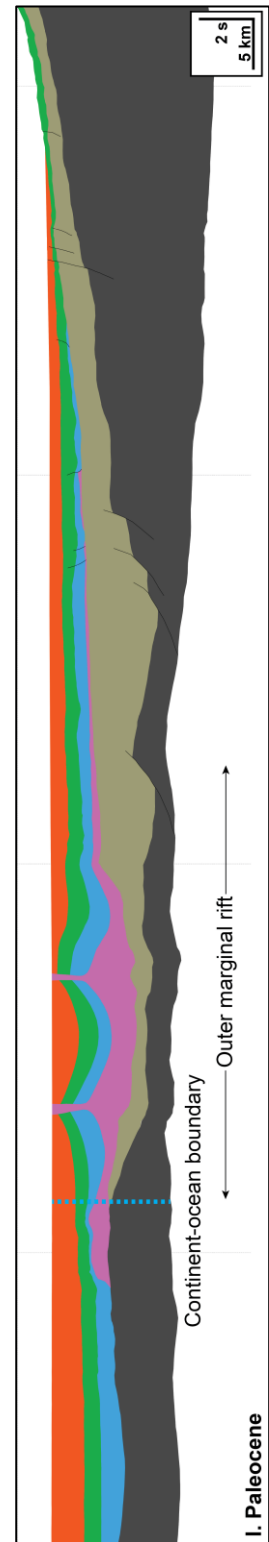
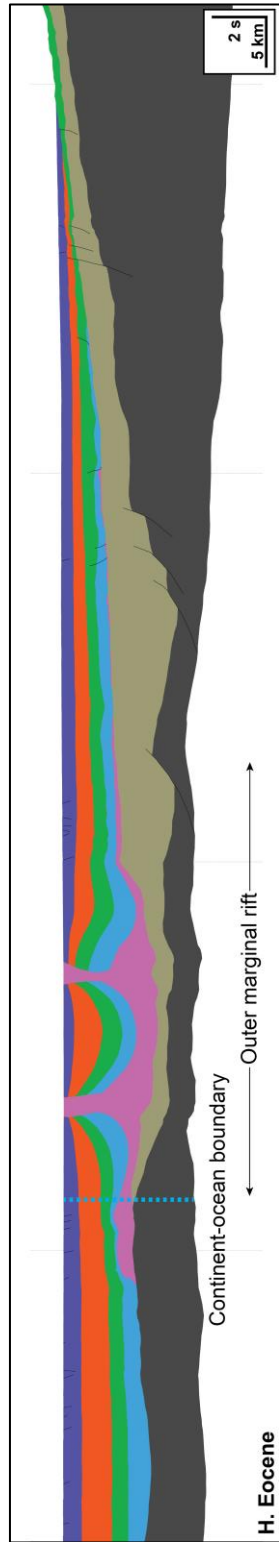
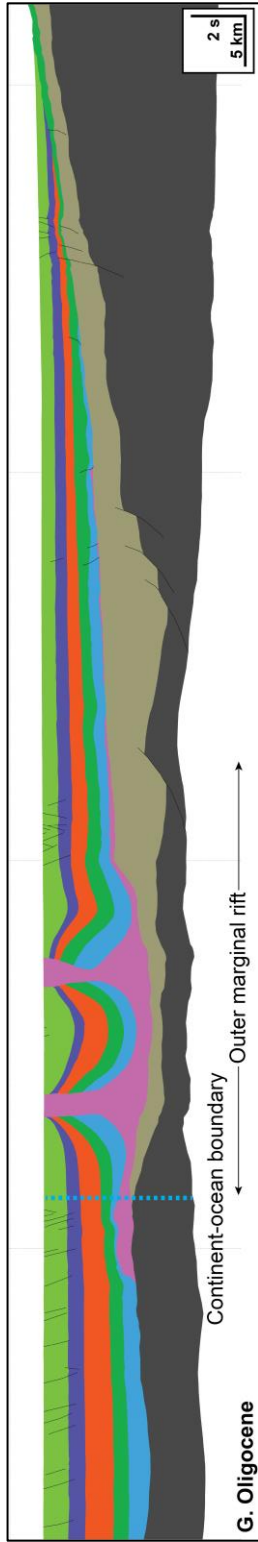


Fig. 13, cont.

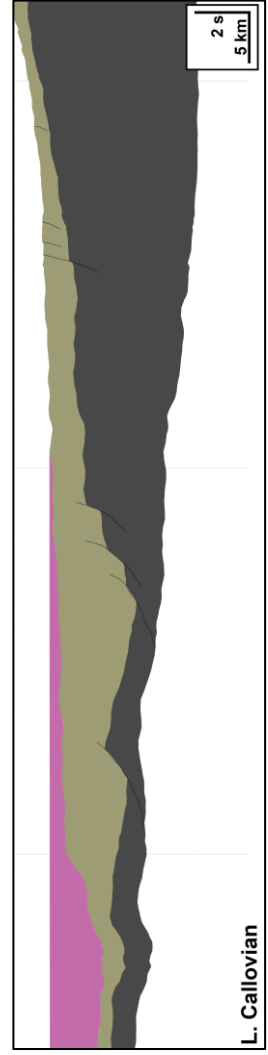
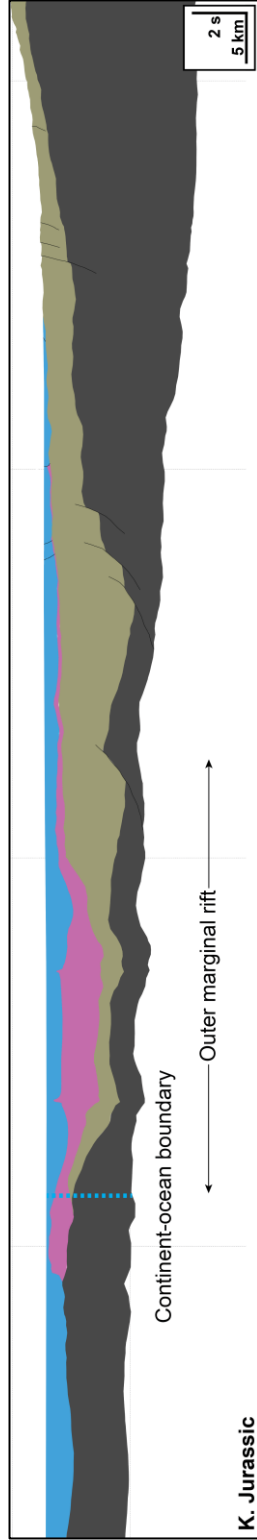
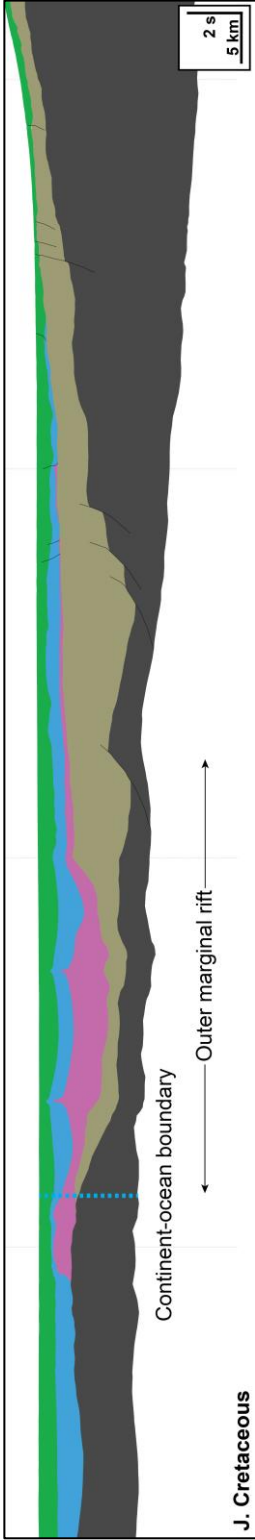


Fig. 13, cont.

6. DISCUSSION

6.1 Timing of salt-assisted gravity sliding on the Yucatan margin and implications for Gulf of Mexico basin evolution

The Callovian salt deposited in the extensive GOM sag basin (Fig. 9a) is assumed by many previous authors to have been deposited with minimal topographic relief at its top (Fig. 14a) (Marton et al., 2000; Hudec and Jackson, 2004; Pilcher et al., 2014; Piedade and Alves, 2017). Above the salt, late Jurassic, terrigenous sediments that include the Norphlet- and Smackover-equivalent units were deposited in thicknesses up to 1400 m (Rosenfeld, 2003) (Fig. 14b).

The slight wedge geometry within these post-salt, late Jurassic, terrigenous units suggest gravity sliding and vertical salt migration was only just beginning by the end of the Jurassic (Fig. 14c). The early (Fig. 14c) and late Cretaceous (Fig. 14d) sections, however, exhibit substantial thickness increases toward the updip, normal fault indicating the majority of downslope movement on the salt detachment occurred during the Cretaceous and likely accompanied progressive deepening of the oceanic area of the central GOM. Above the Cretaceous, Cenozoic strata are generally undeformed (Figs. 7c, 8c), suggesting salt roller development was completed by this time (Fig. 14e).

These stratal thickness changes and the presence of coherent reflectors throughout the Cretaceous period (as opposed to the chaotic seismic facies of mass transport complexes found along steeper slopes) suggest a gradual, downdip translation and concentration of GOM salt into distinct salt bodies on both the northern GOM and Yucatan conjugate margins throughout a period of ~95 Ma from the late Jurassic to the end of the Cretaceous (Figs. 14c, 14d). After late Mesozoic gravity sliding was complete on the underlying salt detachment on both the northern Yucatan (Fig. 3b) and northeastern GOM margins (Fig. 3a), slow subsidence of the GOM basin produced the progressive onlap pattern evident above the late Mesozoic interval of salt

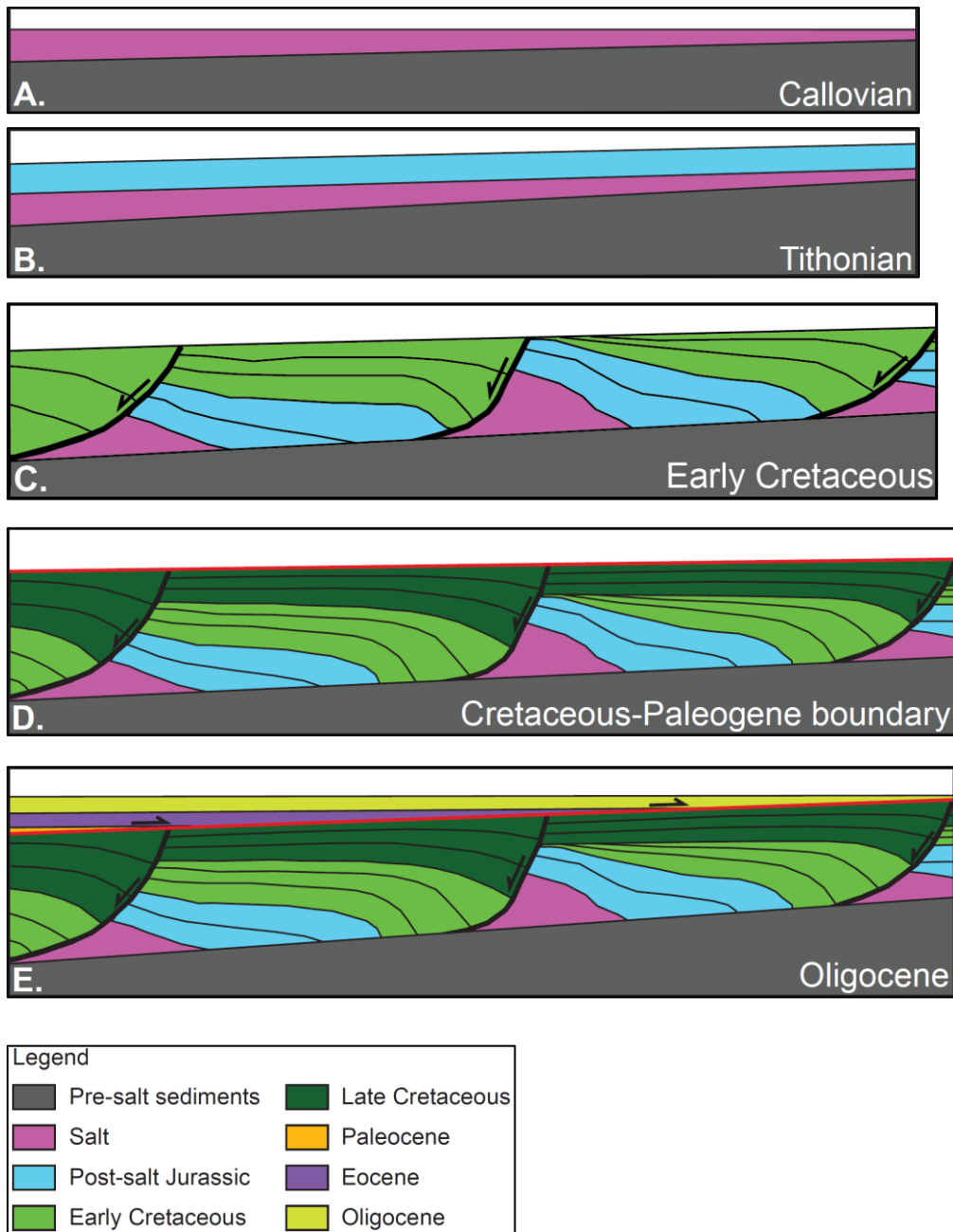


Figure 14. Schematic restorations depicting the development of salt rollers, extensional faulting, and sedimentary growth wedges in the late Jurassic to Cretaceous section and the progressive onlapping of Cenozoic stratigraphy onto the Top Cretaceous surface. Modified from Pilcher et al. (2014) and Piedade and Alves (2017).

deformation (Fig. 14) and large, subsidence-related, Quaternary, normal faults observed in the southern portion of the study area (Figs. 9b, 13).

Contrasting models for GOM subsidence from the origin of the basin in the Triassic and early Jurassic to the present-day include Cassidy and Burke's (2012) subaerial basin below sea level ("SABSEL") model and Pindell et al.'s (2014) outer marginal collapse model. The SABSEL model predicts a large, sedimentary basin existing well below sea level, analogous to the present-day Afar Depression (Beyene and Abdelsalam, 2005). This setting would promote salt deposition in a restricted, sag basin environment prior to geologically-rapid infilling of seawater sufficient to promote carbonate deposition overlying the older, terrigenous strata whose dune morphology was preserved.

In contrast, the outer marginal collapse model requires a dramatic drop in the distal margin at the completion of continental rifting that abruptly decreases the elevation of the basin margins at a rate close to ten times that observed for modern, subsiding basins (Pindell et al., 2014). Pindell et al. (2014) argued it was outer marginal collapse that initiated salt-assisted gravity sliding throughout the GOM soon after the Triassic-Jurassic rift phase of GOM opening. However, slow and gradual salt roller development during the late Jurassic and Cretaceous (Fig. 14c, 14d), continuous mappable reflectors overlying the Callovian salt (Fig. 7c), and the systematic Cenozoic onlapping pattern (Fig. 14e) all suggest gradual, thermal subsidence of the Yucatan margin during the late Jurassic-earliest Cretaceous drift phase of GOM opening and subsequent middle Cretaceous-Cenozoic passive margin phase, rather than a geologically-rapid collapse of the margin. By the early Cretaceous, basin subsidence and sediment loading would have been sufficient to initiate the basinward gravity sliding and salt deformation observed on the Florida and Yucatan conjugate margins (Pilcher et al., 2014).

The gradual nature of GOM subsidence is further supported by the burial histories of different wells around the GOM (Fig. 15a). In order to compare four US GOM wells that penetrate the Oxfordian to the Yucatan study area, a pseudo-well was created in the deep-water along the central seismic section exhibiting many salt rollers (Fig. 15a). To convert the seismic horizons to depth, the velocities from the GUMBO 3 seismic refraction data on the northeastern GOM conjugate margin (Eddy et al., 2014) were projected onto the Yucatan seismic line. The resulting subsidence history of the central, deep-water Yucatan margin correlates well with the burial histories of the US GOM wells (Figs. 15b-15f).

The Titan, Norton, Cheyenne, and Vicksburg wells exhibit very gradual sedimentation from late Jurassic continental break-up until the end of the Albian in the middle Cretaceous (Figs. 15b-15e). Following this, all four wells enter a period of minimal burial from the middle Cretaceous until the middle Miocene. Beginning in the late Miocene, sedimentation increases dramatically in all wells except for Norton (Fig. 15c).

The anomalously high, late Jurassic sedimentation in the Yucatan pseudo-well (Fig. 15f) could easily be attributed to the seismic interpretation of the Top Jurassic at this point, which is not well constrained (see section 3). The biostratigraphic data of the other wells allow for much greater precision in the Mesozoic section. The late Miocene sedimentation increase (Figs. 15b-15f) is a result of the onset of Mississippi fan sedimentation at this time (Weimer et al., 2017). Norton is not affected during this most recent interval as much as other wells due to its westerly location away from the main Mississippi fan depocenter (Fig. 15c). The construction of tectonic subsidence curves for each well removes this effect of sedimentation and gives a clearer image of basin dynamics since the late Jurassic. All tectonic subsidence curves point toward a slow and gradual history of GOM subsidence since the completion of rifting near Callovian time (Figs. 15b-15f). From the immediately post-rift period (late Jurassic) to the pre-Mississippi fan, passive

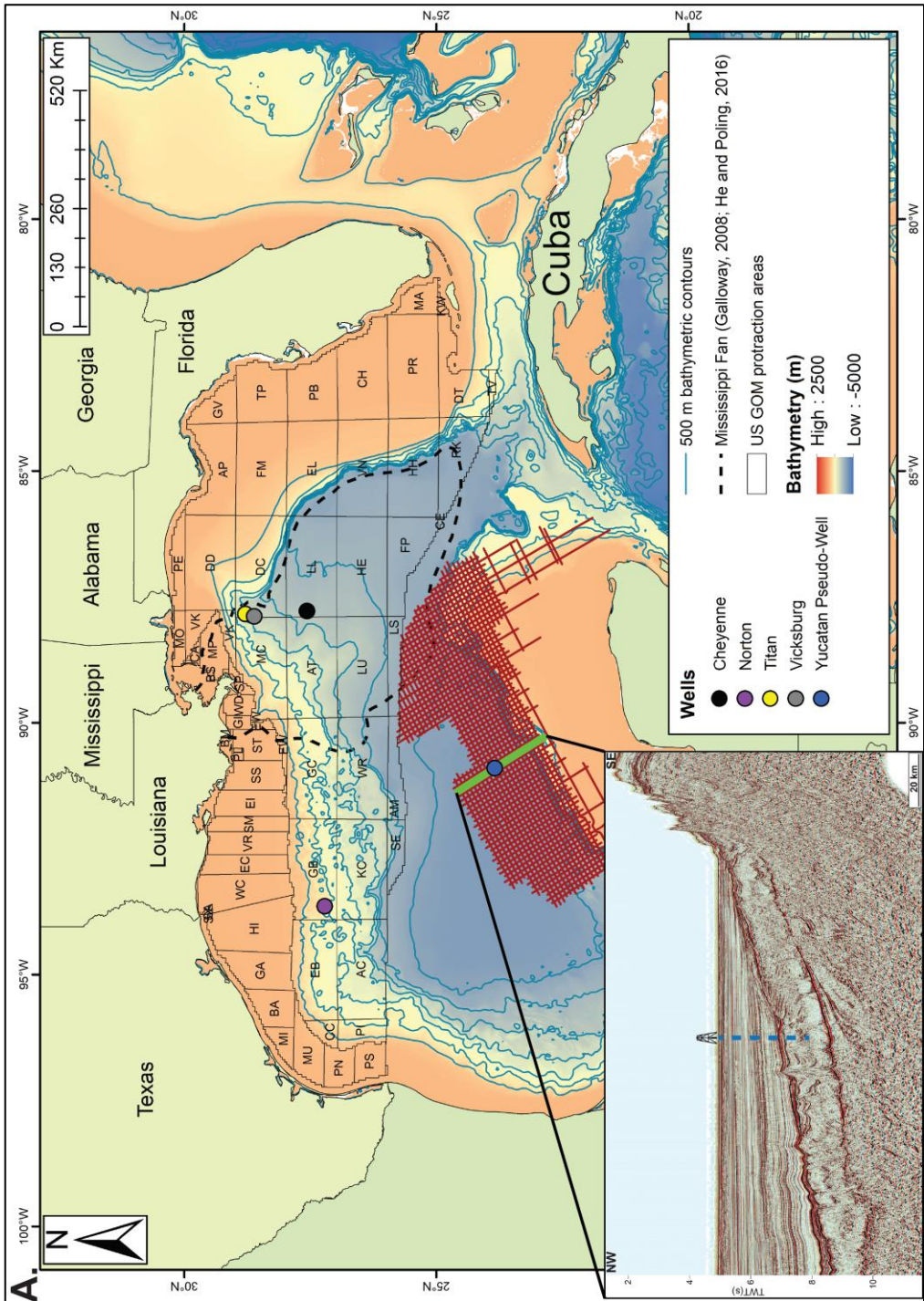


Figure 15. A. Location map of wells in subsidence analysis. Outline of Mississippi fan is shown in black, which heavily influences the total subsidence plots after the mid-Miocene. Location of the pseudo-well on the central Yucatan seismic cross-section is shown in blue in the inset.

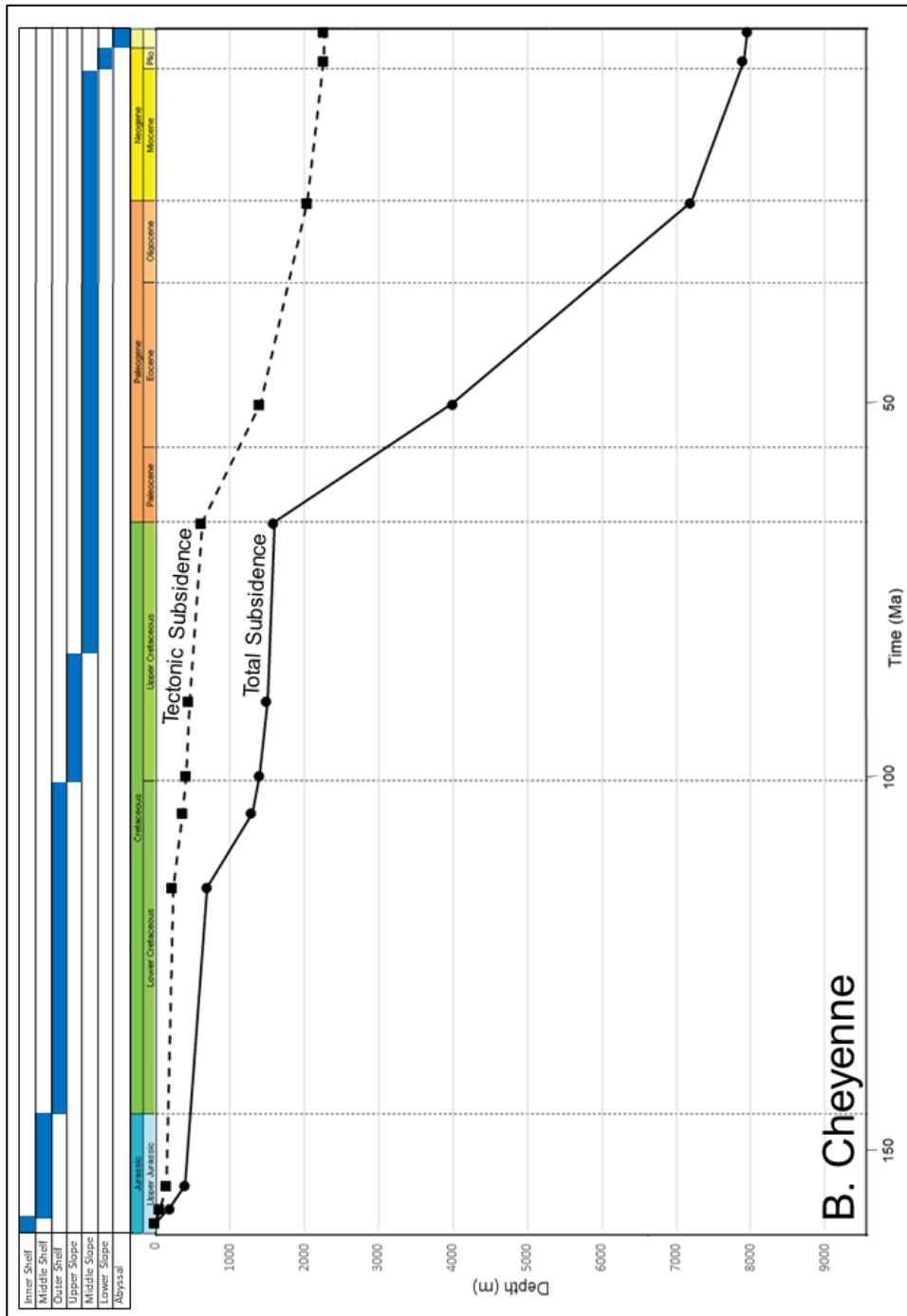


Figure 15 (cont.). B. Plot of tectonic and total subsidence for the Cheyenne well in the US GOM after Ismael (2014). Mississippi fan sedimentation is not as clear as other wells as Ismael (2014) notes that total subsidence increases dramatically in the Paleocene, earlier than the other wells. Estimated paleobathymetry is shown in blue above the subsidence plot.

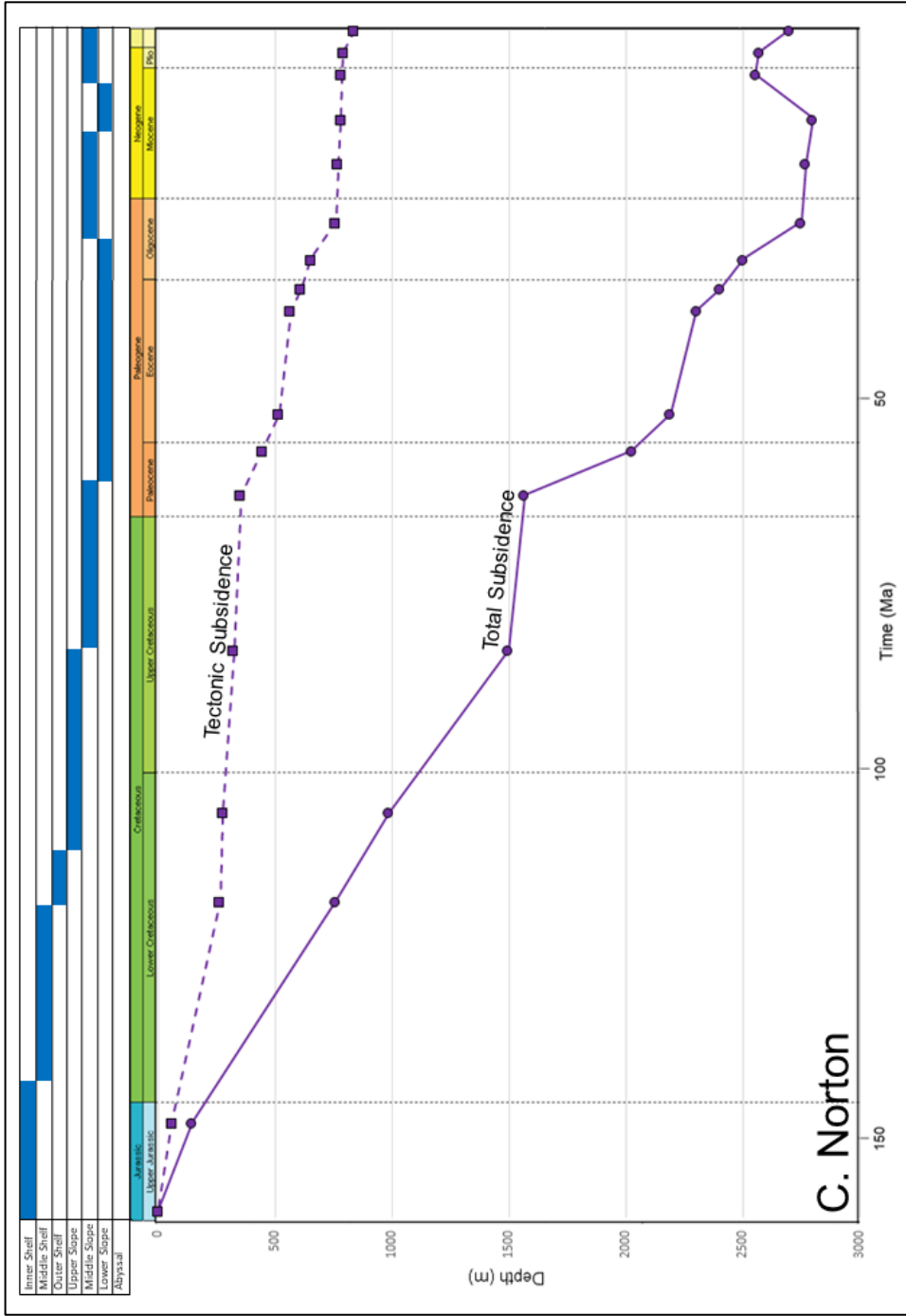


Figure 15 (cont.). C. Plot of tectonic and total subsidence for the Norton well in the US GOM. The effects of Mississippi fan sedimentation are not as evident as the other wells because of its western location away from the primary depocenter. The tectonic subsidence curve illustrates the slow, gradual subsidence of the basin beginning in the late Mesozoic. Estimated paleobathymetry is shown in blue above the subsidence plot.

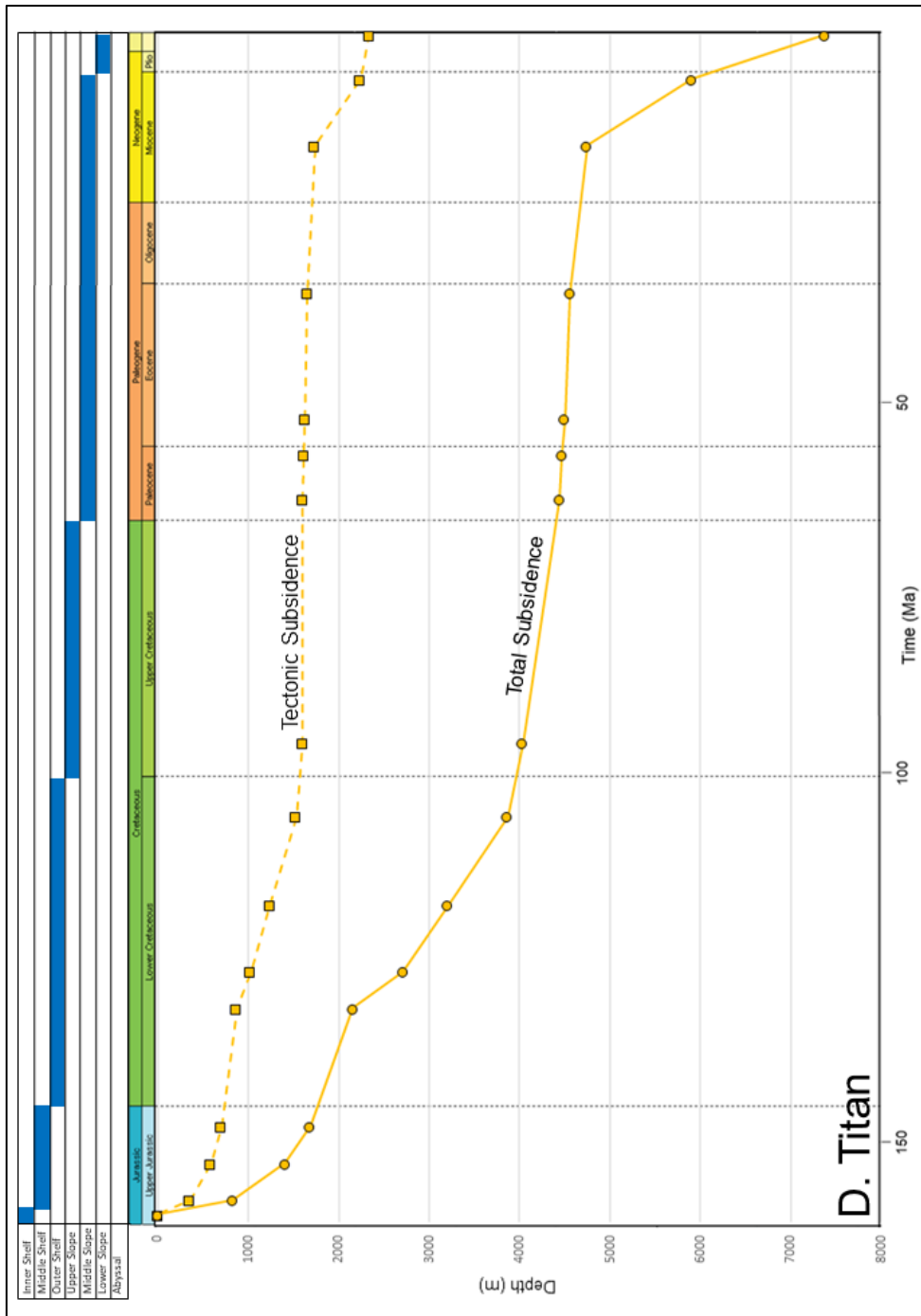


Figure 15 (cont.). D. Plot of tectonic and total subsidence for the Titan well in the US GOM. Mississippi fan sedimentation affects the total subsidence curve greatly beginning in the Miocene. The tectonic subsidence curve, however, removes the effects of sedimentation to reveal a slow, gradual history of basin subsidence. Estimated paleobathymetry is shown in blue above the subsidence plot.

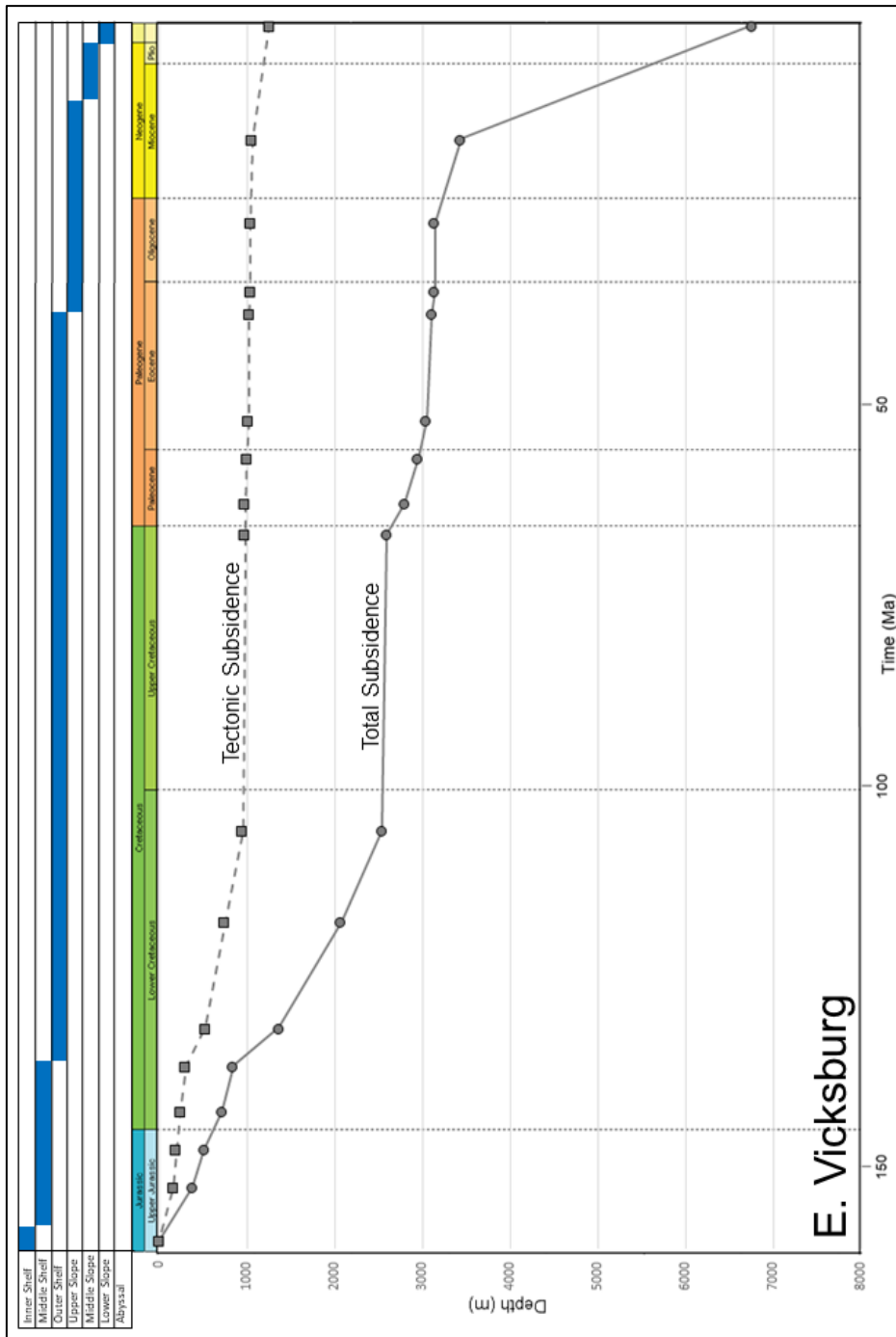


Figure 15 (cont.). E. Plot of tectonic and total subsidence for the Vicksburg well in the US GOM. Similar to Titan, Mississippi fan sedimentation produces large effects on the total subsidence curve from the Miocene to present, but the tectonic subsidence curve again shows the slow, gradual history of basin subsidence. Estimated paleobathymetry is shown in blue above the subsidence plot.

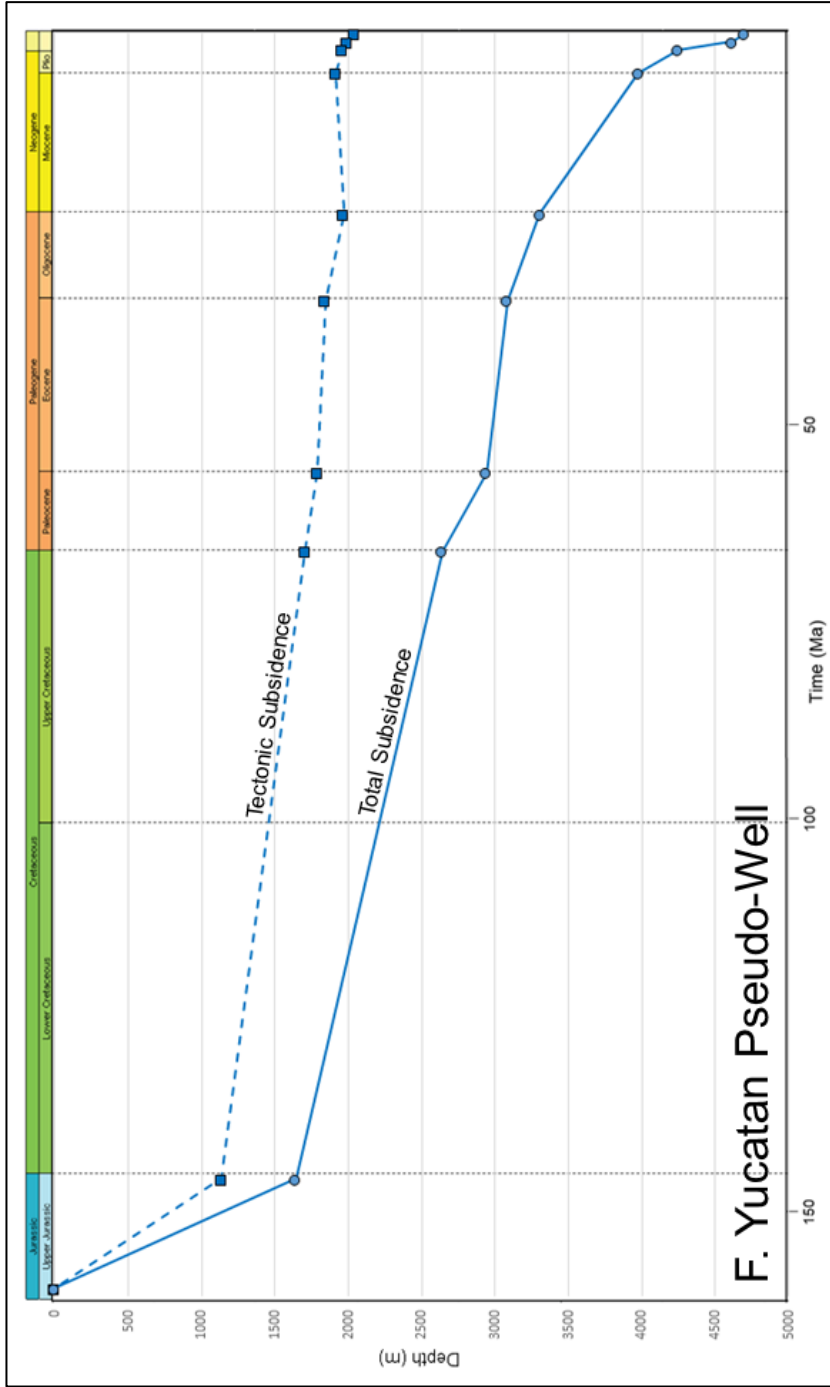


Figure 15 (cont.). F. Tectonic and total subsidence curves for a pseudo-well along a Yucatan seismic cross-section. Despite fewer data points due to no biostratigraphic data, the same trend of slow, gradual subsidence is evident.

margin phase (Cretaceous to middle-Miocene), there is no dramatic change in sedimentation and burial on the total subsidence curves as one might expect had the GOM undergone a geologically-instantaneous increase in basin accommodation due to rapid outer marginal collapse.

6.2 Controls on post-salt sedimentation and structural evolution

Approximately an 11,600 km² area in the central study area beyond the Yucatan shelf edge is identified in which Norphlet-equivalent is commonly observed, although not as a continuous surface on my grid of seismic data with its 10-km-wide, line spacing (Figs. 16a, 16c). Reconstructing the Yucatan continental block back to its pre-rotational location is carried out using fracture zones identified by Nguyen and Mann (2016) (Fig. 16a), which equate to small circles about the pole of rotation that trace the Yucatan's path during seafloor spreading.

The small circles between the two conjugate margins (Fig. 16a) reunite this study's area of mapped Norphlet-equivalent (Fig. 16c) and the area of deep-water Norphlet sandstone previously mapped by Pilcher et al. (2014) on the northern GOM conjugate margin (Fig. 16b). This reveals the predicted pre-drift distribution of mapped Yucatan Norphlet-equivalent sandstone units is adjacent to its northeastern GOM equivalent on the Florida conjugate margin, which together cover a combined area of approximately 15,500 km². It also supports the conclusions by previous workers (Guzman et al., 2000; Rosenfeld, 2003; Hunt et al., 2017) for similar late Jurassic paleoenvironments on both the Yucatan and northern GOM conjugate margins to produce a similar structural setting of small salt rollers separating overlying units of aeolian sandstone (Fig. 3).

Along the Florida margin, Pilcher et al. (2014) suggested that the DeSoto High on the Florida Escarpment represented a paleo-topographic high which dictated sediment transport for the aeolian sands and also created a central, subcircular high from which radially diverging rafts

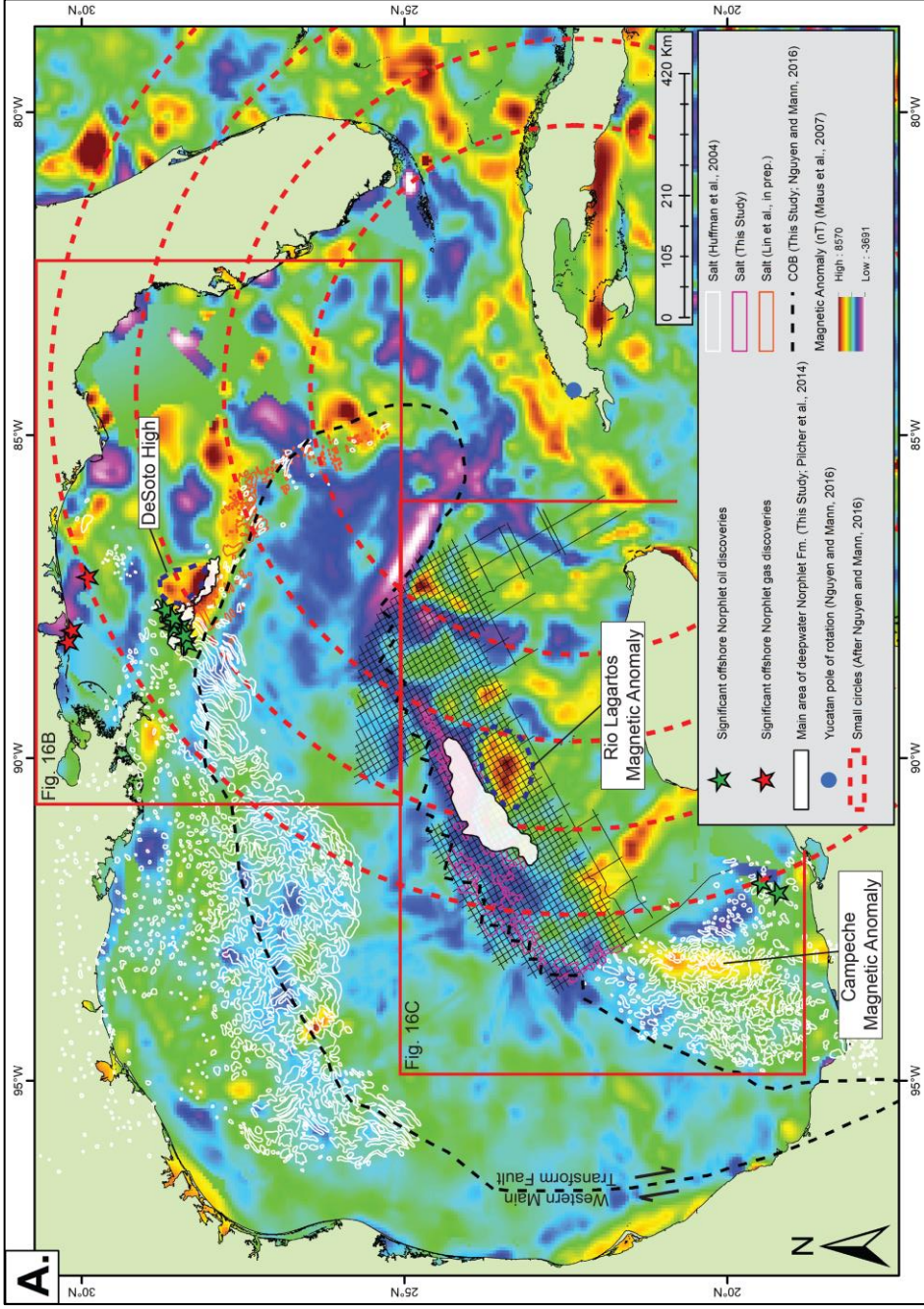


Figure 16. A. Mapped area of prevalent Norphlet-equivalent units on the northern Yucatan margin in relation to the mapping of Pilcher et al. (2014) on the Florida conjugate margin. Magnetic highs near these two areas suggest possible paleo-topographic highs that controlled sediment transport pathways and the direction of salt-assisted gravity sliding away from the area of high Mesozoic elevation. Notable oil (green) and gas (red) discoveries in the Norphlet Formation and Ek-Balam Group are overlaid.

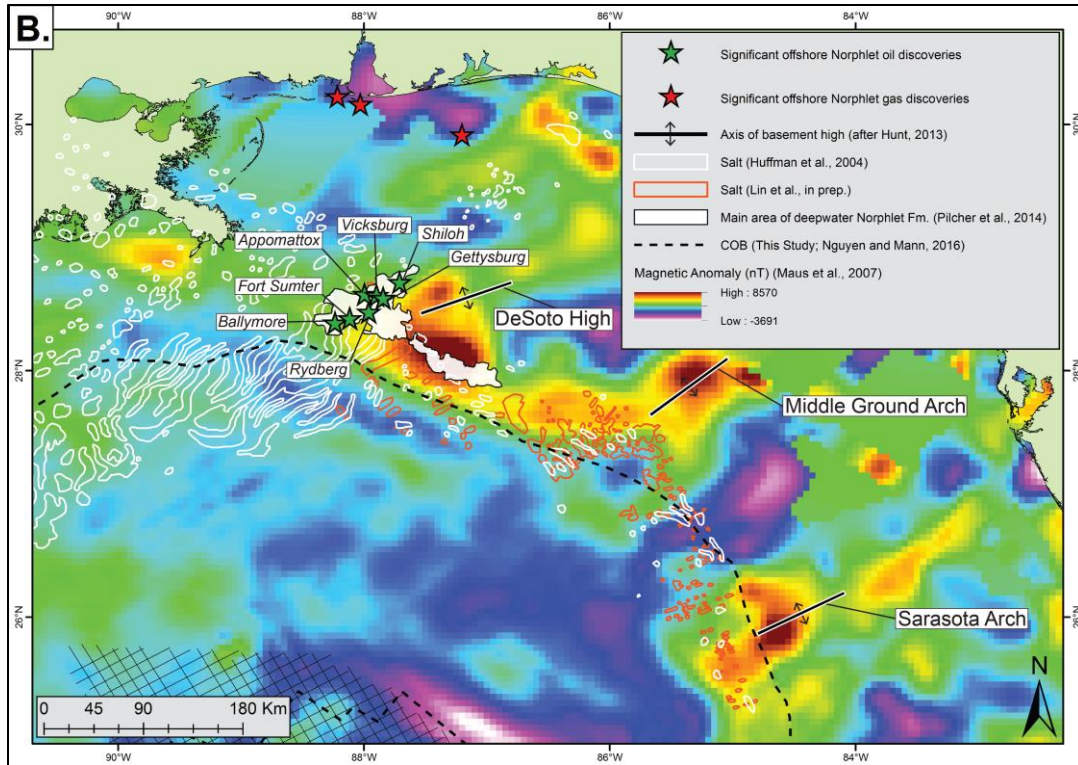


Figure 16 (cont.). B. Zoomed view of the Florida margin with notable hydrocarbon discoveries in the Norphlet Formation labelled.

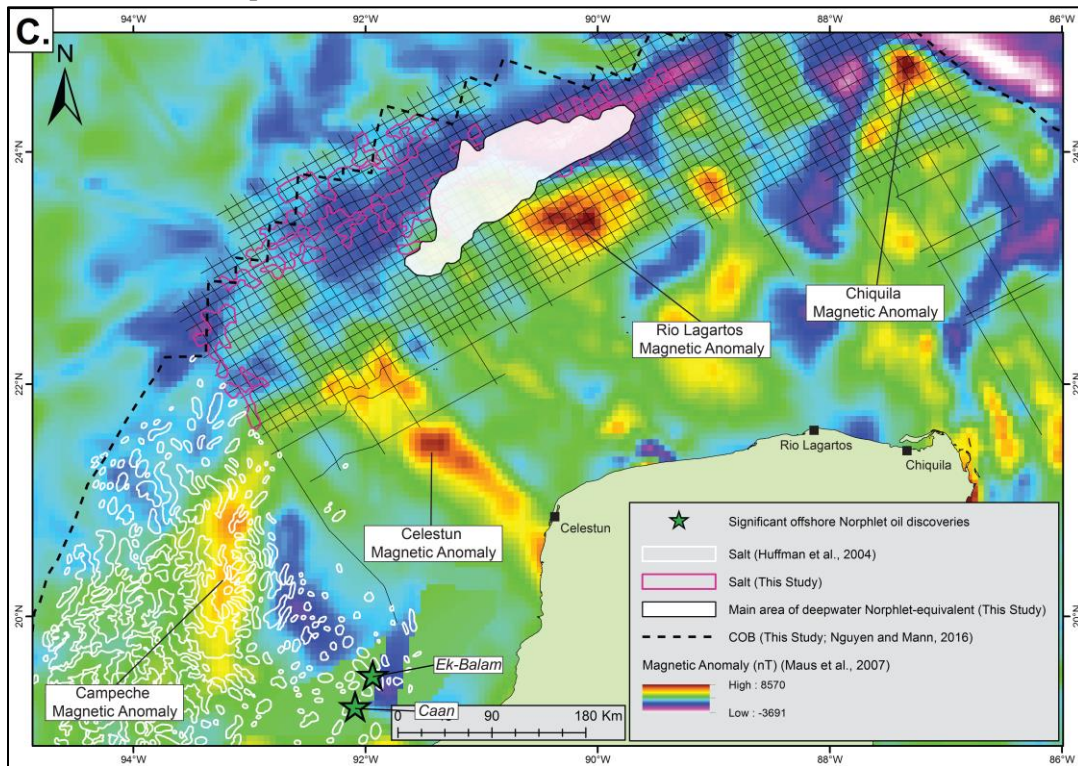


Figure 16 (cont.). C. Zoomed view of the Yucatan margin with notable hydrocarbon discoveries in the Ek-Balam Group's aeolian member labelled.

slid basinward along a basal, salt detachment (Fig 3a). I correlate the high magnetic anomaly of the DeSoto High with a previously unnamed, magnetic high on the Yucatan margin visible on Maus et al.'s (2007) global magnetic grid. This proposed Yucatan magnetic high, named here the Rio Lagartos magnetic anomaly (RLMA) after a nearby coastal town, is a prominent magnetic high located just inboard of the area of mapped salt rollers and Norphlet-equivalent (Fig. 16c). It has a similar extent and magnetic amplitude as the magnetic anomaly associated with the DeSoto High along the Florida margin (Fig. 16b), and could also represent a paleo-topographic high during the late Jurassic.

Two other, unnamed, magnetic highs exist on the northern Yucatan margin which I have named the Celestun Magnetic Anomaly and the Chiquila Magnetic Anomaly (CMA). The spatial relationship of the reconstructed Yucatan magnetic highs to those on the Florida margin (Fig. 17) suggest these magnetic highs are conjugate features that were separated during the oceanic spreading phase of GOM opening by the counter-clockwise rotation of the Yucatan block. Like the DeSoto High, they too may indicate paleo-topographic highs and have controlled both the potential paths of clastic sedimentary input in the Oxfordian section and also the direction of salt-assisted gravity sliding down the detachment surface on both margins. Their northeast-southwest orientation when reconstructed prior to the Yucatan's rotation (Fig. 17) may be related to the northwest-southeast rifting of the Yucatan during phase one rifting (Hunter et al., 2014).

6.3 Late Jurassic paleogeography and implications for hydrocarbon prospectivity

The mapped area of Norphlet-equivalent on the Yucatan margin and the fields producing hydrocarbons from Oxfordian, aeolian sandstone reservoirs in the Bay of Campeche are also restored to their Oxfordian locations prior to late Jurassic-earliest Cretaceous seafloor spreading using the pole of rotation of Nguyen and Mann (2016) (Fig. 17). By integrating the extent of the aeolian facies of the Norphlet Formation from Pilcher et al. (2014) and Pearson (2011) in the US

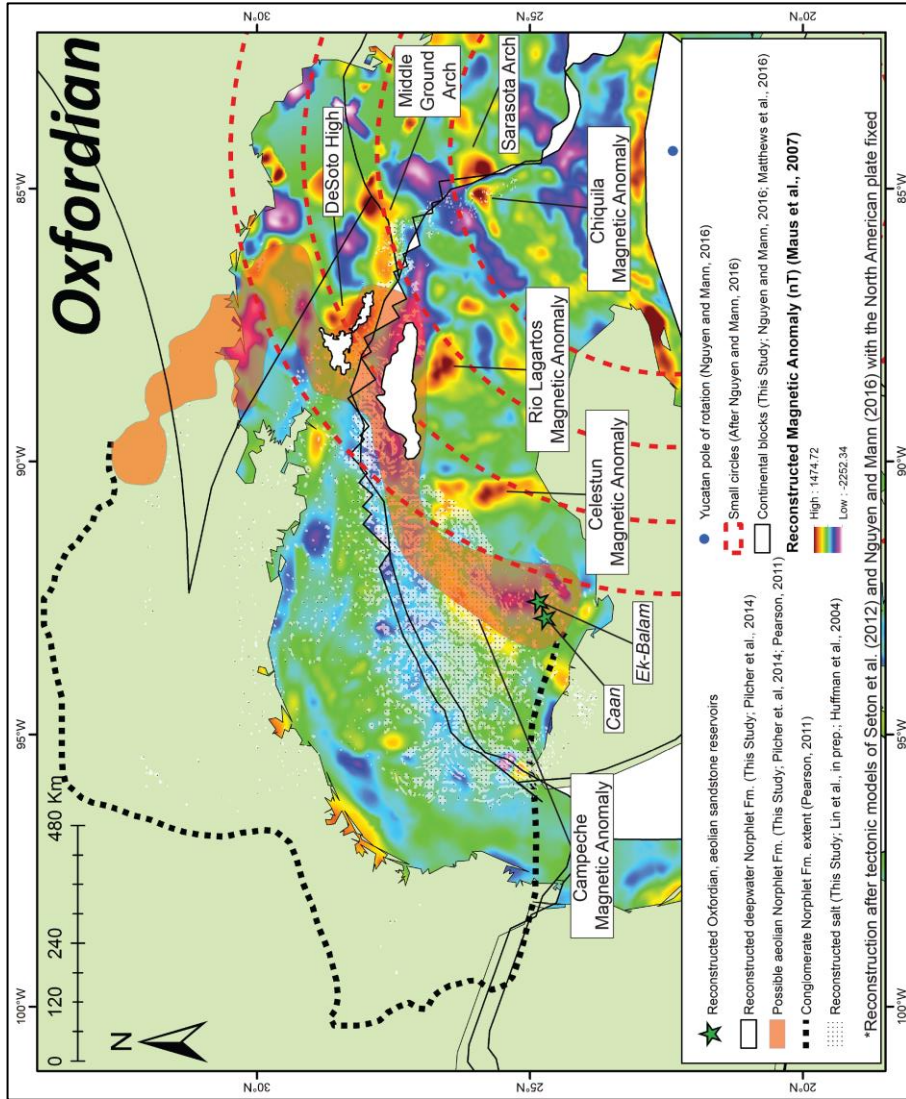


Figure 17. Oxfordian paleogeography showing proposed extent of aeolian sandstone deposition and salt bodies mapped in this study, by Lin (in prep.), and by Huffman et al. (2004). Magnetic data is used to identify paleo-topographic highs on the Yucatan margin where they are less studied than on the conjugate margin in the northeastern GOM. Reconstruction uses a fixed North American plate and restores the Yucatan block to its pre-drift position about a rotational pole from Nguyen and Mann (2016). The reconstructed magnetic grid illustrates the strong spatial correlation between the Sarasota Arch and the Chiquila Magnetic Anomaly, and the DeSoto High and the Rio Lagartos Magnetic Anomaly on the conjugate margins.

GOM and onshore GOM coast, I predict a 167,000 km², continuous area of aeolian sandstone deposition during the Oxfordian that includes both the Norphlet Formation and the Ek-Balam Group described as a Norphlet-equivalent in the Bay of Campeche (Rosenfeld, 2003; Hunt et al., 2017) (Fig. 17). Reconstruction of the GOM magnetic anomalies suggest that the magnetic highs were once adjacent and collinear with one another. The RLMA-DeSoto High and the CMA-Sarasota Arch conjugate pairs potentially formed northeast-southwest trending paleo-topographic highs prior to the Yucatan's counter-clockwise rotation and were related to the Triassic-Jurassic rift phase of GOM opening (Hunter et al., 2014; Lin, in prep.).

Extension of the aeolian sandstone fairway onto the northern Yucatan margin and the northeastern Campeche region would significantly improve the hydrocarbon prospectivity of this unexplored area. Salt mapping has already revealed that trapping styles similar to those utilized at the deep-water Norphlet sandstone discoveries of the northeastern GOM are present on the Yucatan margin where oil seeps are known to exist (Saunders et al., 2016; Pascali et al., 2017) (Fig. 18). Further investigation would be needed to examine whether the seeps were Oxfordian-sourced, the likely Smackover-equivalent that would be needed to charge the Norphlet-equivalent reservoirs of the northern Yucatan margin.

7. CONCLUSIONS

1. Similar to the northeastern GOM (Fig. 3), small (0-600 m thick), Callovian salt rollers overlie a gently-dipping salt detachment along the northern Yucatan margin (Figs. 7c, 8c). Overlying the salt rollers are sedimentary growth wedges that indicate movement along listric, normal faults that root onto the salt detachment. Salt roller deformation is typically limited to the Mesozoic section as relatively undeformed Cenozoic strata overlie and onlap the Top Cretaceous surface.

2. A high-amplitude seismic trough overlies the salt rollers on the updip side, is not a continuous horizon, and exhibits large elevation changes as the reflector is sometimes elevated by underlying salt rollers (Fig. 7b). Following previous studies (Obid, 2006; Hunt, 2013; Hunt et al., 2017), I identify this seismic reflection as a Norphlet-equivalent stratigraphic unit (Fig. 7c). When reconstructed over 250 km to its depositional location in Oxfordian time, the mapped area of Norphlet-equivalent is adjacent to the deep-water Norphlet sandstone of the northeastern GOM (Fig. 17).
3. Three structural salt domains are identified on the northern Yucatan margin: absent or minimal salt, updip salt rollers (0-600 m thick), and downdip salt diapirs (up to 6 km tall) (Fig. 9b). Salt deformation associated with salt rollers is generally limited to the Mesozoic section (Figs. 12, 14) and creates prolific, structural hydrocarbon traps as verified by many discoveries in the northeastern GOM (Fig. 16b). Salt diapirs, however, cause complex deformation throughout the Mesozoic and Cenozoic intervals where salt evacuation produces accommodation and sedimentary thickening and vertical salt migration reduces accommodation and causes sedimentary thinning (Fig. 13). Most of the large salt diapirs of the northern Yucatan are restricted to the outer marginal rift (Fig. 10b) where the basement elevation is at its lowest (Hudec et al., 2013; Ismael, 2014; Pindell et al., 2014; Goswami et al., 2017) (Figs. 10a, 13c).
4. The tectonic subsidence curves of the subsidence analysis of four US GOM wells and one pseudo-well in the central study area of the northern Yucatan margin (Fig. 15) suggest a slow and gradual history of subsidence of the GOM basin since the late Jurassic. Along with the coherent reflectors apparent in sedimentary growth wedges observed from the salt detachment all the way to the Top Cretaceous surface (Fig. 7c), this makes a post-rift, catastrophic collapse of the margin unlikely. Rather, the formation of salt rollers and

sedimentary growth along listric, normal faults rooted on the detachment was slow and methodical throughout the late Jurassic and Cretaceous intervals (Fig. 14).

5. Pilcher et al. (2014) suggest the salt rollers and overlying rafted stratigraphic units in the northeastern GOM dispersed radially by gravity sliding away from a paleo-topographic high, the DeSoto High, which produces a magnetic anomaly (Fig. 16b). Similar magnetic anomalies, the RLMA and CMA, are identified on the Yucatan margin (Fig. 16c). The RLMA's proximity to the mapped Norphlet-equivalent of the northern Yucatan suggests it too may represent a paleo-topographic high that controlled the distribution of salt rollers and overlying stratigraphy that slid down from the elevated, basement high along the salt detachment.
6. Reconstruction of the magnetic grid to the time before seafloor spreading in the GOM places the magnetic highs and lows of the Florida and Yucatan margins adjacent to one another and reveals conjugate pairs of northeast-southwest trending magnetic anomalies (Fig. 17). These magnetic trends may represent the basement structure that resulted from the northwest-southeast directed rift phase of GOM opening during the Triassic and early Jurassic.
7. The mapped extent of deep-water Norphlet-equivalent on the northern Yucatan along with hydrocarbon production from the aeolian sandstone member of the Ek-Balam Group in the Bay of Campeche and the known extent of Norphlet sandstone in the northeastern GOM suggests a large, continuous region of late Jurassic, aeolian sandstone deposition in the GOM basin (Fig. 17). This suggests a hydrocarbon reservoir fairway from the southeastern Bay of Campeche to the central northern Yucatan margin, increasing the known northern GOM reservoir fairway by 84,000 km² in this unexplored region along the western and northern Yucatan margin of Mexico (Fig. 18).

8. REFERENCES

Angeles-Aquino, F., and Cantu-Chapa, A., 2001. Subsurface Upper Jurassic stratigraphy in the Campeche Shelf, Gulf of Mexico. In: Bartolini, C., Buffler, R. T., Cantu-Chapa, A. (Eds.), The western Gulf of Mexico basin: Tectonics, sedimentary basins, and petroleum systems: AAPG Memoir 75, 343-352.

Beyene, A., Abdelsalam, M. G., 2005. Tectonics of the Afar Depression: A review and synthesis. *J. of Afr. Earth Sci.* 41, 41-59.

Cassidy, M., Burke, K., 2012. Sub-aerial basins below sea level provide unexpected reservoirs. *Houston Geological Society Bulletin* 54, 35-37.

Dunnahoe, T., 2018. Total makes largest company discovery in Gulf to date. *Oil and Gas Journal*. 31 Jan. 2018. <www.ogj.com/articles/2018/01/total-makes-largest-company-discovery-in-gulf-to-date.html> Accessed 7 Mar. 2018.

Eddy, D. R., Van Avendonk, H. J. A., Christeson, G. L., Norton, I. O., Karner, G. D., Johnson, C., Snedden, J. W., 2014. Deep crustal structure of the northeastern Gulf of Mexico: Implications for rift evolution and seafloor spreading. *J. Geophys. Res. Solid Earth* 119, 6802-6822.

Galloway, W. E., 2008. Depositional evolution of the Gulf of Mexico sedimentary basin. In: Miall, A. D. (Ed.), *Sedimentary basins of the world* 5, 505-548.

Godo, T., 2006. Norphlet aeolian dunes in the deep-water Gulf of Mexico. *Houston Geological Society Bulletin* 49, 11.

Godo, T. J., Chuparova, E., McKinney, D. E., 2011. Norphlet aeolian sand fairway established in the deep-water Gulf of Mexico. *AAPG Annual Convention and Exhibition, Houston, 10-13th April 2011.*

Godo, T., 2017. The Appomattox field: Norphlet Aeolian sand dune reservoirs in the deep-water Gulf of Mexico. In: Merrill, R. K., Sternbach, C. A. (Eds.), *Giant fields of the decade 2000-2010. AAPG Memoir 113, 29-54.*

Goldhammer, R. K., Johnson, C. A., 2001. Middle Jurassic-Upper Cretaceous Paleogeographic evolution and sequence-stratigraphic framework of the northwest Gulf of Mexico rim. In: Bartolini, C., Buffler, R. T., Cantu-Chapa, A. (Eds.), *The western Gulf of Mexico basin: Tectonics, sedimentary basins, and petroleum systems. AAPG Memoir 75, 45-81.*

Goswami, A., Haire, E., Pindell, J., Horn, B. W., 2017. Pre-salt in the deepwater Gulf of Mexico: Evolution and play potential in the syn-rift and sag fill in offshore Mexico. *AAPG Annual Convention and Exhibition, Houston, 2-5th April 2017.*

Gray, G. G., Lawton, T. F., Murphy, J. J., 2008. Looking for the Mojave-Sonora megashear in northeastern Mexico. In: Moore, G. (Ed.), *Geological Society of America Field Guide 14. Geological Society of America Joint Annual Meeting, Houston, 5-9th October 2008. 26 pp.*

Guzman, A. E., Limon-Gonzalez, M., Marquez-Dominguez, B., 2000. The Gulf of Mexico basin south of the border, *the* petroleum province of the 21st century. Second Annual Wallace E. Pratt Memorial Conference, San Diego, 12-15th January 2000. 19 pp.

Guzman-Vega, M. A., Mello, M. R., 1999. Origin of oil in the Sureste Basin, Mexico. AAPG Bull. 83, 1068-1095.

He, L., Poling, R., 2016. Post-Jurassic sedimentary history of the eastern Gulf of Mexico. Gulf Coast Association of Geological Societies Transactions 66, 759-762.

Hudec, M. R., Jackson, M. P. A., 2004. Regional restoration across the Kwanza Basin, Angola: Salt tectonics triggered by repeated uplift of a metastable passive margin. AAPG Bull. 88, 971-990.

Hudec, M. R., Norton, I. O., Jackson, M. P. A., Peel, F. J., 2013. Jurassic evolution of the Gulf of Mexico salt basin. AAPG Bull. 97, 1683-1710.

Huffman, A. C., Kinney, S. A., Biewick, L. R. H., Mitchell, H. R., Gunther, G. L., 2004. Gulf Coast Geology (GCS) Online—Miocene of Southern Louisiana. USGS Data Series 90-A, v. 1.0.

Hunt, B. W., 2013. Regional Norphlet facies correlation, analysis, and implications for paleostructure and provenance, eastern Gulf of Mexico. Unpublished Master of Science Thesis, University of Alabama, 112 pp.

Hunt, B., Robinson, D. M., Weislogel, A. L., Ewing, R. C., 2017. Sediment source regions and paleotransport of the Upper Jurassic Norphlet Formation, eastern Gulf of Mexico. AAPG Bull. 101, 1519-1542.

Hunter, I. S., Robinson, D. M., Weislogel, A., 2014. Origin and development of the Apalachicola Basin. AAPG Annual Convention and Exhibition, Houston, 9 April 2014.

Ismael, M., 2014. Tectonostratigraphic stages in the Mesozoic opening and subsidence of the Gulf of Mexico based on deep-penetration seismic reflection data in the salt-free-eastern part of the basin. Unpublished Master of Science Thesis, University of Houston, 126 pp.

Lin, P., in prep. Crustal structure, tectonostratigraphic evolution, and source rock distribution and maturity of the eastern Gulf of Mexico basin. PhD thesis, University of Houston.

Lopez, J. J. R., 1996. Disposicion de los cuerpos de areniscas y su relacion en el mantenimiento de la produccion del campo Ek-Balam, Campeche. Boletin de la Asociacion Mexicana de Geologos Petroleros 45, 1-38.

Lovell, T., 2010. Detrital Zircon U-Pb age constraints on the provenance of the upper Jurassic Norphlet Formation, eastern Gulf of Mexico: Implications for paleogeography. Gulf Coast Association of Geological Societies Transactions 60, 443-460.

Mann, P., Padilla y Sanchez, R., Nguyen, L., Lankford-Bravo, D., 2016. Geologic and geophysical evidence for a Pacific origin for seawater filling the Callovian Gulf of Mexico evaporite basin. AAPG Annual Convention and Exhibition, Calgary, 19-22nd June 2016.

Marton, G., Buffler, R. T., 1994. Jurassic reconstruction of the Gulf of Mexico basin. *Int. Geol. Rev.* 36, 545-586.

Marton, L. G., Tari, G. C., Lehmann, C. T., 2000. Evolution of the Angolan passive margin, West Africa, with emphasis on post-salt structural styles. *Geophys. Mon.* 115, 129-149.

Matthews, K. J., Maloney, K. T., Zahirovic, S., Williams, S. E., Seton, M., Muller, R. D., 2016. Global plate boundary evolution and kinematics since the late Paleozoic. *Global and Planetary Change* 146, 226-250.

Maus, S., Sazonova, T., Hemant, K., Fairhead, J. D., Ravat, D., 2007. National Geophysical Data Center candidate for the World Digital Magnetic Anomaly Map. *Geochem., Geophys., Geosystems* 8, 10 pp.

Mitra, S., Gonzalez, J. D. A., Garcia, J. H., Ghosh, K., 2007. Ek-Balam field: A structure related to multiple stages of salt tectonics and extension. *AAPG Bull.* 91, 1619-1636.

Nguyen, L., Mann, P., 2016. Gravity and magnetic constraints on the Jurassic opening of the oceanic Gulf of Mexico and the location and tectonic history of the Western Main transform fault along the eastern continental margin of Mexico. *Interpretation* 4, SC23-SC33.

Obid, J. A., 2006. Sequence and seismic stratigraphy of the Jurassic strata in northeastern Gulf of Mexico. Unpublished PhD Thesis, University of Alabama, 270 pp.

Padilla y Sanchez, R. J., 2017. The late Triassic-late Cretaceous flooding of the Gulf of Mexico from the Pacific through Mexico. AAPG Annual Convention and Exhibition, Houston, 2-5th April 2017.

Pascali, A., Bugti, M. N., Mann, P., 2017. A search for controls on the distribution of natural, submarine oil seeps in the Gulf of Mexico. AGU Fall Meeting, New Orleans, 11-15th December 2017.

Payeur, T., Weimer, P., Gutterman, W., Zimmermann, E., Cumella, S., 2017. Stratigraphic evolution of upper Jurassic strata, northeastern Gulf of Mexico: Preliminary results. Gulf Coast Association of Geological Societies Transactions 67, 235-257.

Pearson, O. N., 2011. Undiscovered hydrocarbon resources in the U.S. Gulf Coast Jurassic Norphlet and Smackover Formations. Gulf Coast Association of Geological Societies Transactions 61, 329-340.

Piedade, A., and Alves, T. M., 2017. Structural styles of Albian rafts in the Espirito Santo Basin (SE Brazil): Evidence for late raft compartmentalization on a 'passive' continental margin. Mar. Pet. Geol. 79, 201-221.

Pilcher, R. S., Murphy, R. T., Ciosek, J. M., 2014. Jurassic raft tectonics in the northeastern Gulf of Mexico. Interpretation 2, SM39-SM55.

Pindell, J., Kennan, L., 2009. Tectonic evolution of the Gulf of Mexico, Caribbean and northern South America in the mantle reference frame. In: James, K. H., Lorente, M. A., Pindell, J. L. (Eds.), The origin and evolution of the Caribbean plate. Geol. Soc. Lond. Spec. Publ. 328, 1-55.

Pindell, J., Graham, R., Horn, B., 2014. Rapid outer marginal collapse at the rift to drift transition of passive margin evolution, with a Gulf of Mexico case study. Basin Res. 26, 1-25.

Pindell, J., Miranda C., E., Ceron, A., Hernandez, L., 2016. Aeromagnetic map constrains Jurassic-Early Cretaceous synrift, break up, and rotational seafloor spreading history in the Gulf of Mexico. GCSSEPM Foundation Perkins-Rosen Annual Research Conference, Houston, 8-9th December, 2016.

Rodriguez, A. B., 2011. Regional structure, stratigraphy, and hydrocarbon potential of the Mexican sector of the Gulf of Mexico. Unpublished Master of Science Thesis, University of Texas at Austin, 177 pp.

Rosenfeld, J. H. 2003. Economic potential of the Yucatan Block of Mexico, Guatemala, and Belize. In: Bartolini, C., Buffler, R. T., Blickwede, J. (Eds.), The Circum-Gulf of Mexico and the Caribbean: Hydrocarbon habitats, basin formation, and plate tectonics. AAPG Memoir 79, 340-348.

Rowan, M. G., Peel, F. J., Vendeville, B. C., 2004. Gravity-driven fold belts on passive margins. In: McClay, K. R. (Ed.), Thrust tectonics and hydrocarbon systems. AAPG Memoir 82, 157-182.

Rowan, M. G., Ratliff, R. A., 2012. Cross-section restoration of salt-related deformation: Best practices and potential pitfalls. *J. Struct. Geol.* 41, 24-37.

Salvador, A., 1987. Late Triassic-Jurassic paleogeography and origin of Gulf of Mexico basin. *AAPG Bull.* 71, 419-451.

Sandwell, D. T., Muller, R. D., Smith, W. H. F., Garcia, E., Francis, R., 2014. New global marine gravity model from CryoSat-2 and Jason-1 reveals buried tectonic structure. *Science* 346, 65-67.

Sanford, J. C., Snedden, J. W., Gulick, P. S., 2016. The Cretaceous-Paleogene boundary deposit in the Gulf of Mexico: Large-scale oceanic basin response to the Chicxulub impact. *J. Geophys. Res. Solid Earth* 121, pp. 22.

Saunders, M., Geiger, L., Rodriguez, K., Hargreaves, P., 2016. The delineation of pre-salt license blocks in the deep offshore Campeche-Yucatan Basin. AAPG Annual Convention and Exhibition, Calgary, 19-22nd June 2016.

Saunders, M., Geiger, L., Steier, A., Lin, P., 2017. Mapping the Jurassic Norphlet Sandstone along the northern margin of the Yucatan Peninsula. AAPG Annual Convention and Exhibition, Houston, 2-5th April 2017.

Sclater, J. G., Christie, P. A. F., 1980. Continental stretching: An explanation of the post-mid-Cretaceous subsidence of the central North Sea Basin. *J. Geophys. Res. Solid Earth* 85, 3711-3739.

Seton, M., Muller, R. D., Zahirovic, S., Gaina, C., Torsvik, T., Shephard, G., Talsma, A., Gurnis, M., Turner, M., Maus, S., Chandler, M., 2012. Global continental and ocean basin reconstructions since 200 Ma. *Earth-Sci. Rev.* 113, 212-270.

Snedden, J. W., Norton, I. O., Christeson, G. L., Sanford, J. C., 2014. Interaction of deepwater deposition and a mid-ocean spreading center, eastern Gulf of Mexico basin, USA. *Gulf Coast Association of Geological Societies Transactions* 64, 371-383.

Tew, B. H., Mink, R. M., Mann, S. D., Bearden, B. L., and E. A. Mancini. 1991. Geologic framework of Norphlet and pre-Norphlet strata of the onshore and offshore eastern Gulf of Mexico area. *Gulf Coast Association of Geological Societies Transactions* 31, 590-600.

Weimer, P., Bouroullec, R., Adson, J., Cossey, S. P. J., 2017. An overview of the petroleum systems of the northern deep-water Gulf of Mexico. *AAPG Bull.* 101, 941-993.